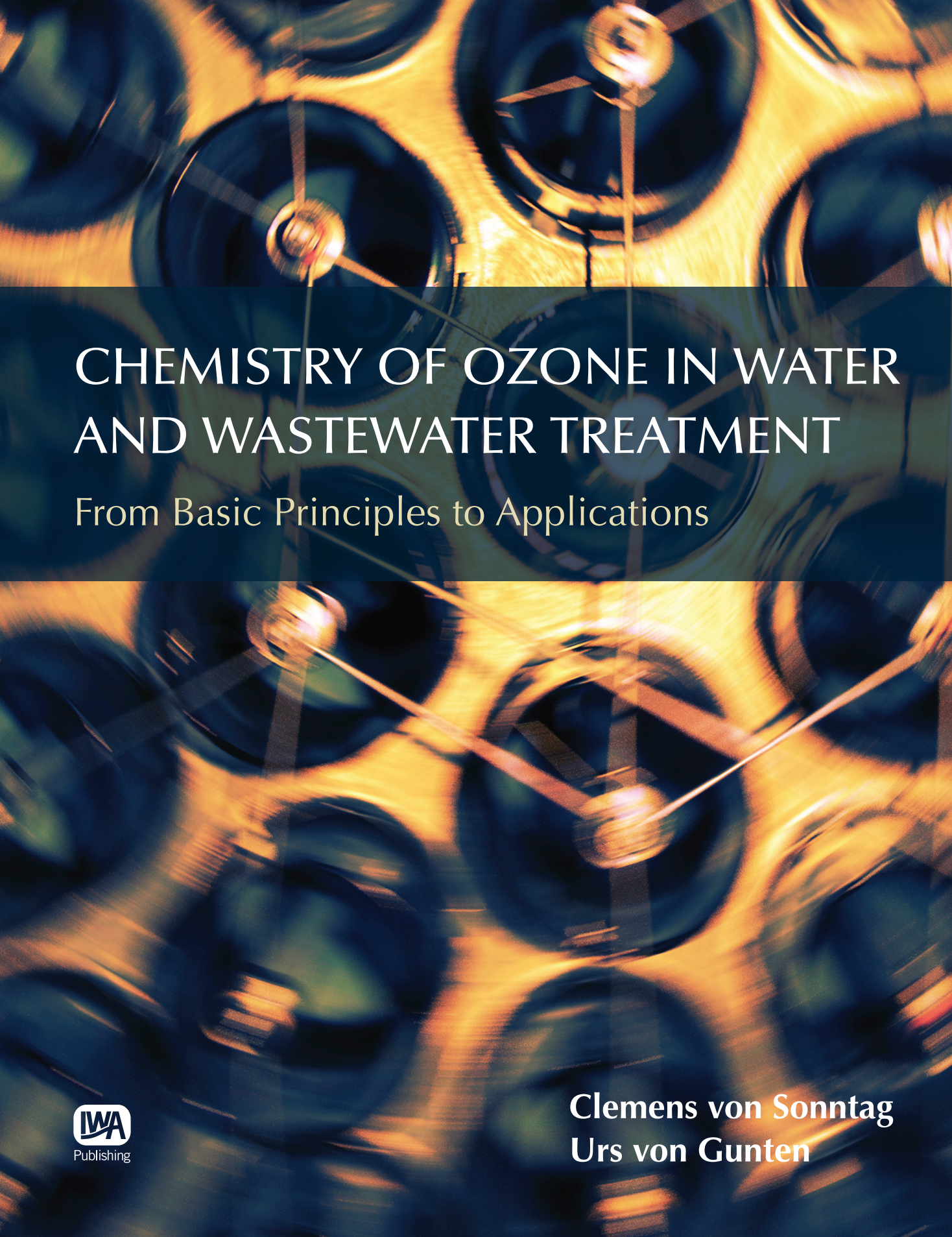

CHEMISTRY OF OZONE IN WATER AND WASTEWATER TREATMENT

From Basic Principles to Applications

Clemens von Sonntag
Urs von Gunten

IWA Publishing

Chemistry of Ozone in Water and Wastewater Treatment

Chemistry of Ozone in Water and Wastewater Treatment

From Basic Principles to Applications

Clemens von Sonntag and Urs von Gunten

IWA Publishing
London • New York

Published by **IWA Publishing**
Alliance House
12 Caxton Street
London SW1H 0QS, UK
Telephone: +44 (0)20 7654 5500
Fax: +44 (0)20 7654 5555
Email: publications@iwap.co.uk
Web: www.iwapublishing.com

First published 2012

Cover image: Ozone Generator Ozonia, Degrement Technologies, with permission.
Photograph: Urs von Gunten.
Cover Design: Timo von Gunten and Sixteen Design (www.sixteen-design.co.uk)

British Library Cataloguing in Publication Data
A CIP catalogue record for this book is available from the British Library

ISBN 9781843393139 (Paperback)
ISBN 9781780400839 (eBook)

Contents

About the Authors

Prof. Dr Clemens von Sonntag
Max-Plack-Institut für Bioanorganische Chemie, D-45470 Mülheim an der Ruhr, Germany,
(retired: postal address: Bleichstr. 16, D-45468 Mülheim an der Ruhr)

and

Institut für Instrumentelle Analytik, Universität Duisburg-Essen, D-45117 Essen.
(email: clemens@vonsonntag.de)

Prof. Dr Urs von Gunten
Department of Water Resources and Drinking Water, Eawag, Swiss Federal Institute of Aquatic Science and Technology, CH-8600 Dübendorf, Switzerland

and

Institute of Environmental Engineering, School of Architecture, Civil and Environmental Engineering, ENAC, Ecole Polytechnique Fédérale Lausanne, EPFL, CH-1012 Lausanne.
(email: vongunten@eawag.ch)

Chapter 1

Historical background and scope of the book

The discoverer of ozone, *Christian Friedrich Schönbein* (1799–1869, cf. Figure 1.1) was born in Metzingen (Germany) as the son of a dyer. With only one exam in his life, which he passed on his own, without a regular education, he became one of the leading chemists in Europe. Before being nominated Professor at the University of Basel, he studied in Germany, England and France. In 1830, he received an honorary doctoral degree from the University of Basel. He also became an honorary citizen of the City of Basel in 1840 and later on was politically active in the legislative and executive government of this city (Nolte, 1999). He is best known for his discovery of ozone (1839), but he also discovered the principle of the fuel cell (1839), and gun cotton (1846). The test for ozone that he had developed on the basis of the guajac resin led to the discovery of peroxidases (1855) and is still in use as a simple screening test for colon cancer (the haemoglobin in the faeces act like peroxidases). He also was the first (von Sonntag, 2006) to use the Fe^{2+} plus H_2O_2 reaction (Schönbein, 1859), which was later termed the Fenton reaction after *Henry John Horstman Fenton* (1854–1929) who nearly forty years later looked into the reaction in more detail (Fenton, 1894; Fenton & Jackson, 1899). *Schönbein* gave the new oxygen species the name "ozone" because of its strong smell [taken from Greek "ὄζειν" (ózein): to smell (see Chapter 2) (Schönbein, 1840)] and was very close to deducing the right structure (Schönbein, 1854). He also described the reaction with iodide and the most sensitive indigo assay (Schönbein, 1854). This assay is still in use today (Chapter 2). His famous 1854 review was requested by *Justus von Liebig* (1803–1873) to be published in his "Annalen", in which he writes: "*Herr Professor Schönbein hat auf meinen Wunsch seine Untersuchungen über diesen Gegenstand für die Leser der Annalen zusammengestellt. Ich betrachte die Erscheinungen und Beobachtungen, welche dieser ausgezeichnete Forscher beschreibt, für eben so wichtig wie bedeutungsvoll für die Wissenschaft, denn es ist von jeher die Entdeckung einer neuen Eigenschaft der Materie die Quelle neuer Naturgesetze und die Quelle der Einsicht in bis dahin unerklärliche Erscheinungen gewesen*. – On my request, professor Schönbein has compiled his studies on this subject. I consider the phenomena and observations described by this distinguished scientist as important as well as significant for science, since the discovery of a novel property of matter has always been the source of new laws of nature and the source of comprehension of hitherto unexplainable phenomena."

Schönbein was not only an excellent scientist but must also have been good company (Oesper, 1929a; Oesper, 1929b). *Justus von Liebig* wrote to *Friedrich Wöhler* (1800–1882): "*Schönbeins Humor ist unschätzbar; wenn ich nur seinen Magen hätte.* – Schönbein's sense of humour is invaluable; I wish I had his stomach."

Figure 1.1 *Christian Friedrich Schönbein* (1799−1868). University Library Basel, Portrait Collection, with permission.

The history of the first hundred years of ozone chemistry has been reported in eight excellent articles by M.C. Rubin (Rubin, 2001, 2002, 2003, 2004, 2007, 2008, 2009; Braslavsky & Rubin, 2011), and here we can give only a very short account.

Schönbein had discovered ozone when he electrolysed dilute sulfuric acid and observed that it was also formed in the autoxidation of white phosphorus ("the phosphorus smell"). The latter was the standard method for obtaining ozone in the first years of ozone chemistry. He reported his discovery to the Basel Natural Science Society on 13 March 1839: "*Über den Geruch an der positiven Elektrode bei der Elektrolyse des Wassers* – On the odour at the positive electrode during electrolysis of water." *Schönbein* had already realised that low concentrations of carbon, iron, tin, zinc and lead hindered ozone production (Schönbein, 1844). For *Schönbein*, this was proof of the oxidising properties of ozone. Yet, it was more difficult at the time to derive the structure of ozone. Originally, *Schönbein* thought that ozone is related to halogens, because of its smell, which is similar to chlorine and bromine. Later, he hypothesised that it contained oxygen and hydrogen (Schönbein, 1844). Only years later, did he accept that ozone was a modification of oxygen as was described by *Jacob Berzelius* (1779–1848) in 1846 (Nolte, 1999). He writes to *Michael Faraday* (1791–1861): "*Wir können nicht länger an der Tatsache zweifeln, dass Sauerstoff in zwei verschiedenen Zuständen, in einem aktiven und einem inaktiven, in dem ozonischen und dem normalen Zustand exisitiert.* – We can no longer doubt the fact that oxygen exists in two different states, an active and an inactive one, in the ozonic and normal state."

The ozone generator that we use today for its production was invented by *Werner von Siemens* (1816–1882) in 1857, and only this invention made industrial applications of ozone possible.

Applications often very rapidly follow technical progress. It was less than a fortnight after the discovery of x-rays by *Wilhelm Konrad Röntgen* (1845–1923), when a physicist in Chicago realised that this biologically active radiation might be used in cancer therapy, and the first patient was treated (Grubbé, 1933; von Sonntag, 1987). Also, when reliable UV-lamps became available (Perkin, 1910), the first plant providing UV-disinfected drinking water to a community of 20,000 people was installed in the same year (von Sonntag, 1988). Similarly, very shortly after the discovery of the pathogenic agents of anthrax in 1876 and of cholera in 1884 by *Robert Koch* (1843–1910), the disinfecting power of ozone was reported (Sonntag, 1890) in the same issue as that of chlorine (Nissen, 1890). The implementation of ozone in water treatment followed about one decade later (see below and Chapter 5).

The ozone chemistry of organic compounds was first studied systematically by *Carl Friedrich Harries* (1866–1923), professor at the University of Kiel and son-in-law of *Werner von Siemens*, and it was he who coined the name "ozonide" for compounds formed in the reaction of ozone with organic compounds, notably olefins (Rubin, 2003).

A breakthrough in the understanding of ozone reactions mechanistically was achieved by *Rudolf Criegee* (1902–1975, Figure 1.2), with experiments starting in the late 1940s, and the reaction of olefins with ozone (Criegee, 1975) rightly carries his name. One of us (CvS) knew Criegee quite well, as Criegee had been his PhD examiner in Organic Chemistry at the Technical University of Karlsruhe, but, at the time, trained as a photochemist and as a radiation chemist; the candidate would never have dreamt that, one day, ozone chemistry may find his own interest as well.

Figure 1.2 *Rudolf Criegee* (1902–1975). Chemistry Department of the Karlsruhe Institute of Technology (formerly the Technical University of Karlsruhe), with permission.

In those times, ozone chemistry was carried out largely in organic solvents (Bailey, 1978; Bailey, 1982) [for aqueous solutions see (Bailey, 1972)]. *Werner Stumm* (1924−1999) (Giger & Sigg, 1997), director of Eawag (1970−1992) realised the high potential of ozone in water treatment, but also the very limited knowledge of its reactions in aqueous solution (Stumm, 1956). He thus enforced his group by asking *Jürg Hoigné* (Giger & Sigg, 1997) to join in, and due to *Hoigné's* pioneering work on ozone chemistry in aqueous solution, the topic of this book, found more than a little interest. It was he who showed that ozone reactions in aqueous solution may induce free-radical reactions (Hoigné & Bader, 1975), reactions that seem not to occur in organic solvents. *Hoigné* also started off as a radiation chemist, and a friendship with one of us (CvS) dates back to the mid-1960s, when *Hoigné* was still an active member of the radiation chemistry community. With this background knowledge, he introduced radiation-chemical tools for elucidating aspects of ozone chemistry in aqueous solution (Bühler *et al.*, 1984; Staehelin *et al.*, 1984). The other author of this book (UvG) joined the *Hoigné* group at Eawag in 1992 and later became his successor. We (CvS and UvG) profited greatly from discussions with *Jürg Hoigné*, and it is our great pleasure to dedicate this book to him.

The disinfecting power of ozone (Sonntag, 1890) and chlorine (Nissen, 1890) were realised practically at the same time in the late 19th century. The first ozone disinfection unit was installed in 1906 in Nice (France)

(Kirschner, 1991). Not much later (1911), a UV-disinfection plant was built in nearby Marseille (von Sonntag, 1988). Despite this very early start of ozone- and UV-disinfection technologies, chlorination dominated over many decades, and it was only in the 1970s and even later, when the shortcomings of chlorination became apparent (chlorination by-products, lack of inactivation of the cysts of *Giardia* and oocysts of *Cryptosporidium*) that disinfection with ozone and UV gained in importance. Later on, the oxidation of micropollutants also became an important field of ozone application (Chapter 5).

Based on the increasing importance of ozone in drinking water and wastewater, a number of books appeared on this topic (Evans, 1972; Langlais *et al.*, 1991; Beltrán, 2004; Rakness, 2005; Gottschalk *et al.*, 2010). They often dealt with technical aspects or, when ozone chemistry was in the foreground, they no longer covered the recent developments in this area of research. Most scientific papers at conferences and in publications report interesting details, but they are not embedded in a general mechanistically based concept of ozone chemistry in aqueous solution. The present book intends to fill this apparent gap and should enable researchers to sharpen their research by applying basic mechanistic principles. Mechanistic considerations "hypotheses" are the basis of scientific progress: "*Hypothesen sind Netze, nur der wird fangen, der auswirft.* – Hypotheses are nets, only those who cast will catch." (*Friedrich Philipp Freiherr von Hardenberg* (1772–1801), "*Novalis*", German poet and scholar). Yet, there is a *caveat* that we should not stick to these concepts slavishly: "*Hypothesen sind Wiegenlieder, womit der Lehrer seine Schüler einlullt, der denkende treue Beobachter lernt immer mehr seine Beschränkung kennen, er sieht: je weiter sich das Wissen ausbreitet, desto mehr Probleme kommen zum Vorschein.* – Hypotheses are lullabies, by which the teacher lulls his pupils; the thinking and careful observer increasingly realises his limitations; he sees: the further knowledge expands, the more problems appear." (*Johann Wolfgang von Goethe* (1749–1832), German poet and scholar). Mechanisms are always open to revision, since concepts in science can never be proven and must contain the potential of falsification – otherwise they are too general and useless [*Karl Raimund Popper* (1902–1984), Austrian philosopher]. The reader will see this principle operating in relation to our work also; we had to revise our already published mechanistic suggestions when new experimental data became available. Here, we are in accord with *Schönbein* who is reported (Oesper, 1929a) to have said: "As for me, the determination of the truth is far more important than the maintenance of my views, for why should one hold fast to notions that will not withstand the criticisms of facts. The sooner they fall, the better, even though prima facie they appear ever so ingenious."

Yet, mechanistic considerations are not hatched in the ivory tower for the amusement of physical chemists, but are of great predictive value. As in analytical chemistry, one typically only finds what one is looking for. Mechanistic considerations lead to more detailed and in-depth studies.

With this concept in mind, *Maggie Smith*, responsible for IWA Publishing, and the authors agreed to launch this book at as low a price as possible to make it not only affordable for senior scientists but also for students of environmental sciences and engineering. For expanding the knowledge in ozone chemistry and application or finding an entry into the field, as many references as possible were included and updated in early 2012. Ozone rate constants in aqueous solution are compiled, updating an earlier compilation (Neta *et al.*, 1988). Managers of water supplies and wastewater treatment plants will find here the state-of-the-art in disinfection and pollution abatement using ozone and ozone-based advanced oxidation processes and a discussion of certain limitations that may be caused by problematic by-products such as bromate. Furthermore, examples of the incorporation of ozone into water and wastewater treatment schemes are given. Finally, as our drinking water resources become scarcer, notably in arid countries, a paragraph is devoted to the contribution of ozone treatment in reclamation technologies.

While writing this book, we spent much of our limited spare time in front of the computer screen or correcting drafts. This was a considerable burden on our families, and in particular on our wives, Ilsabe and Birgit, who had to miss activities that would have been fun to share. We were in the most fortunate situation that despite these sacrifices Ilsabe and Birgit gave us their loving support, which is reflected in the successful termination of this project. We are more than just most thankful for this.

Chapter 2

Physical and chemical properties of ozone

2.1 INTRODUCTORY REMARKS

Schönbein gave ozone its name because of its strong smell (Chapter 1). In his 1854 review, he calculated that ozone should be detectable by its smell at a concentration of 1 ppm (Schönbein, 1854). He also raised the question of why the nose is that sensitive in detecting ozone. One of us (CvS) hypothesises that the receptors in the nose do not record ozone as such but a strongly smelling as yet unknown product formed upon the reaction of ozone with some material contained in the skin. Evidence for this comes from a typical lab experience. When one spills some ozone water on one's hands, they smell like ozone, even after a time, when all the ozone must have evaporated/reacted completely. The smell of iron is due to the formation of unsaturated aldehydes and ketones on the skin which are in contact with iron (Glindemann *et al.*, 2006). Similarly, it might be possible that strongly smelling volatile compounds form when ozone is in contact with skin.

The nose is a most sensitive instrument for warning that some ozone must be in the air with an indicative level of about 15 $\mu g/m^3$ and a clear detection at around 30–40 $\mu g/m^3$ (Cain *et al.*, 2007). However, the sensitivity soon fades away, and one has the impression that ozone is no longer present to the same extent. Thus measures have to be taken *immediately* to ventilate the room and free it from toxic ozone.

The toxicity of ozone has already been described by *Schönbein*, and he mentions that about 2 mg kills a large rabbit (Schönbein, 1854). Prolonged exposures should hence be avoided. The maximum daily allowance in air at work is 200 $\mu g/m^3$ (8-h-value) in most industrialised countries (Rakness, 2005). Information on the human toxicity limits for ozone exposure is available (Kirschner, 1991; Rakness, 2005).

Some physical properties of ozone are compiled in Table 2.1.

Table 2.1 Compilation of some physical properties of ozone

Property	Value
Molecular weight	48 Da
Dipole moment	0.537 Debye
Bond length	1.28 Å

(*Continued*)

Table 2.1 Compilation of some physical properties of ozone (*Continued*)

Property	Value
Bond angle	117°
Melting point	–192.7°C
Boiling point	–110.5°C
Solubility in water at 0°C	2.2×10^{-2} M
Solubility in water at 20°C	1.19×10^{-2} M
Henry constant at 0°C	35 atm M^{-1}
Henry constant at 20°C	100 atm M^{-1}
Explosion threshold	10% Ozone

2.2 GENERATION OF OZONE

Schönbein discovered ozone, when he electrolysed dilute sulfuric acid. Electrolysis of sulfuric acid (20%) with gold or platinum anodes at high current density and cooling may yield oxygen with an ozone content of 4–5%. Yields may be even further increased using a platinum wire anode and by cooling to –14°C.

Electrolysis, albeit with other electrodes and ozone-resistant membranes, continues to be a convenient means for producing ozone in aqueous solution (McKenzie *et al.*, 1997). Such equipment is commercially available, but most commercial ozone generators work on the basis of a silent discharge first developed by *Werner von Siemens* in 1857. Dry air or oxygen (dew point minimum –65°C) may be used. With air, an ozone concentration of 1–5% (by weight) and with oxygen 8–16% may be reached (Rakness, 2005). Depending on pressure and energy of ignition, ozone concentrations >10% can be explosive (Koike *et al.*, 2005). Thus, high-ozone-yield systems have to be operated according to the guidelines of the suppliers. The energy requirement for ozone production is about 12–15 kWh/kg for ozone including oxygen production, transport and destruction (Hollender *et al.*, 2009; Katsoyiannis *et al.*, 2011). Based on this approach to generating ozone, the cost/energy requirements of ozone in technical applications has been evaluated (Ried *et al.*, 2009) and will be discussed in more detail in Chapter 3.

The chemistry in the plasma of the microdischarge columns is quite complex with about 300 reactions that may have to be considered (Eliasson *et al.*, 1987; Okazaki *et al.*, 1988). Under optimised conditions, the major fraction of the energy of the electrons gained in the electric field leads to excited atomic and molecular states of oxygen (feed gases: O_2 and air) and nitrogen (feed gas: air). The excited states of O_2 (O_2^*, $A^3\Sigma_u^+$, $B^3\Sigma_u^-$) dissociate according to reactions (1) and (2) (Kogelschatz *et al.*, 1988; Kogelschatz, 2003).

$$O_2 + e^- \longrightarrow O_2^* + e^- \quad (1)$$

$$O_2^* \longrightarrow 2\,O \quad (2)$$

In this oversimplified scheme, there is no differentiation between triplet O atoms, $O(^3P)$, and singlet O atoms, $O(^1D)$. Since O_2 has a triplet ground state, reaction (3) proceeds only readily with $O(^3P)$ (spin conservation rule). Ozone formation is facilitated through a three-body reaction (3) with M (O_2, O_3, O, or in case of air, N_2) being a collision partner.

$$O + O_2 + M \longrightarrow O_3^* + M \longrightarrow O_3 + M \quad (3)$$

O_3^* is the initial transient excited state of ozone. Ozone formation in reaction (3) is in competition with reactions (4)–(6) which also consume O atoms (Kogelschatz, 2003).

$$O + O + M \longrightarrow O_2 + M \quad (4)$$

$$O + O_3 + M \longrightarrow 2\,O_2 + M \quad (5)$$

$$O + O_3^* + M \longrightarrow 2\,O_2 + M \quad (6)$$

When air is used as the feed gas, several nitrogen species such as N^+, N_2^+, N and excited atomic and molecular species increase the complexity of the reaction system. This leads to the additional reactions (7)–(10), involving nitrogen atoms and excited molecular states of N_2 (A: $^3\Sigma_u^+$, B: $^3\Pi_g$) (Kogelschatz, 2003).

$$N + O_2 \longrightarrow {}^\bullet NO + O \quad (7)$$

$$N + {}^\bullet NO \longrightarrow N_2 + O \quad (8)$$

$$N_2(A) + O_2 \longrightarrow N_2O + O \quad (9)$$

$$N_2(A, B) + O_2 \longrightarrow N_2 + 2\,O \quad (10)$$

Approximately 50% of the ozone formed in air-fed systems is produced from these nitrogen-based processes. Ozone formation through these processes is slower (ca. 100 μs) than in O_2 (10 μs), and a significant part of the electron energy which is lost through collisions with nitrogen molecules can be recovered for ozone formation by reactions (7)–(10) followed by reaction (3) (Kogelschatz, 2003). In addition to reactions (7)–(10), several other nitrogen oxide species, ${}^\bullet NO_2$, ${}^\bullet NO_3$, N_2O_5, are formed that consume ozone [reactions (11)–(14)] (Kogelschatz & Baessler, 1987).

$$ {}^\bullet NO + O_3 \longrightarrow {}^\bullet NO_2^* + O_2 \quad (11)$$

$$ {}^\bullet NO_2^* \longrightarrow {}^\bullet NO_2 + h\nu \quad (12)$$

$$2\,{}^\bullet NO + 3\,O_3 \longrightarrow N_2O_5 + 3\,O_2 \quad (13)$$

$$ {}^\bullet NO_2 + O_3 \longrightarrow {}^\bullet NO_3 + O_2 \quad (14)$$

${}^\bullet NO_2$* is an excited form of ${}^\bullet NO_2$. In typical air-fed ozone generators, ${}^\bullet NO_x$ formation is nearly 2% of ozone formation.

Feed-gases for ozone generators should be dry to avoid undesired effects on ozone generation. The singlet O atom, $O(^1D)$, reacts very quickly with water vapour by insertion [reaction (15)], cf. (Taube, 1957). The thus-formed H_2O_2 retains much vibrational energy and readily decomposes into two ${}^\bullet OH$ radicals [reaction (16)], which induce the decomposition of ozone (Chapter 13).

$$O(^1D) + H_2O \longrightarrow H_2O_2^* \longrightarrow 2\,{}^\bullet OH \quad (15)/(16)$$

Furthermore, ${}^\bullet OH$ radicals react readily with ${}^\bullet NO$ and ${}^\bullet NO_2$ to HNO_2 and HNO_3. N_2O_5 also hydrolyses to HNO_3 in water (Kogelschatz & Baessler, 1987). Therefore, when the air-feed is not dry, formation of nitrous and nitric acids can lead to corrosion of metal parts in ozone generators and tubing (Kaiga *et al.*, 1997).

Even in large-scale ozone generators where typically pure oxygen is used, the presence of nitrogen (1%) has a beneficial effect on ozone generation by increasing the ozone yield compared to pure oxygen owing to the O-forming reactions (7)−(10) (Kogelschatz, 2003).

2.3 OZONE SOLUBILITY IN WATER

Ozone is about ten times more soluble in water than oxygen (Figure 2.1), and this allows one to obtain rather high ozone concentrations by saturating water with an ozone/oxygen mixture from an ozone generator that

is still rich in oxygen. For the solubility of ozone at high ozone concentrations in the gas phase, see Mizuno & Tsuno (2010).

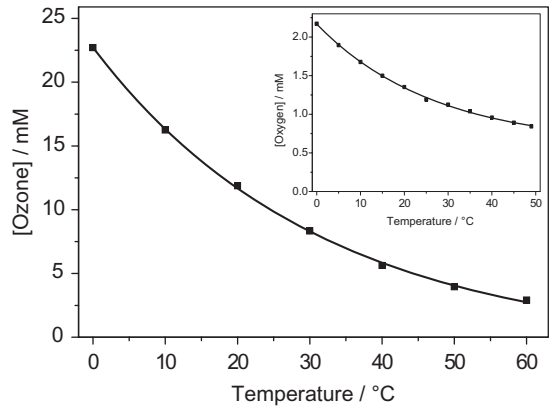

Figure 2.1 Solubility of ozone and oxygen (inset) in water as a function of the temperature for pure gases. The maximum aqueous ozone concentration for a given ozone/oxygen gas mixture can be calculated by Henry's law according to the ozone partial pressure which is achieved by a given ozone generation system.

Ozone solubility strongly depends on temperature. Ozone solubility is about twice as high at 0°C than at room temperature (Figure 2.1). Hence, cooling with ice can be used with advantage when ozone-rich stock solutions are desired. Ozone concentrations then range near 1–1.5 mM as is often required for kinetic studies (Ramseier *et al.*, 2011).

2.4 UV–VIS SPECTRUM OF OZONE

The first absorption band of ozone in aqueous solution is at 590 nm. Its absorption is only weak [$\varepsilon = 5.1 \pm 0.1$ $M^{-1}cm^{-1}$ (Hart *et al.*, 1983)], and this weak absorption in the visible region causes the blue colour of concentrated solutions. The second absorption band is in the UV region, and its maximum centres at 260 nm (Figure 2.2).

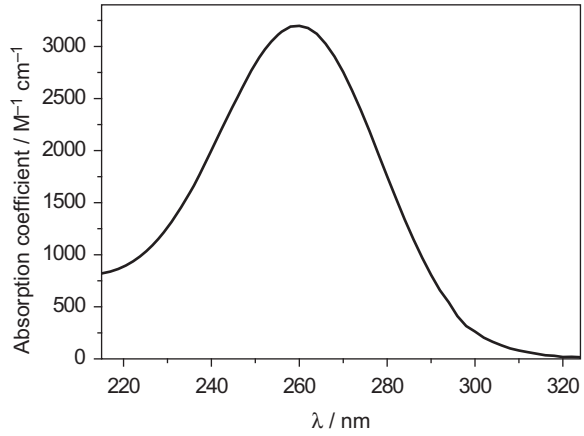

Figure 2.2 Ozone spectrum in the UV region taking a molar absorption coefficient of 3200 $M^{-1}cm^{-1}$ at the maximum (260 nm) (courtesy A. Tekle-Röttering).

Its absorption coefficient at the maximum is a matter of continuing debate. This is not an academic question, as the ozone concentration in water is often determined by measuring the ozone absorption. The difference between the highest and the lowest reported values is about 20% (Table 2.2). This may not seem much, but when a complete material balance is attempted, 20% is non-negligible.

Table 2.2 Molar absorption coefficient of ozone at 255–260 nm in aqueous solution

Molar absorption coefficient/$M^{-1}\,cm^{-1}$	Reference
3600	Taube, 1957
2930 ± 70	Kilpatrick *et al.*, 1956
2000	Boyd *et al.*, 1970
2900	Bader & Hoigné, 1982
3314 ± 70	Forni *et al.*, 1982
2950	Gilbert & Hoigné, 1983
3292 ± 70	Hart *et al.*, 1983
3150	Hoigné, 1998

For two of those (Hoigné, 1998; Forni *et al.*, 1982), no information is given as to how these values have been obtained. Except for the value that was based on the oxidation of Fe^{2+} (Hart *et al.*, 1983), all values were determined by reacting ozone with I^- and measuring the iodine formed. It has been mostly assumed that one mole of ozone produces one mole of iodine according to reactions (17) and (18).

$$O_3 + I^- \longrightarrow IO^- + O_2 \tag{17}$$

$$IO^- + I^- + H_2O \longrightarrow I_2 + 2\,OH^- \tag{18}$$

Yet, a ratio of 1.5 (without explaining the chemistry behind this higher value) has also been given (Boyd *et al.*, 1970); reported ratios range between 0.65 and 1.5 mol/mol (Rakness *et al.*, 1996). Experiments confirming a somewhat higher value have as yet not been carried out, but a speculation may still be at place here. It is recalled that in reaction (17) oxygen is released to some extent as singlet oxygen ($^1O_2$) (Muñoz *et al.*, 2001). I^- reacts moderately fast with $^1O_2$ ($k = 7.2 \times 10^6\,M^{-1}\,s^{-1}$) in competition with a decay to the ground state ($k \approx 3 \times 10^5\,s^{-1}$, in H_2O) (Wilkinson *et al.*, 1995). At an I^- concentration near 4×10^{-2} M about 50% of $^1O_2$ has reacted with I^-. This reaction is reported to lead to I_3^- (Wilkinson *et al.*, 1995). Thus, reaction (19), which gives rise to peroxoiodide ($\Delta G^0 = -11$ kJ mol^{-1}, Naumov and von Sonntag, 2010, unpublished results) may take place.

$$I^- + {}^1O_2 \rightleftarrows IOO^- \tag{19}$$

Peroxoiodide is in equilibrium with its conjugate acid [reaction (20)].

$$IOO^- + H^+ \rightleftarrows IOOH \tag{20}$$

The free acids of this group of compounds have very low O–O BDEs [cf. ONOOH: 92 ± 8.5 kJ mol^{-1} (Brusa *et al.*, 2000)], and undergo rapid homolysis such as reaction (21).

$$IOOH \longrightarrow IO^\bullet + {}^\bullet OH \tag{21}$$

$IO^{\bullet}$ provides three oxidation equivalents and $^{\bullet}OH$ provides one leading to the overall reaction (22).

$$IOO^- + 3\ I^- + 4\ H^+ \longrightarrow 2\ I_2 + 2\ H_2O \quad (22)$$

Reaction (19) is in competition with the reversion of $^1O_2$ to the ground state ($t_{1/2} = 5$ µs in H_2O) and hence its importance should depend on the I^- concentration used in such experiments. Reactions (19) and (20) have to occur only to a small extent to increase the value of the absorption coefficient, as two molecules of iodine are formed per $^1O_2$ reacting according to reaction (22). It is noteworthy, that Hoigné used increasingly higher absorption coefficients as his experience with ozone reactions increased (Table 2.2). There is also some information that may be drawn from the ozonolysis of olefins (Chapter 8). Without steric hindrance by bulky substituents, they give rise to a carbonyl compound and an α-hydroxyalkylhydroperoxide. Taking an absorption coefficient of 3314 M^{-1} cm^{-1}, a material balance (mol product per mol ozone) is obtained with a tendency of an excess of up to 5% (typically less, near 2%, cf. Table 6.3). This seems to indicate that the chosen absorption coefficient may be somewhat on the high side. Correcting for this, the value would come very close to the most recent value chosen by Hoigné, and it is suggested here to use a molar absorption coefficient of 3200 M^{-1} cm^{-1} for the determination of the ozone concentration in water.

2.5 DETERMINATION OF THE OZONE CONCENTRATION

Analytical methods for determining ozone concentrations in water and the gas phase have been reviewed (Gottschalk *et al.*, 2010). The most straightforward method is measuring its absorption at 260 nm (the spectrum near the maximum is relatively broad, and an absorption maximum at 258 nm is also found in the literature. Due to this broadness, measurements at either 260 nm or 258 nm give practically identical results). We suggested above basing such measurements on an absorption coefficient of $\varepsilon(260\ nm) = 3200\ M^{-1}\ cm^{-1}$. It is well suited for the determination of ozone in stock solutions (Ramseier *et al.*, 2011b) and in waters with low UV absorbance [$A(258\ nm) < 1\ m^{-1}$] (Hoigné & Bader, 1994). Such measurements require, however, that there is no other material such as dissolved organic matter (DOM), turbidity and iron that absorb at this wavelength (Hoigné, 1994). For coping with such conditions, assays have been developed that are discussed below (Hoigné & Bader, 1994).

For on-line measurements of ozone, amperometric electrodes without and with membranes can be used (Stanley & Johnson, 1979; Langlais *et al.*, 1991; Rakness, 2005; Gottschalk *et al.*, 2010). Many systems are commercially available and are not discussed any further.

2.5.1 The *N,N*-diethyl-*p*-phenylenediamine (DPD) method

The first studies with *p*-phenylenediamines for the determination of ozone used tolidine as a substrate (Zehender, 1952; Zehender & Stumm, 1953).

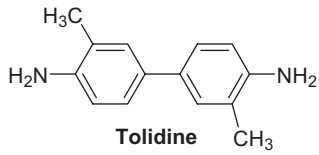

Tolidine

The yellow colour that is formed was measured at 440 nm, but this colour faded away too rapidly, and quenching ozone first with Mn^{2+} in sulfuric acid solution has been suggested. This reaction gives rise to MnO_2 solution (Chapter 12). The subsequent addition of tolidine gave a more stable colour. *p*-Phenylenediamine and its *N*-alkylated derivatives have low reduction potentials. For the parent, a value

of +309 mV and for *N*,*N*,*N*′,*N*′-tetramethyl-*p*-phenylenediamine (TMPD) a value of +266 mV is given (Wardman, 1989). The value for DPD must lie in-between. In its reactions with one-electron oxidants, stable radical cations are formed [reaction (23)]. For TMPD this is commonly known as Wurster's blue. DPD is widely used for the determination of free and combined chlorine in drinking water (Eaton *et al.*, 2005). The DPD radical cation is red and absorbs strongly at 551 nm.

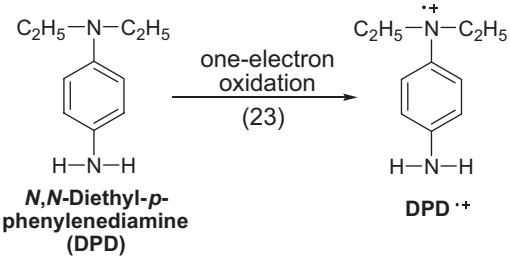

DPD has also been proposed as an agent for the determination of ozone (Gilbert, 1981; Gilbert & Hoffmann-Glewe, 1983; Gilbert & Hoigné, 1983). Based on $\varepsilon_{app}(260\ nm) = 2.950\ M^{-1}\ cm^{-1}$ for ozone, an absorption coefficient of $\varepsilon = 19.900 \pm 400\ M^{-1}\ cm^{-1}$ has been derived (Gilbert & Hoigné, 1983). This value is different from that given for the H_2O_2 assay: $\varepsilon_{app}(551\ nm) = 21.000 \pm 500\ M^{-1}\ cm^{-1}$ (Bader *et al.*, 1988). This difference may be due to an error in the absorption coefficient of ozone (see above) and/or in a more complex reaction.

In the reaction of TMPD with ozone, $^{\bullet}OH$ radicals are generated (via $O_3^{\bullet -}$) in a yield near 70% (Chapter 8, Table 8.4) [reaction (24)].

$$TMPD + O_3 \longrightarrow TMPD^{\bullet +} + O_3^{\bullet -} \qquad (24)$$

Based on the DMSO test for $^{\bullet}OH$ formation (Chapter 14), the $^{\bullet}OH$ yield in the reaction of ozone with DPD is only 23% [Jarocki & von Sonntag (2011), unpublished results], that is, its precursor $O_3^{\bullet -}$ and hence primary $DPD^{\bullet +}$ is also only 23%. A detailed study that would have elucidated other potential reactions giving rise to $DPD^{\bullet +}$ has still to be carried out. From radiation-chemical studies it is known that $^{\bullet}OH$ in its reaction with the stronger reductant TMPD gives rise to $TMPD^{\bullet +}$ (partially via an adduct), and the reduction potential of TMPD is so low that even peroxyl radicals can also undergo this reaction. Rate constants range from 1.1×10^6 to $1.9 \times 10^9\ M^{-1}\ s^{-1}$ depending on the nature of the substituents (Neta *et al.*, 1989; Schuchmann & von Sonntag, 1988). To what extent all this also holds for the less reducing DPD is not yet known. If not, $^{\bullet}OH$ scavenging by the water matrix may lower $DPD^{\bullet +}$ yields.

In Mn(II)-containing waters, the MnO_2 colloids that are formed upon ozonation (Chapter 12) also readily oxidise DPD. This may result in an overestimate of residual ozone concentrations when such waters are assayed by the DPD method. At an extremely high Mn(II) concentration of 8.5 mg/L (154 μM) converted to MnO_2, an ozone equivalent of 1.01 mg/L (21 μM) has been reported (Gilbert, 1981). For more typical Mn(II) concentrations of the order of 1 mg/L, the interference would be much smaller but still mimic an ozone residual. Additionally, the presence of Br^- and its oxidation to HOBr during ozonation (Chapter 10) can result in a false positive ozone residual because HOBr also reacts with DPD (Pinkernell *et al.*, 2000). Similar interferences are observed with the indigo method (see below).

2.5.2 The indigo method

For the quantification of ozone, *Schönbein* developed the indigo method, and in his 1854 review (Schönbein, 1854) he writes at the end of it: "*Um die in einem gegebenen Luftvolumen vorhandene Menge ozonisirten*

Sauerstoffes dem Gewichte nach zu bestimmen, bediene ich mich schon seit Jahren der Indigolösung, und vielfache Versuche haben mich überzeugt, daß dieses Mittel rasch zum Ziele führt; denn mit Hülfe desselben läßt sich der Gehalt einiger Liter Luft an ozonisirtem Sauerstoff in wenigen Minuten bis zu einem kleinen Bruchtheil eines Milligrammes bestimmen, wie sich aus nachstehenden Angaben ergeben wird. – For the determination of the amount per weight of ozonised oxygen in a given volume of air, I have been using a solution of indigo for years, and many experiments have convinced me that this agent leads quickly to the goal; with its help the content of ozonised oxygen can be determined up to a fraction of a milligram within a few minutes, as can be seen from the ensuing description."

The indigo solution that *Schönbein* used has also been sulfonated. At present, the bleaching of indigotrisulfonate by ozone is measured to determine ozone concentrations. As a decrease (base: 100% with a given uncertainty) rather than an increase (base: 0%, no uncertainty) is measured, there is an intrinsic analytical uncertainty. The indigotrisulfonate that is commercially available is a technical product with an unknown purity (possibly near 85%). This material reacts very quickly with ozone, $k = 9.4 \times 10^7\,M^{-1}\,s^{-1}$ (Muñoz & von Sonntag, 2000a). Details of the reaction have not yet been investigated, but if the site of ozone attack is the central C–C double bond, sulfonated isatine and the corresponding α-hydroxyhydroperoxide should be the primary products (Chapter 6). In contrast to the reaction of ozone with DPD, no $^{\bullet}OH$ is generated in the reaction of ozone with indigotrisulfonate [Jarocki & von Sonntag (2011), unpublished results].

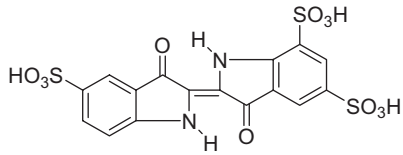

Indigotrisulfonic acid

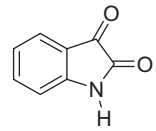

Isatine

The indigo method, now a kind of standard method, is not a primary method, and the extent of bleaching has been based on the molar absorption coefficient of ozone (for its value see above). The purity of the indigo sample, the ozone absorption coefficient and the reaction efficiency thus determine the value of ε(600 nm) to be used for the indigo assay. A value close to 20,000 $M^{-1}\,cm^{-1}$ has been found (Bader & Hoigné, 1982; Muñoz & von Sonntag, 2000a).

Indigotrisulfonate is also readily oxidised by some products that may be generated by ozone with water containing impurities such as Mn(II). The rate constant with the MnO_2 colloids is $k > 10^7\,M^{-1}\,s^{-1}$ and with permanganate, which is also formed to some extent, it is $k = 1.3 \times 10^3\,M^{-1}\,s^{-1}$. The Mn(III) species dominating in acid solution reacts at $2 \times 10^4\,M^{-1}\,s^{-1}$ (Reisz *et al.*, 2008). HOBr may also react with indigo. Currently, the extent of interference is, however, not entirely clear.

The use of indigotrisulfonate for the determination of ozone residual concentrations in drinking water plants has been assessed. Indigo stock solutions are not stable and using solutions that have been standing for several weeks can cause a major underestimate of ozone residual concentrations (Rakness *et al.*, 2010).

2.6 METHODS FOR MEASURING OZONE KINETICS

To measure rate constants for the reaction of ozone with a substrate under first-order conditions, experiments can be performed in excess of ozone or the selected substrate. Typically, a substrate concentration is chosen in excess of ozone (e.g. tenfold), and the ozone decrease is measured as a function of time. Because, the stoichiometry of the ozone–substrate reaction may deviate from 1.0, more than 1 mol of ozone may be consumed per mol of degraded substrate. Therefore, under first-order conditions, the determined rate

constant for the decrease of ozone or the decrease of the substrate may deviate by more than a factor of 3 (e.g. phenol, triclosan and diclofenac, paragraph 2.6.4; monochloramine, Chapter 8). For water treatment, this has to be considered, because in real systems ozone is typically in large excess over the substrate. Thus, the second-order rate constant determined by the decrease of the substrate should be used for the assessment of substrate abatement.

There are several methods for determining the rate constant of ozone with a given compound. The most reliable ones are the direct methods. A larger error may be involved in the method that uses competition kinetics, as there is already an uncertainty, albeit typically small, in the rate constant of the competitor. Direct methods, however, may also have their problems, but these are not as straightforward. In all cases, the determination of rate constants with ozone requires extreme care to avoid reactions with $^{\bullet}OH$, which may be formed during ozonation. Therefore, kinetic measurements should be carried out at low pH, where ozone is more stable and/or in presence of $^{\bullet}OH$ scavengers (Hoigné & Bader, 1983a). Methods based on reactive ozone absorption are not easy to perform and some have led to results not compatible with more straightforward methods (see below) and should be avoided if possible.

2.6.1 Ozone decay measurements

Following ozone decay as a function of time is a direct method and thus possibly the most reliable one. Here, the compound whose rate constant is to be determined is typically present in large excess (e.g. tenfold) over ozone. The other way round, ozone in a large excess over the substrate is also feasible but often not as convenient. Under such conditions, the reaction is kinetically of (pseudo-) first order. For the substrate (**M**) in excess, one may write equations (25) and (26).

$$O_3 + M \longrightarrow P \tag{25}$$

$$\frac{-d[O_3]}{dt} = k_1[O_3] \times [M] \tag{26}$$

As the concentration of **M** does not significantly change during the reaction, [**M**] becomes a constant and equation (26) can be integrated to equation (27).

$$\ln\left(\frac{[O_3]}{[O_3]_0}\right) = -k_1[M] \times t = -k_{obs} \times t \tag{27}$$

A plot of $\ln([O_3]/[O_3]_0)$ vs. the time (t) yields a straight line from the slope of which k_{obs} is calculated and division by [**M**] yields the bimolecular rate constant k_1 (unit: $M^{-1}\,s^{-1}$). The ozone decay can be followed spectrophotometrically at 260 nm. The absorption coefficient of ozone at this wavelength is high (3200 $M^{-1}\,cm^{-1}$; for a discussion see above), but its exact value is not required here as only the absorption ratios are of relevance. Absorption of **M** in the same wavelength region as ozone does usually not affect the determination of the rate constant by this method as the same kinetics are followed even if **M** is bleached or an absorption due to the formation of **P** builds up. Strong absorptions by **M** may impede such measurements. This is typically avoided in the batch quench method (see below).

For low rate constants, kinetics can be followed in a UV-spectrophotometer set at the time-drive mode. A variation of the direct determination of ozone rate constants is the batch quench method. Here, a solution of indigotrisulfonate is added at different times, and the remaining ozone concentration is determined by the bleaching of the indigotrisulfonate (Bader & Hoigné, 1981). Alternatively, the reaction solution is

dispensed into sampling tubes containing indigotrisulfonate, which quenches the residual ozone (Hoigné, Bader, 1994). The reaction of ozone with indigo is so fast [$k = 9.4 \times 10^7\ M^{-1}\ s^{-1}$ (Muñoz, von Sonntag, 2000)] that it occurs practically instantaneously.

For high rate constants, the stopped-flow technique is of advantage. Here, the available time range allows the determination of rate constants near $10^6\ M^{-1}\ s^{-1}$. Alternatively, quench flow techniques can be used, in which the ozone consumption is measured for various predetermined reaction times by quenching the solution with indigotrisulfonate. The bleaching of indigo, a measure for the ozone residual concentration, can then be measured off-line by spectrophotometry. The determination of rate constants with this method is in a similar range as stopped-flow – in the order of 10^5–$10^6\ M^{-1}\ s^{-1}$ (Buffle *et al.*, 2006b). For higher rate constants, methods based on competition kinetics are required.

For dissociating compounds where the base reacts too fast to be monitored, kinetics may be carried out in a more acidic environment. Sufficiently far from the pK_a, the observed rate constant, k_{obs}, drops by one order of magnitude per pH unit as does the concentration of the more reactive base in equilibrium. This allows one to measure the rate of reaction on a convenient timescale. Taking the pK_a of the substrate into account, extrapolation to high pH allows the calculation of the rate constant of the highly reactive base (Hoigné, Bader, 1983b). Typical examples are amines and phenols, where this difference in the rate constants is several orders of magnitude. At lower pH, the poorly reactive conjugate acid (BH^+) is present in excess, but the base (B) dominates the rate of reaction. Under such conditions, the pH-specific rate constant (k_{obs}) can be conveniently determined by equation (28).

$$k_{obs} = k(BH^+) + k(B) \times 10^{(pH - pKa)} \tag{28}$$

2.6.2 Quenching of ozone with buten-3-ol

There may be conditions where spectral interference does not allow following the 260 nm absorption as a function of time and quenching with indigotrisulfonate cannot be used because oxidising species build up during ozonation, the progress of the reaction may then be followed by quenching ozone with buten-3-ol (Chapter 6) and measuring formaldehyde [e.g. spectrophotometrically (Nash, 1953)] generated in a 100% yield according to reaction (29) (Dowideit & von Sonntag, 1998).

$$CH_2{=}CH_2C(OH)HCH_3 + O_3 \longrightarrow CH_2O + H_2O_2 + HC(O)C(OH)HCH_3 \tag{29}$$

2.6.3 Reactive absorption

Ozone rate constants are sometimes also determined by making use of reactive absorption measurements. In a typical setup, 0.5 ml of a solution containing the compound whose rate constant is to be determined is placed in a polystyrene tube (12 mm i.d.) (Kanofsky & Sima, 1995). An ozone/oxygen flow passes 1.2 cm above the solution at 1.25 ml s^{-1}. The difference between the ozone concentration in the gas inlet and outlet is measured, and the fraction of ozone absorbed after 2 min is plotted against the logarithm of the substrate concentration. Such data are evaluated on the basis of the *Reactive Absorption Theory* discussed in detail in the given reference. Another approach has also been described (Utter *et al.*, 1992). In some cases, reliable (supported by more direct methods) rate constants were obtained. This approach has been extended to ozone and substrate uptake measurements in a stirred bubble column (Andreozzi *et al.*, 1996). As long as there is a 1:1 ratio of ozone uptake and substrate disappearance, this approach may also yield acceptable rate constants. But when this prerequisite is not met, the method may fail (typically, values may come out too low). For example, the rate constant of diclofenac by this method gave a value of $1.8 \times 10^4\ M^{-1}\ s^{-1}$ (Vogna *et al.*, 2004), while the more reliable determination by

competition kinetics yielded $6.8 \times 10^5\ M^{-1}\ s^{-1}$ (Sein *et al.*, 2008) (Chapter 8). Therefore, we recommend that, whenever possible, one should stick to more direct methods including determination by competition kinetics. These methods are addressed in the next paragraph.

2.6.4 Competition kinetics

The determination of ozone rate constants of a given compound **M** requires that the ozone rate constant of the competitor **C** is known to a high accuracy, that is, it should have been determined by a reliable direct method.

In competition kinetics, two substrates **M** and the competitor **C** react with ozone [reactions (30), rate constant k_m and (31), rate constant k_c] (Dodd, 2008).

$$M + O_3 \longrightarrow \text{oxidation products of M} \tag{30}$$

$$C + O_3 \longrightarrow \text{oxidation products of C} \tag{31}$$

The relative degradations as a function of the ozone concentration are then given by equation (32).

$$\ln\left(\frac{[M]}{[M]_0}\right) = \ln\left(\frac{[C]}{[C]_0}\right) \times \frac{k_m}{k_c} \tag{32}$$

For this approach, it is required that **M** and **C** are degraded by ozone with the same efficiency, for example, unity efficiency. An efficiency of unity is often found, for example, with olefins (Chapter 6). But, with some aromatic compounds, marked deviations from an efficiency of unity have been reported, for example, phenol [~0.42 (Mvula & von Sonntag, 2003)], triclosan [0.41 (Suarez *et al.*, 2007)] and diclofenac [~0.4 (Sein *et al.*, 2008)] (Chapters 7 and 8). The reasons for such deviations are not yet fully understood. Apparently, there are fast side reactions that compete with the destruction of the substrate. These will continue to occur under the conditions of the competition kinetics as well. Thus, such deviations will result in an under/overestimation of the rate constant when determined according to equation (32). The error will be typically not more than a factor of two or three, and this is often quite acceptable.

The second approach is based on the measurement of just the competitor **C**. While the product of the reaction with **C** can be monitored, the reaction with **M** remains silent. Detection can be by bleaching of **C** or build-up of absorption or by the formation of a specific product due to the formation of **C***.

$$C + O_3 \longrightarrow C^* \text{ (detected)} \tag{33}$$

$$M + O_3 \longrightarrow P \text{ (not detected)} \tag{34}$$

At a given ozone concentration ($[O_3]_0 \ll [\mathbf{M}]$ and $[\mathbf{C}]$) relationship (35) holds ($[\mathbf{C}^*]_0$ is the concentration of **C*** in the absence and $[\mathbf{C}^*]$ in the presence of **M**).

$$\frac{[C^*]}{[C^*]_0} = \frac{k_c[C]}{k_c[C] + k_m[M]} \tag{35}$$

This can be rearranged into equation (36).

$$\frac{[C^*]_0}{[C^*]} = \frac{k_c[C] + k_m[M]}{k_c[C]} = 1 - \frac{k_m[M]}{k_c[C]} \tag{36}$$

Plotting $([\mathbf{C}^*]_0/[\mathbf{C}^*] - 1)$ vs. $[\mathbf{M}]/[\mathbf{C}]$ yields a straight line with a slope of k_m/k_c. Since k_c is known, k_m can be calculated.

Various potential competitors have been discussed (Muñoz & von Sonntag, 2000a). A most convenient one is buten-3-ol. Its solubility in aqueous solution is high, as is its ozone rate constant [$k = 7.9 \times 10^4\ \mathrm{M^{-1}\ s^{-1}}$ (Dowideit & von Sonntag, 1998)]. One of its ozonation products, formaldehyde, can be readily determined (cf. Paragraph 2.6.2). The use of competitors with pH-dependent rate constants, for example, phenol or olefinic acids should be avoided, as a small uncertainty in the pH changes the observed rate constant significantly.

2.7 REDUCTION POTENTIALS OF OZONE AND OTHER OXYGEN SPECIES

The reduction potential of ozone is of relevance, whenever one-electron transfer reactions have to be considered. Although other ozone reactions dominate (e.g. Chapters 6, 7 and 8), one-electron transfer reactions often take place in competition. There are two potential routes, an inner sphere type electron transfer, that is, when an adduct is formed first that subsequently decays into $O_3^{\bullet -}$ and the corresponding radical cation. Alternatively, an outer-sphere electron transfer may take place. The energetics of the latter is given by the reduction potential shown in Table 2.3. Reduction potentials [indicated by (g)] corrected for the solubility of ozone and oxygen can be calculated by equation (37).

Table 2.3 Reduction potentials, $E°$ (vs. NHE) at pH 7 in V at 25°C, of O_2 and water, partially reduced intermediates, ozone, and singlet dioxygen according to (Koppenol *et al.*, 2010). Reduction potentials of gases are based on their saturated solutions, that of other solutes on their 1 M solution. For making reduction potentials comparable with the reduction potentials of solids, such standard reduction potentials [indicated by (g)] were converted in the table to the basis of 1 M according to the solubility of ozone and O_2 (see Figure 2.1)

Reaction	Reduction potential/V
$O_2 + e_{aq}^- \rightleftarrows O_2^{\bullet -}$	−0.18
$O_2(g) + e_{aq}^- \rightleftarrows O_2^{\bullet -}$	−0.35
$^1O_2 + e_{aq}^- \rightleftarrows O_2^{\bullet -}$	+0.81
$^1O_2(g) + e_{aq}^- \rightleftarrows O_2^{\bullet -}$	+0.64
$O_3 + e_{aq}^- \rightleftarrows O_3^{\bullet -}$	+1.03
$O_3(g) + e_{aq}^- \rightleftarrows O_3^{\bullet -}$	+0.91
$O_2^{\bullet -} + e_{aq}^- + 2H^+ \rightleftarrows H_2O_2$	+0.91
$HO_2^{\bullet} + e_{aq}^- + H^+ \rightleftarrows H_2O_2$	+1.05
$O_2 + 2e_{aq}^- + 2H^+ \rightleftarrows H_2O_2$	+0.36
$O_2(g) + 2e_{aq}^- + 2H^+ = H_2O_2$	+0.28
$H_2O_2 + e_{aq}^- + H^+ \rightleftarrows {}^{\bullet}OH + H_2O$	+0.39
$H_2O_2 + 2e_{aq}^- + 2H^+ = 2\ H_2O$	+1.35
$O_2 + 4e_{aq}^- + 4H^+ \rightleftarrows H_2O$	+0.85
$O_2(g) + 4e_{aq}^- + 4H^+ \rightleftarrows H_2O$	+0.81
$^{\bullet}OH + e_{aq}^- + H^+ \rightleftarrows H_2O$	+2.31

$$E = E^0 - 0.059 \log[\text{red}]/[\text{ox}] \quad (37)$$

For O_2 reduction to $O_2^{\bullet -}$ ($[O_2] \approx 1.2$ mM) this leads to equations (38)–(40).

$$E = E^0 - 0.059 \log[O_2^{\bullet -}]/[O_2] = E^0 + 0.059 \log[O_2] - 0.059 \log[O_2^{\bullet -}] \quad (38)$$

$$E = -0.18 - 0.059 \times 2.92 - 0.059 \log[O_2^{\bullet -}] \quad (39)$$

$$E = -0.35 - 0.059 \log[O_2^{\bullet -}] \text{ (i.e., } E^0[O_2]/[O_2^{\bullet -}] = -0.35\text{V for a saturated oxygen solution)} \quad (40)$$

2.8 STABILITY OF OZONE SOLUTIONS

Aqueous ozone solutions are unstable. Many effects contribute to this instability, but not all of them are fully elucidated. In basic solutions, ozone is especially unstable. This is due to the formation of $^{\bullet}OH$ by OH^- (Chapter 11) and the reaction of $^{\bullet}OH$ with ozone (Chapter 13). This reaction proceeds even in neutral solutions, where the OH^- concentration is very low (1×10^{-7} M). Acidification and the addition of $^{\bullet}OH$ scavengers such as bicarbonate further increase the ozone stability in aqueous solutions. In acid solutions and at 31°C, the rate constant of ozone decomposition has been reported at 3×10^{-6} s^{-1} ($E_a = 82.5 \pm 8.0$ kJ mol^{-1}) (Sehested *et al.*, 1992). Mechanistic details of the 'spontaneous decomposition' are not yet fully understood.

In natural waters, the dissolved organic matter (DOM) contributes significantly to ozone decay, and waters that have a low DOM and high bicarbonate content show relatively high ozone stability (Chapter 3), which is of relevance for the disinfection efficiency of ozone (Chapter 4).

2.9 REACTIVITY OF OZONE

In micropollutant abatement, for example, the reactivity of a micropollutant determines the efficiency of its elimination by an ozone treatment. Ozone rate constants may vary 8–10 orders of magnitude even within one group of compounds. Cases in point are olefins (Chapter 6) and aromatic compounds (Chapter 7) and also compounds which carry C–H functions as only ozone-reactive sites (Chapter 10). In general, ozone rate constants depend on temperature, but there are only very few cases, where details have been measured. The temperature dependence of the second order rate constants can be expressed by the Arrhenius equation [A: pre-exponential factor, E_a: Activation energy, R: Universal gas constant, T: absolute temperature (K)] (41).

$$k = \text{A} \times e^{-\frac{E_a}{RT}} \quad (41)$$

To determine the parameters A and E_a, equation (41) can be logarithmised, yielding equation (42).

$$\log k = \log A - \frac{1}{2.3}\frac{E_a}{RT} \quad (42)$$

A plot of $\log k$ versus $1/T$ allows the determination of $\log A$ and E_a. Available data are compiled in Table 2.4 and some plots are shown in Chapters 9 and 10.

All these compounds react only slowly with ozone. For the more reactive ones, much lower activation energies are expected and hence the temperature dependence of the rate constants will be less pronounced.

There may be a dramatic effect of pH when the site of ozone attack can be deprotonated/protonated, such as in the case of phenols/amines or inorganic ions (Chapters 7, 8, 11and 12).

Table 2.4 Compilation of available reaction parameters (rate constants at 20°C) for ozone reactions in aqueous solution

Compound	$k/M^{-1}s^{-1}$	log A	E_a/kJ mol^{-1}	Reference
Cl^-	1.4×10^{-3}	10.3	74	Yeatts & Taube, 1949
Br^-	160	8.8	37	Haag & Hoigné, 1983a
ClO^-	35	12.2	59.8	Haag & Hoigné, 1983b
BrO^-	505	13.4	60	Haag & Hoigné, 1983a
$(CH_3)_2SO$	1.8	11.5	63.1	Reisz & von Sonntag, 2011*
H_2O_2	0.036	11.5	73.5	Sehested *et al.*, 1992
$HC(O)O^-$	82	10.9	50.3	Reisz & von Sonntag, 2011*
$HC(O)O^-$	46**	11.4	54.6	Reisz & von Sonntag, 2011*
$HC(CH_3)_2OH$	0.83	12.5	70.7	Reisz & von Sonntag, 2011*
$(CH_3)_3COH$	0.0011	9.3	68.7	Reisz & von Sonntag, 2011*

*Reisz & von Sonntag, 2011 (unpublished results)
**In the presence of tBuOH

2.9.1 pH dependence of ozone reactions and the "reactivity p*K*"

Whenever ozone reacts with a compound that can be present in different protonation states, there will be a pH dependence of the rate constant. When deprotonated, the electron density within a given molecule is higher, and due to the electrophilicity of ozone the rate constant for the reaction with ozone is also higher. The magnitude of this pH effect strongly depends on the type of ozone reaction. With amines, for example, where ozone adds to the lone pair at nitrogen, the high reactivity of the free amine (in the order of $10^6\,M^{-1}\,s^{-1}$) drops to nearly zero when this reaction site is blocked upon protonation or is significantly lowered by complexation with a transition metal ion (Chapter 8). With phenols, on the other hand, there is already a marked activation of the aromatic ring by the OH group ($k = 1.3 \times 10^3\,M^{-1}\,s^{-1}$). This is, however, strongly increased upon deprotonation of the phenol, resulting in a rate constant of $1.4 \times 10^9\,M^{-1}\,s^{-1}$ for the phenolate ion (Chapter 7). In olefinic acids the anion supplies some additional electron density to the C–C double bond, and in acrylic acid, for example, the rate constant of the free acid is $k = 2.8 \times 10^4\,M^{-1}\,s^{-1}$, while that of the anion is $1.6 \times 10^5\,M^{-1}\,s^{-1}$ (Chapter 6). This is only a factor of 5.7, while deprotonation of phenol increases the rate constant by a factor of about one million. Quantum-chemical calculations discussed in Chapter 7 can account for this dramatic difference.

pH effects are not restricted to organic compounds but are also observed with inorganic compounds. A case in point is As(III). With $As(OH)_3$, ozone reacts with $5.5 \times 10^5\,M^{-1}\,s^{-1}$, while $As(OH)_2O^-$ reacts with $1.8 \times 10^8\,M^{-1}\,s^{-1}$ (Chapter 12). Similarly, HS^- reacts five orders of magnitude faster than H_2S (Chapter 11).

Such differences in the rate constants may result in marked effects on product distribution as a function of pH, which does not follow the pK_a of the starting material. This effect has been termed "reactivity p*K*".

If compound **MH** is an acid that is in equilibrium with its anion $\mathbf{M}^-$ [equilibrium (43)], it reacts with ozone according to equation (44), where α is the degree of dissociation and $k(O_3{+}\mathbf{MH})$ and $k(O_3{+}\mathbf{M}^-)$ are the ozone rate constants of **M** and $\mathbf{M}^-$, respectively.

$$MH \rightleftarrows M^- + H^+ \tag{43}$$

$$d[MH]_{total}/dt = (\alpha \times k(O_3 + MH) + (1 - \alpha)\ k(O_3 + M^-)) \times [MH]_{total} \times [O_3] \tag{44}$$

The degree of dissociation (α) can be calculated on the basis of the dissociation constant (K) and the pH [equation (45)].

$$\alpha = 1/(1 + K/[H^+]) \tag{45}$$

The situation for phenol is shown in Figure 2.3. On the basis of the above rate constants, a reactivity pK_a of 4 is calculated. This means that despite the fact that phenol has a pK_a of 10, a predominant reaction of ozone with the neutral form will only occur below pH 4.

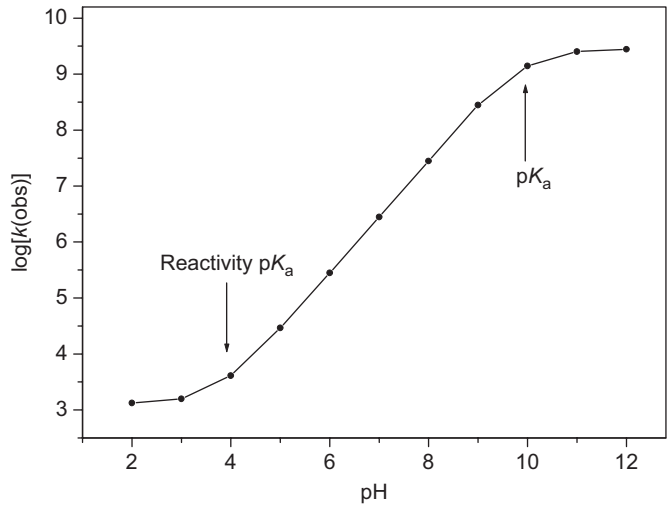

Figure 2.3 Plot of the logarithm of the observed rate constant of the reaction of phenol with ozone as a function of pH. pK_a(phenol) and its reactivity pK_a are indicated by arrows.

2.9.2 Multiple reaction sites within one molecule

There may be different ozone-reactive sites within a molecule such as an aromatic ring and an aliphatic amino group. This situation is found in some pharmaceuticals such as in the beta blocker metoprolol. For other compounds with multiple sites of attack, the situation may become more complicated.

In metoprolol, a compound containing an amino group and an aromatic ring (for its structure see Chapter 8), the amino group loses its ozone reactivity upon protonation. Thus at low pH, the overall reactivity will only be due to the rate constant of the aromatic ring [in the case of metoprolol: k(metoprolol–H^+) = $330\ M^{-1}\ s^{-1}$, (Benner *et al.*, 2008)], while at high pH the ozone reactivity is determined by the reaction of the free amine [pK_a(metoprolol) = 9.7; k(metoprolol) = $8.6 \times 10^5\ M^{-1}\ s^{-1}$ (Benner *et al.*, 2008)]. The percentage of ozone reacting with the free amine in equilibrium as a function of pH is shown in Figure 2.4.

The pH at which the two reaction sites, aromatic ring and amino group, react equally fast is again a kind of "reactivity pK". Due to the much higher rate constant of the free amine, the reactivity pK of metoprolol is much lower than its pK_a value. The reactivity pK for metoprolol (Meto) is calculated at 6.3 on the basis of equations (46–52).

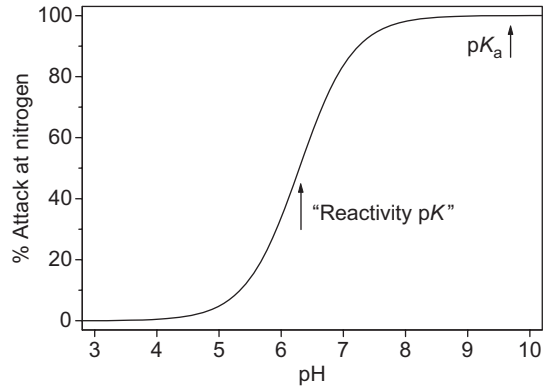

Figure 2.4 Reaction of ozone with metoprolol (p$K_a = 9.7$). Percentage of ozone attack at nitrogen as a function of the pH. The "reactivity pK" is at 6.3.

$$k(\text{Meto} - \text{H}^+) \times [\text{Meto} - \text{H}^+] = k(\text{Meto}) \times [\text{Meto}] \quad (46)$$

$$[\text{Meto}] = [\text{Meto}]_{\text{total}} \times K_a/(K_a + [\text{H}^+] \quad (47)$$

$$[\text{Meto} - \text{H}^+] = [\text{Meto}]_{\text{total}} \times [\text{H}^+]/(K_a + [\text{H}^+]) \quad (48)$$

$$k(\text{Meto} - \text{H}^+) \times [\text{Meto}]_{\text{total}} \times [\text{H}^+]/(K_a + [\text{H}^+]) = k(\text{Meto}) \times [\text{Meto}]_{\text{total}} \times K_a/(K_a + [\text{H}^+]) \quad (49)$$

$$k(\text{Meto} - \text{H}^+) \times [\text{H}^+] = k(\text{Meto}) \times K_a \quad (50)$$

$$\log\left[(k(\text{Meto} - \text{H}^+))\right] - \text{pH} = \log[k(\text{Meto})] - \text{p}K_a \quad (51)$$

$$\text{"reactivity p}K\text{"} = \text{p}K_a - \log[k(\text{Meto})] + \log\left[k\left(\text{Meto} - \text{H}^+\right)\right] \quad (52)$$

This is of a practical consequence for the formation of transformation products. In wastewater that has typically a pH of 7–8, metoprolol is almost entirely degraded via a reaction of ozone at the amino group despite the fact that the pK_a of protonated metoprolol is 9.7. Therefore, under these conditions, mainly transformation products resulting from an ozone attack on the amino group will be formed.

Chapter 3

Ozone kinetics in drinking water and wastewater

3.1 STABILITY OF OZONE IN VARIOUS WATER SOURCES

The stability of ozone in drinking water and in wastewater is largely determined by its reaction with the dissolved organic matter (DOM). The nature of DOM varies among waters of different origin as does its concentration. For example, in drinking waters, DOM, measured as DOC, is typically below 4 mg/L, while in wastewaters it ranges between 5 and 20 mg/L. The nature of DOM has an influence on the rate of its reaction with ozone and thus on the ozone lifetime in these natural waters, drinking waters and wastewaters. Carbonate alkalinity influences ozone stability by scavenging $^{\bullet}OH$ (see below). This is of major importance, as the two desired effects of ozone, disinfection and micropollutant abatement, depend on the lifetime of ozone in these waters (see below). Therefore, it will be necessary to discuss the properties of aquatic DOM as much as they are known today and then discuss the lifetime of ozone in different waters.

An aspect of considerable consequence in this context is $^{\bullet}OH$ production, resulting from a side reaction of ozone with DOM. The $^{\bullet}OH$ radical is an important intermediate in the decomposition of ozone in water (Hoigné & Bader, 1975). In a study on wastewater that may be generalised on this point to other DOMs as well, it has been suggested that ozone reacts with the electron-rich aromatic components of DOM by electron transfer [reaction (1)] (Nöthe *et al*., 2009; Pocostales *et al*., 2010).

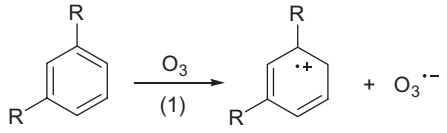

DOM model

The $O_3^{\bullet-}$ radical gives rise to $^{\bullet}OH$ [reactions (2) and (3)] (Merényi *et al*., 2010a) (Chapter 11).

$$O_3^{\bullet-} \rightleftarrows O_2 + O^{\bullet-} \quad (2)$$

$$O^{\bullet-} + H_2O \rightleftarrows {}^{\bullet}OH + OH^- \quad (3)$$

Production of $^{\bullet}OH$ does not cease when the electron-rich aromatics present in DOM have reacted with ozone (Nöthe *et al*., 2009). Hence, new electron-rich sites must be created upon the action of ozone. A

typical reaction of ozone with aromatic compounds is hydroxylation, and it has been suggested that phenols thus formed are responsible for the continuing $^{\bullet}OH$ production (Nöthe *et al.*, 2009). In this context, it may be recalled that ozone adducts to aromatic compounds [reaction (4)] can eliminate singlet oxygen [$^1O_2$, reaction (5)], and the resulting zwitterion rearranges into phenol [reaction (6)] (Mvula *et al.*, 2009) (cf. Chapter 7).

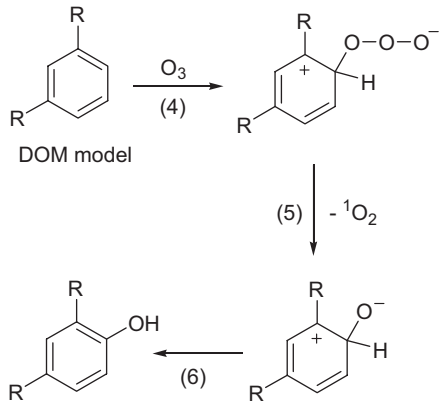

Phenols belong to the group of electron-rich aromatics that undergo electron transfer to ozone, cf. reaction (1) (Mvula & von Sonntag, 2003) and thus are capable of continuing $^{\bullet}OH$ production according to reactions (2) and (3). Moreover, $^{\bullet}OH$ adds to aromatic compounds of DOM [reaction (7)].

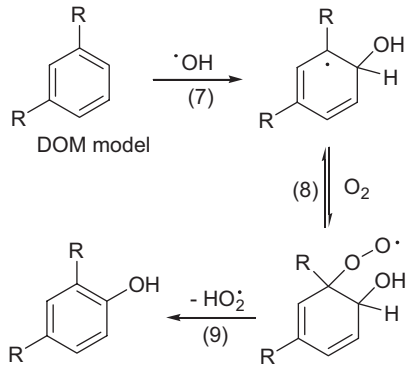

In the presence of O_2 (available at high concentrations during ozonation), the thus-formed hydroxycylohexadienyl radicals are in equilibrium with the corresponding peroxyl radicals [equilibrium (8)], which eliminate $HO_2^{\bullet}$ (in competition with other reactions) (Pan *et al.*, 1993; Fang *et al.*, 1995; Naumov & von Sonntag, 2005) [reaction (9)]. In wastewater but also in drinking water, $HO_2^{\bullet}$ is deprotonated to $O_2^{\bullet-}$ [equilibrium (10), $pK_a(HO_2^{\bullet}) = 4.8$ (Bielski *et al.*, 1985)], and the latter reacts rapidly with ozone [reaction (11)] (Chapter 13). There are indications of the formation of $O_2^{\bullet-}$ in the reaction of ozone with DOM [cf. reaction (9) and (10)] (Staehelin & Hoigné, 1982).

$$HO_2^{\bullet} \rightleftarrows O_2^{\bullet-} + H^+ \quad (10)$$

$$O_2^{\bullet-} + O_3 \longrightarrow O_2 + O_3^{\bullet-} \quad (11)$$

In these reactions, the aromatic DOM subunits are not yet mineralised but only hydroxylated. This is the likely reason why •OH generation does not cease during ozonation even at elevated ozone doses. In addition, other moieties of DOM such as aliphatic C—H bonds also lead to superoxide and eventually •OH through the above reactions (see below and Chapter 14). These reactions also apply to DOM in drinking waters.

Figure 3.1 shows the ozone stability in five Swiss waters with various compositions (DOC and alkalinity).

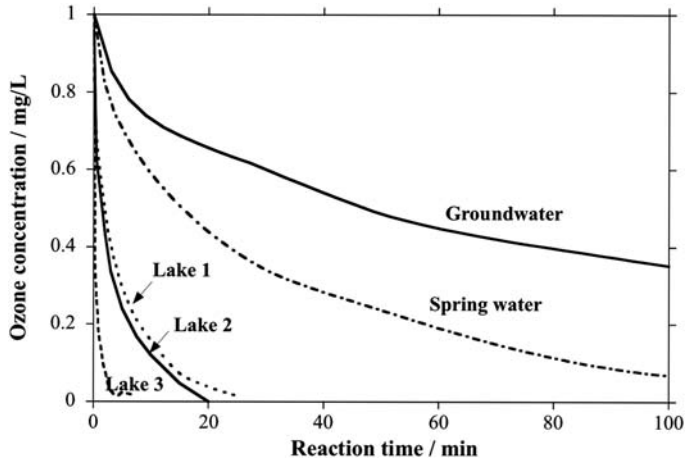

Figure 3.1 Stability of ozone in various Swiss natural waters at pH 8 and 15°C (ozone dose 1 mg/L). Water quality data: Groundwater (DOC 0.7 mg/L, carbonate alkalinity 6.7 mM); Spring water (DOC 0.9 mg/L, carbonate alkalinity 5.4 mM); Lake 1 (DOC 1.3 mg/L, carbonate alkalinity 2.5 mM); Lake 2 (DOC 1.6 mg/L, carbonate alkalinity 3.6 mM); Lake 3 (DOC 3.2 mg/L, carbonate alkalinity 3.4 mM). From Urfer *et al.*, 2001 with permission.

At pH 8, ozone stability decreases in the sequence groundwater > spring water > lake water 1, 2 > lake water 3. This corresponds to an increasing trend in DOC concentration and a decreasing trend in alkalinity. Ozone has a very similar stability in lake waters 1 and 2, even though the DOC is higher in lake water 2. Carbonate alkalinity which has a stabilising effect on ozone is, however, higher in lake water 2. The effect of carbonate alkalinity has been systematically tested in Lake Zurich water, by varying the carbonate/bicarbonate concentration from 0 to 2.5 mM at pH 8. While keeping the DOC constant, an increase in carbonate alkalinity leads to a significantly lower rate of ozone decomposition (Elovitz *et al.*, 2000a).

In a survey of eleven DOM isolates, a hundredfold variation of the approximate pseudo-first-order rate constant, k_{DOC}, for the ozone decrease was observed for synthetic waters containing 2 mg/L of the DOM isolate and 2.5 mM HCO_3^- at pH 7 (Figure 3.2) (Elovitz *et al.*, 2000b). This figure shows that Suwannee River fulvic and especially humic acids are outliers and do not represent ozone consumption kinetics of typical DOM in surface waters. Therefore, results from the wide application of these sources of organic matter to simulate drinking water ozonation have to be interpreted with caution and do not allow generalisations on other water sources.

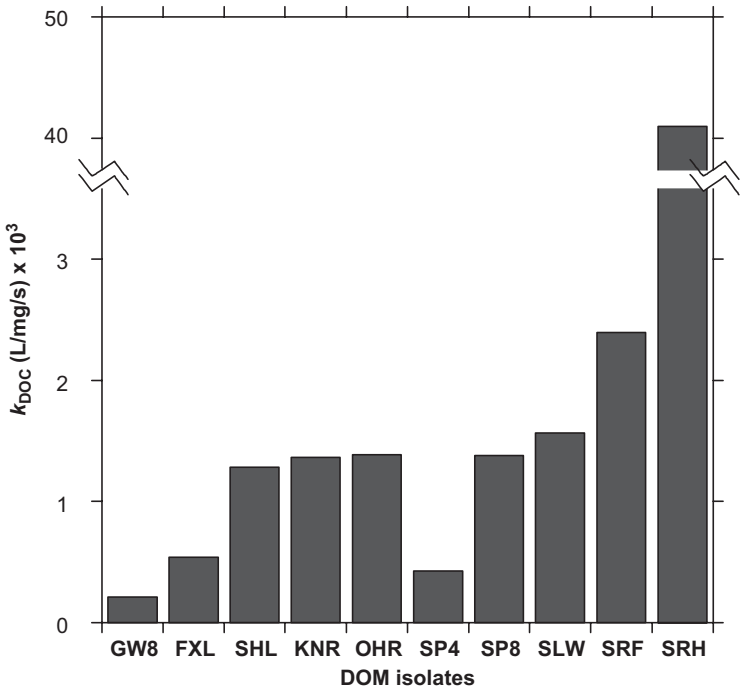

Figure 3.2 First-order rate constants of ozone decomposition (k_{DOC}) in model waters containing ≅ 2 mg/L DOC, 2.5 mM HCO_3^- at pH 7. DOM isolates XAD-8: GW8, Groundwater Minnesota, USA; FXL, Lake Fryxell, Antarctica; SHL, Lake Shingobee, Minnesota; KNR, Yakima River, Washington; OHR, Ohio River, Ohio; SP8, California State Project Water, California; SLW, Silver Lake, Colorado. DOM isolate XAD-4: SP4, California State Project Water, California. SRF and SRH: Suwannee River, Georgia fulvic and humic acid, respectively. Reprinted with permission from Elovitz *et al.*, 2000b. Copyright (2000) American Chemical Society.

The role of DOM and alkalinity for ozone stability can be explained by (i) the direct reaction of DOM with ozone and (ii) $^{\bullet}$OH scavenging by DOM and carbonate/bicarbonate. Whereas the type of DOM is highly relevant for ozone reactions, it is of minor importance for $^{\bullet}$OH scavenging. Second order rate constants for the reaction of various DOM sources with $^{\bullet}$OH are reported to vary within about a factor of two with an average value of $(2.3 \pm 0.77) \times 10^4$ $(\text{mgC/L})^{-1}\,\text{s}^{-1}$ (Brezonik & Fulkerson-Brekken, 1988; Reisz *et al.*, 2003). This value is very close to a more recent study with DOM isolates with an average value of 1.9×10^4 $(\text{mgC/L})^{-1}\,\text{s}^{-1}$ (Westerhoff *et al.*, 2007). The DOM isolate with the highest rate constant is a wastewater [3.9×10^4 $(\text{mgC/L})^{-1}\,\text{s}^{-1}$] which might have significantly different properties, that is, less coiling and a higher fraction of the carbon available for reaction with $^{\bullet}$OH compared to natural DOM sources. In other wastewater studies, values of 3×10^4 $(\text{mgC/L})^{-1}\,\text{s}^{-1}$ and 3.5×10^4 $(\text{mgC/L})^{-1}\,\text{s}^{-1}$ were found (Nöthe *et al.*, 2009; Katsoyiannis *et al.*, 2011).

The scavenging of $^{\bullet}$OH by DOM and bicarbonate has different effects on ozone stability. Note that at the typical pH values of drinking water and wastewater (pH ≤ 8.5) the contribution of $^{\bullet}$OH scavenging by carbonate is smaller despite the fact that the rate constant of carbonate with $^{\bullet}$OH ($k = 3.9 \times 10^8\ \text{M}^{-1}\,\text{s}^{-1}$) is higher than that of bicarbonate ($k = 8.5 \times 10^6\ \text{M}^{-1}\,\text{s}^{-1}$). The reason for this is the high pK_a of

bicarbonate [$pK_a(HCO_3^-) = 10.3$; the corresponding reactivity pK (cf. Chapter 2) is 8.6]. The reaction of $^\bullet OH$ with bicarbonate leads to carbonate radicals, $CO_3^{\bullet-}$ [reaction (15); $pK_a(HCO_3^\bullet) < 0$ (Czapski *et al.*, 1999)], Part of the $^\bullet OH$ reaction with DOM leads to $O_2^{\bullet-}$ (see above), and $O_2^{\bullet-}$ reacts quickly with ozone to $^\bullet OH$, whereas $CO_3^{\bullet-}$ further reacts by self-reaction [reaction (16)] and with DOM [Suwannee River Fulvic acid, $k = 280 \pm 90$ (mg of C/L)$^{-1}$ s^{-1} (Canonica *et al.*, 2005)].

Because of the fast reaction of $O_2^{\bullet-}$ with ozone, leading to $^\bullet OH$ (Chapter 13), this pathway leads to a destabilisation of ozone. Hoigné introduced the concept of "promoter" and "inhibitor" for compounds that accelerate or reduce the rate of ozone decay (Staehelin & Hoigné, 1985). This concept, often cited in the literature and repeated like a prayer wheel, is sometimes misunderstood, and it seems to be helpful to discuss it here in some detail. A typical promoter is methanol at pH 8. The reaction may be induced by the slow reaction of ozone with methanol, which may generate $^\bullet CH_2OH$ radicals (cf. Chapter 10). These react readily with O_2 present in excess [reaction (12)]. The resulting peroxyl radical can eliminate $HO_2^{\bullet-}$, but this reaction is slow ($k < 3$ s^{-1}) (Rabani *et al.*, 1974). At pH 8, the OH^- concentration is 1×10^{-6} M. OH^- induces an $O_2^{\bullet-}$ elimination with a bimolecular rate constant close to 1.8×10^{10} M^{-1} s^{-1} (Rabani *et al.*, 1974). Thus at pH 8, the rate of $O_2^{\bullet-}$ formation is near 1×10^4 s^{-1} [reaction (12)–(14), for details see Chapter 14].

$$^\bullet CH_2OH + O_2 \longrightarrow {}^\bullet OOCH_2OH \quad (12)$$

$$^\bullet OOCH_2OH \longrightarrow CH_2O + HO_2^\bullet \quad (13)$$

$$^\bullet OOCH_2OH + OH^- \longrightarrow CH_2O + H_2O + O_2^{\bullet-} \quad (14)$$

The product of reaction (16) gives rise to percarbonate upon hydrolysis. This sequence induces a very efficient chain reaction, that is, ozone decay is promoted. Scavenging of $^\bullet OH$ by bicarbonate [reactions (15) and (16), $2k_{16} = 1.25 \times 10^7$ M^{-1}s^{-1} (Weeks & Rabani, 1966)] or carbonate, interrupts the chain and enhances the lifetime of ozone. It acts as an inhibitor.

$$HCO_3^- + {}^\bullet OH \longrightarrow CO_3^{\bullet-} + H_2O \quad (15)$$

$$2\ CO_3^{\bullet-} \longrightarrow (CO_3^-)_2 \text{ (precursor of percarbonate)} \quad (16)$$

The formation of percarbonate according to reaction (16) deserves a note. Percarbonate is in equilibrium with H_2O_2 and bicarbonate (Richardson *et al.*, 2000), and is a stronger oxidant than H_2O_2 (Bennett *et al.*, 2001; Yao & Richardson, 2000). It has been suggested as a suitable agent for pollution control, at least in a limited number of cases (Xu *et al.*, 2011).

Other $^\bullet OH$ scavengers such as tertiary butanol (tBuOH) and acetate also interrupt the chain, although some $O_2^{\bullet-}$ is also formed in the bimolecular decay of their peroxyl radicals [for tBuOH see Schuchmann & von Sonntag (1979), details in Chapter 14, for acetate see Schuchmann *et al.*, (1985)], the dominant decay routes do not give rise to $O_2^{\bullet-}$. Thus, these compounds also act effectively as inhibitors, although with a small promoting contribution. Other organic compounds act in a similar way, promoting and inhibiting as well. A case in point is DOM as discussed above. Thus, a careful look at the concept of "promoter" and "inhibitor" is required, and its discussion should take into consideration the advantages and the limitations of this approach.

To mimic the interaction between DOM moieties leading to $O_2^{\bullet-}$ formation and components (promoters) that scavenge $^\bullet OH$ without further reaction with ozone (inhibitors), ozone stability was investigated in a synthetic system containing methanol which releases $O_2^{\bullet-}$ after H-abstraction by $^\bullet OH$ and oxygen addition and either acetate, tBuOH or bicarbonate, which do not react further with ozone (Elovitz & von Gunten, 1999).

Table 3.1 shows the results for the synthetic systems at pH 8. For a methanol concentration of 70 µM (scavenging rate $k(^\bullet OH + MeOH) \times [MeOH] = 7 \times 10^4$ s^{-1}), the pseudo-first-order rate constant for ozone decrease k_d is very similar for all scavengers, which act as inhibitors in this case.

Table 3.1 Pseudo first-order rate constants for ozone decomposition (k_d) and calculated R_{ct} values for model systems containing 70 µM methanol and the inhibitors acetate, tertiary butanol (tBuOH) and bicarbonate at pH 8 [according to Elovitz & von Gunten, 1999]

Inhibitor S	Conc./µM	$k(^{\bullet}OH + [S]) \times [S]/s^{-1}$	k_d (s^{-1})	R_{ct}
None	–	–	$\sim 1.4 \times 10^{-2}$	–
Acetate	350	2.8×10^{4}	1.9×10^{-3}	1.4×10^{-8}
tBuOH	46	2.7×10^{4}	1.9×10^{-3}	1.3×10^{-8}
HCO_3^-	2600	2.7×10^{4}	2.4×10^{-3}	1.9×10^{-8}

This shows that the interplay between promotion and inhibition of ozone decomposition is independent of the inhibitor and leads to similar ozone stability. Furthermore, the R_{ct}, the ratio between the concentrations of $^{\bullet}OH$ and ozone also is very similar in the range of $(1.3–1.9) \times 10^{-8}$ (see below). Due to their high reactivity towards the water matrix and ozone, $^{\bullet}OH$ radicals have very low steady-state concentrations during ozonation, typically below 10^{-12} M. Because direct measurement of $^{\bullet}OH$ concentrations during ozonation is impossible, there are basically two ways to tackle this problem: (i) Modelling ozone decay and thereby calculating the $^{\bullet}OH$ concentrations (Chelkowska *et al*., 1992; Westerhoff *et al*., 1997). The application of these models to natural waters is difficult due to the varying reactivity of DOM (see above). Usually, some rate constants have to be fitted to mimic kinetics of ozone decay in real water systems (Chelkowska *et al*., 1992; Westerhoff *et al*., 1997). Therefore, model predictions for transient $^{\bullet}OH$ concentrations generally disagree with experimental observations. (ii) Experimental calibration of $^{\bullet}OH$ formation by ozone in natural waters with the help of an ozone-resistant probe (Hoigné & Bader, 1979; Elovitz & von Gunten, 1999; Haag & Yao, 1992; Haag & Yao, 1993). Here, the decrease of an added probe (in low concentrations, ≤ 1 µM) which does not react with ozone but reacts quickly with $^{\bullet}OH$ is measured either as a function of the ozone dose (Hoigné & Bader, 1979) or continuously during ozonation (Elovitz & von Gunten, 1999; Haag & Yao, 1992; Haag & Yao, 1993). The first approach leads to the integral $^{\bullet}OH$ exposure and the corresponding ozone dose required for eliminating a particular compound to a certain percentage. The latter approach yields information on the dynamics of the oxidation by ozone and $^{\bullet}OH$. Haag & Yao (1993) used continuous ozonation experiments for arriving at steady-state concentrations of $^{\bullet}OH$. Part of the scavenging capacity of DOM was lost during these experiments and the mean steady-state concentration of $^{\bullet}OH$ became very high, resulting in a ratio of the concentrations of $^{\bullet}OH$ and O_3 of about 10^{-7}. In single ozone dosage experiments, ratios in the order of 10^{-8}–10^{-9} were obtained (Elovitz & von Gunten, 1999). Such ratios are more typical for ozonation and ozone-based AOPs under more realistic conditions.

The kinetics of the decrease of a probe (e.g. *p*-chlorobenzoic acid, pCBA) can be expressed as follows [equations (17) and (18)] (Elovitz & von Gunten, 1999).

$$-\frac{d[\text{pCBA}]}{dt} = k(^{\bullet}\text{OH} + \text{pCBA}) \times [\text{pCBA}][^{\bullet}\text{OH}] \tag{17}$$

Rearranging and integrating equation (17) leads to equation (18).

$$-\ln\left(\frac{[\text{pCBA}]}{[\text{pCBA}]_0}\right) = k(^{\bullet}\text{OH} + \text{pCBA}) \times \int [^{\bullet}\text{OH}]\, dt \tag{18}$$

The term $\int [^{\bullet}OH]dt$ represents the time-integrated concentration of $^{\bullet}OH$, which is equal to $^{\bullet}OH$ exposure or $^{\bullet}OH$-ct. The $^{\bullet}OH$ exposure can therefore be determined by measuring the relative decrease of, for example, pCBA as a function of the reaction time. The term R_{ct} defined in equation (19) describes the ratio of $^{\bullet}OH$ exposure to ozone exposure (or $^{\bullet}OH$-ct and O_3-ct) (Elovitz & von Gunten, 1999).

$$R_{ct} = \frac{\int [^{\bullet}OH]\, dt}{\int [O_3]\, dt} \tag{19}$$

Substitution of equation (19) into equation (18) results in equation (20).

$$-\ln\left(\frac{[pCBA]}{[pCBA]_0}\right) = k(^{\bullet}OH + pCBA) \times R_{ct} \int [O_3]\, dt \tag{20}$$

Ozone exposure can be calculated from the integral of "ozone concentration versus time data" (von Gunten & Hoigné, 1994).

For many natural waters, a plot of the logarithm of the relative decrease of pCBA vs. ozone exposure showed basically two phases for which fairly good linear correlations of the two parameters were obtained (Elovitz *et al*., 2000a, b). This is quite similar to the behaviour of ozone (see below). This means that the ratio R_{ct} of the exposures (*ct* values) of $^{\bullet}OH$ and ozone remains constant, and for these conditions the ratio of the concentrations of $^{\bullet}OH$ and ozone ($[^{\bullet}OH]/[O_3]$) can be considered constant. This empirical concept is based on the observation that during ozonation the pseudo-first-order rate constant for transforming ozone into $^{\bullet}OH$ and scavenging of $^{\bullet}OH$ or their ratios remain constant. R_{ct} is typically in the range of 10^{-8}–10^{-9} (M/M) for various waters and varying water quality parameters such as pH, alkalinity, DOC and temperature (Elovitz *et al*., 2000a). During the initial fast decomposition of ozone, the ratio is usually higher (by about a factor of 10) and varies as a function of the ozone dose (Pinkernell & von Gunten, 2001). Even during the initial phase of ozonation, R_{ct} can be approximately expressed by just one value without significant deviations in calculated micropollutant degradation (Acero *et al*., 2000, 2001). Therefore, measurement of the ozone concentration and the oxidation of a probe allow prediction of the oxidation of a particular micropollutant during ozonation when rate constants for its reaction with ozone and $^{\bullet}OH$ are known (Acero *et al*., 2000; Peter & von Gunten, 2007).

Ozone kinetics in most waters is multi-phasic (e.g. Figure 3.3). In drinking waters and wastewaters, kinetics may be adequately described by breaking it down in to three components following first-order kinetics (Nöthe *et al*., 2009) (Figure 3.3) or to two components when the very fast and comparatively little ozone consuming component is disregarded (Schumacher *et al*., 2004b; Buffle *et al*., 2006b).

At a DOC of 7.2 mg/L and an ozone dose of 10 mg/L, the first component consumes ~1 mg/L ozone at $k = 0.071$ (mg DOC)$^{-1}$ s^{-1}. The second component ($k = 0.011$ (mg DOC)$^{-1}$ s^{-1}) consumes 5 mg/L ozone, while the third component consumes 4 mg/L ozone at 0.0019 (mg DOC)$^{-1}$ s^{-1}. These data are normalised to the DOC in Table 3.2.

It seems that the variability of the ozone decomposition rate in wastewaters with similar DOC concentrations is much smaller than in natural waters which contain DOM of quite variable composition (see above). Figure 3.4 shows results for ozone decrease in Opfikon wastewater (DOC 4.5 mg/L) and Berlin wastewater (DOC 8.5 mg/L). For the same ozone dose (2.5 mg/L) and pH 8, ozone consumption in undiluted Berlin wastewaters is much faster than in Opfikon wastewater. However, for a 1:1 dilution of Berlin wastewater, adjusting the DOC to a similar level, ozone consumption rate is very similar for both waters. Thus, the concentrations of the ozone-reactive moieties must be very similar.

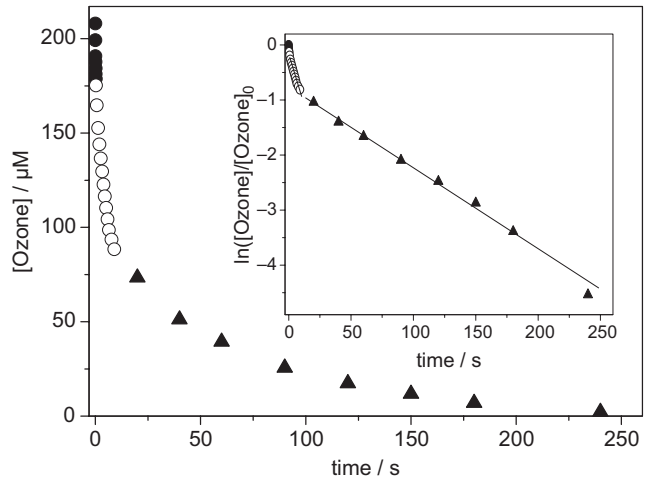

Figure 3.3 Ozone decay as followed by stopped flow (circles) and batch-quench (triangles) at 17.3 °C and pH 8. Wastewater (WWTP Bottrop) and ozone solution were mixed in a 4:1 ratio leading to concentrations of [DOC] = 7.2 mg/L and [O_3] = 10 mg/L (208 µM); [HCO_3^-] = 5.08 mM. Inset: data plotted as ln([ozone]/[ozone]$_0$) vs. time. Reprinted with permission from Nöthe *et al.*, 2009. Copyright (2009) American Chemical Society.

Table 3.2 Rate of ozone decay and ozone consumption in wastewater according to (Nöthe *et al.*, 2009)

Process	Rate/(mg DOC)$^{-1}$ s^{-1}	Ozone consumption/mg O_3 (mg DOC)$^{-1}$
Initial	0.071	0.15
Fast	0.011	0.7
Slow	0.0019	>0.85

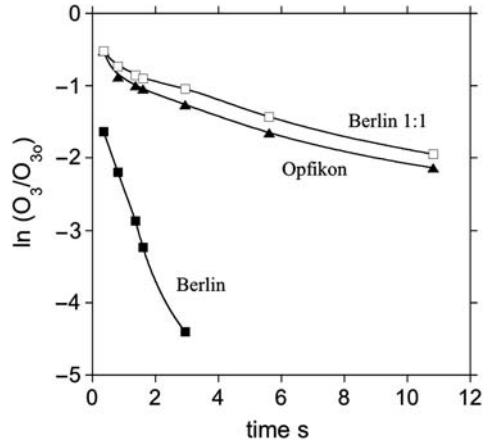

Figure 3.4 Ozone consumption in Berlin (DOC 8.5 mg/L) and Opfikon (DOC 4.5 mg/L) wastewater for an ozone dose of 2.5 mg/L at pH 8. Data for a 1:1 dilution of Berlin wastewater (DOC 4.25 mg/L) with ultrapurified water are also shown. According to Buffle *et al.*, 2006a, with permission.

To reflect the continuum of the reactive moieties in DOM, the reactivity of ozone with DOM can conceptually be described by a model in which DOM is divided into, for example, five classes of compounds with second-order rate constants ranging from 10 to 10^7 $M^{-1}s^{-1}$ (Buffle *et al*., 2006a). For a wastewater, these individual moieties were assigned with fictitious concentrations in the range between 10 and 70 µM. With this approach it was possible to describe the ozone decrease in a particular wastewater (Buffle *et al*., 2006a). A similar approach allowed the modelling of reactions occurring in a bubble column (Nöthe *et al*., 2010).

3.2 MOLECULAR WEIGHT DISTRIBUTION OF DISSOLVED ORGANIC MATTER

Gel permeation chromatography (GPC), also called size exclusion chromatography (SEC), has been widely used for the determination of the distributions of molecular weights of the DOMs in various waters. In brief, a solution of the analyte (here DOM) is injected onto a chromatographic column containing the separation gel. Low-molecular-weight material can penetrate into the pores of the gel, wherefrom it is eluted slowly while high-molecular-weight material that cannot penetrate the pores elutes faster. Lacking exact reference material, it is not possible to correlate a given retention time with the exact molecular weight of that fraction, but the order of elution, high-molecular-weight material first, low-molecular-weight material later will continue to be approximately correct. In wastewater, for example, the various GPC fractions have a different specific UV absorbance (SUVA). This is a clear indication, that one deals with polymers of different chemical properties and that the above caveat as to the uncertainties of the molecular weights of the various fractions is justified.

The development of detection systems that record not only UV absorbance but also DOC have been essential for the present topic (Huber *et al*., 1990; Huber & Frimmel, 1991; Huber & Frimmel, 1992; Huber & Frimmel, 1996; Her *et al*., 2002). Figure 3.5 shows an example of a SEC-OCD chromatogram of a wastewater before and after ozonation.

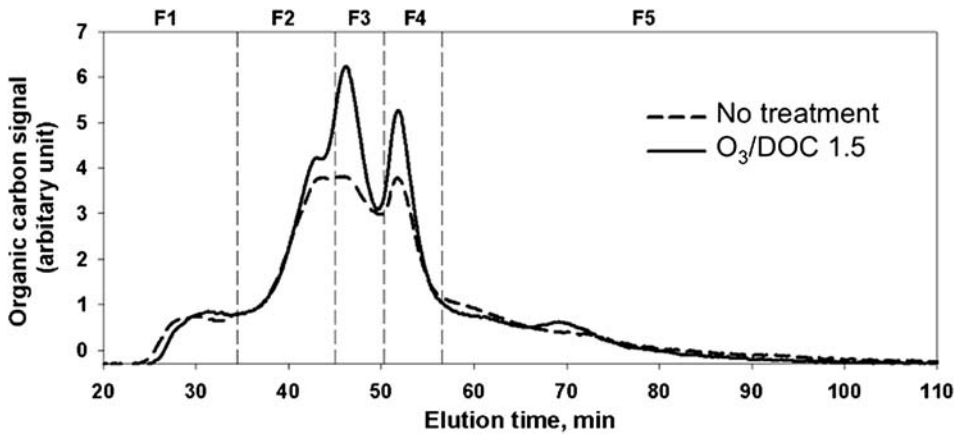

Figure 3.5 Changes in the SEC-OCD chromatogram due to ozonation of 8-µm-filtered secondary effluent of the Kloten-Opfikon wastewater treatment plant (Switzerland). SEC-OCD chromatogram before and after ozonation (specific ozone dose 1.5 gO_3/g DOC). Regensdorf wastewater: TOC 5 mg/L, DOC 4.7 mg/L, HCO_3^- 2.86 mM, pH 7.0. F1, Biopolymers; F2, Humics; F3, Building blocks; F4, Low-molecular-weight humics and acids; F5, Low-molecular-weight neutrals (Lee & von Gunten, unpublished).

Irrespective of the origin of a water, there are always various partially-separated fractions detected. In natural waters and wastewaters, there is barely a fraction that may be associated with really low-molecular-weight material (<150 Da). SEC-OCD chromatograms of natural waters, drinking waters, soluble microbial products and wastewater have been published (Fuchs, 1985a, b, c; Allpike *et al*., 2005; Meylan *et al*., 2007; Jiang *et al*., 2010). As expected, waters from different origins such as groundwaters, surface waters and wastewaters show substantial differences. Waters contained in barrages that are fed by nutrients from nearby agricultural activities may be rich in extracellular organic matter (EOM) of algae (Hoyer *et al*., 1985) or groundwaters in peaty areas may be enriched in humics. Such differences are reflected in differences in ozone reactivity (Figure 3.2) but (obviously) also in SEC-OCD chromatograms. Common study objects are fulvic and humic acids, and data as to their structures are becoming increasingly available (Reemtsma & These, 2005; Reemtsma *et al*., 2006a, b, 2008; These & Reemtsma, 2003, 2005; These *et al*., 2004)

Figure 3.6 shows the changes of the various DOM fractions caused by ozone reactions. The so-called hydrophobic DOM fraction is retained by the chromatographic column, that is, not the entire DOC is accounted for by SEC-OCD.

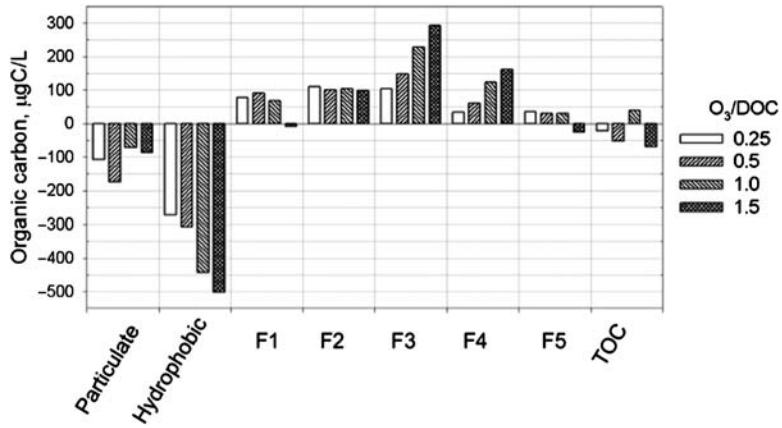

Figure 3.6 Changes in the SEC-OCD chromatogram due to ozonation of 8-µm-filtered secondary effluent of the Kloten-Opfikon wastewater treatment plant (Switzerland). Changes of individual fractions (mgC/L) for various specific ozone doses between 0.25−1.5 gO_3/gDOC. Regensdorf wastewater: TOC 5 mg/L, DOC 4.7 mg/L, HCO_3^- 2.86 mM, pH 7.0. F1, Biopolymers; F2, Humics; F3, Building blocks; F4, Low-molecular-weight humics and acids; F5, Low-molecular-weight neutrals (Lee & von Gunten, unpublished).

The hydrophobic fraction can be determined from the difference between measured DOC and the sum of all fractions. This hydrophobic fraction decreases significantly with increasing ozone dose. This means that this part of DOC becomes detectable upon ozone treatment as fractions denoted 'building blocks and low-molecular-weight humics and acids'. The higher molecular weight fractions 'biopolymers' and 'humics' are only marginally changed. Note that at the very high ozone dose of 7.5 mg/L only about 10% of the DOM-DOC is converted to low-molecular-weight compounds.

The specific ozone doses in Figures 3.5 and 3.6 are given on a gO_3/gDOC basis. This unit has been chosen, because it is very practical for water treatment purposes, notably in wastewaters (Hollender *et al*., 2009).

For any calculations of the reaction of ozone with DOM on the molecular level, the ozone concentration has to be given in units of M instead of mg/L and for the DOM (unit: mgC/L) an equivalent unit also has to be found. Considering that DOM is polymeric, one may express its concentration, as conveniently done with other polymers, in subunits. In DOM, which is not made up of repeating subunits of known molecular weight, this is not possible, but one may make the assumption that such subunits are made up of ten carbon atoms on average (Nöthe *et al*., 2009). For aromatic subunits (see below), this would imply six for the core benzene ring and four for substituents and linking these subunits to one another. Potential polymeric carbohydrate-based polymers would have six carbon atoms for the core unit and two further carbon atoms when *N*-acetylated. This is not far from the ten carbon atoms assumed for the aromatic units. Heteroatoms (O, N, S) and hydrogens do not have to be included in this simplified approach, as it is only based on carbon atoms (DOC). With this assumption, water that has a DOC of 12 mgC/L is 100 μM in DOM subunits. This approach now allows us to discuss many aspects of ozone chemistry in drinking water and wastewater on the molecular level. For example in a wastewater that contains a DOC of 10 mg/L (83 μM in subunits), at an ozone dose of only 4 mg/L (83 μM), each DOC subunit has reacted with ozone – on average. This approach will be used for a semi-quantitative assessment of certain DOM properties [Chemical Oxygen Demand (COD), absorption spectra, etc.].

3.3 MINERALISATION AND CHEMICAL OXYGEN DEMAND

The degree of mineralisation of DOM is typically very small, of the order of 10% for an ozone/DOC mass ratio of 1.0 (Nöthe *et al*., 2009). For the determination of the chemical oxygen demand (COD), another bulk method to characterise the organic matter in water treatment systems, two oxidants, namely dichromate and permanganate, are in use. Dichromate is the stronger oxidant and is capable of oxidising >95% of the DOC. Thus the COD value as determined with dichromate is typically 1.5 times higher than the permanganate value.

It has been observed in a wastewater that the COD drops by ~23% at an ozone to DOC mass ratio of 1.0. Typically, one out of the three O-atoms in ozone is transferred in ozone reactions. This indicates that the COD is reduced by about 0.65 mol O_2 (1.3 mol O) at an ozone/DOC mass ratio of 1.0. From the above, one would expect a value of 0.5 mol O_2 (1.0 mol O). Thus, it seems that the oxidation of wastewater is somewhat more efficient than suggested by the above stoichiometry. This is most likely due to the formation of $^{\bullet}OH$ radicals which induce peroxyl radical reactions, where O_2 serves as the oxidant (Chapter 14). In comparison, the DOC concentration is much less affected (Nöthe *et al*., 2009). This is understood, as the DOC concentration only decreases when decarboxylation reactions set in, that is, when already substantially oxidised material is further oxidised (note that naturally occurring DOM is already partially oxidised). Mechanistic aspects of ozone-induced decarboxylation reactions are discussed in Chapters 6 and 14.

3.4 FORMATION OF ASSIMILABLE ORGANIC CARBON

As a consequence of the reaction of ozone with DOM, assimilable organic carbon (AOC) or biodegradable organic carbon (BDOC) is formed. This leads to the formation of smaller oxygen-rich molecules, such as carboxylic acids, aldehydes, ketones, etc. (Richardson *et al*., 1999b), which are typically more biodegradable and can be summarised under AOC or BDOC (Hammes *et al*., 2006; van der Kooij *et al*., 1989; Siddiqui *et al*., 1997). The mechanisms and kinetics of the formation of these compounds is governed by the reaction of ozone with DOM moieties such as phenols or other activated aromatic systems (Chapter 7). Upon ozonation, this leads to various olefins and eventually small organic acids

and aldehydes (Chapter 6). Even though this is only a model approximation of the interaction between DOM and ozone, similar processes occur under realistic conditions (Figure 3.7).

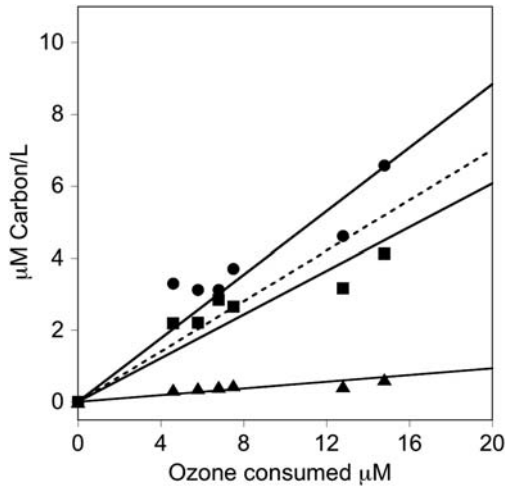

Figure 3.7 Formation of AOC (circles), organic acids (squares) and aldehydes (triangles) during ozonation of Lake Zurich water. Dashed line: sum of acids, ketones and aldehydes. DOC 1.4 mg/L, T = 22 °C, pH 8, bicarbonate = 2.6 mM. Adapted from Hammes *et al.*, 2006, with permission.

In presence of tBuOH (as an $^{\bullet}OH$ scavenger), formation of organic acids is almost identical to that in absence of tBuOH in natural waters (Hammes *et al.*, 2006). Therefore, the formation of AOC which is mostly composed of carboxylic acids and aldehydes in the investigated waters is most likely due to direct ozone reactions with fast reacting moieties present in the humic fraction of DOM. In the case of Lake Zurich water, AOC can be mostly explained by carboxylic acids, whereas aldehydes and ketones contribute little. The results look different when algae are present during (pre-) ozonation. In this case, a significant portion of the AOC results from the lysis of algal cells and consists of intracellular cytoplasmic DOM (Hammes *et al.*, 2007). This material is released very quickly, even though the algae are not completely destroyed. Significant AOC formation of up to 740 µg C/L has also been observed during ozonation of wastewater (Zimmermann *et al.*, 2011).

The removal of these compounds, measured as AOC or BDOC, is one of the major tasks in water treatment plants containing an ozonation step. Their removal can be achieved in a biological filtration step (sand, biological activated carbon filtration) after ozonation (cf. Chapter 5). This avoids regrowth of micro-organisms in the distribution systems, which is particularly important in countries where no or only limited disinfectant residual is used in the distribution systems (e.g. Germany, Netherlands, Austria, Switzerland).

Figure 3.8 shows the formation and removal of AOC, carboxylic acids and aldehydes/ketones during ozonation and biological filtration, respectively, in a drinking water treatment plant. Even though the AOC concentration at the effluent of the plant is similar to that of Lake Zurich water, the treatment train including pre- and intermediate ozonation and several biological filtration steps leads to a significant overall reduction of DOC which is very beneficial for the general water quality. Similarly, during

post-sand filtration of ozonated wastewater, AOC concentration was reduced significantly (up to 50%) (Zimmermann *et al*., 2011).

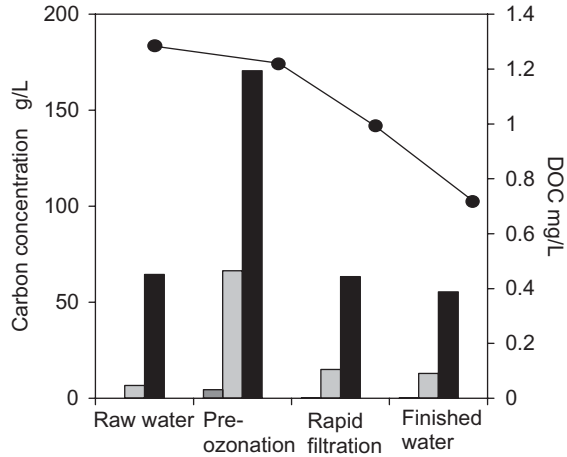

Figure 3.8 Formation and removal of AOC, carboxylic acids, aldehydes and ketones in the Lake Zurich drinking water treatment plant (Lengg, Zurich, Switzerland). Shaded bar: aldehydes and ketones; grey bars: total organic acids; black bars: assimilable organic carbon (AOC); circles: DOC. Adapted from Hammes *et al*., 2006, with permission.

3.5 FORMATION AND MITIGATION OF DISINFECTION BY-PRODUCTS

As shown above, the application of ozone leads to a transformation of electron-rich moieties of the DOM. This has consequences for the formation of disinfection by-products (DBPs) during post-disinfection in, for example, the distribution system, and mostly leads to a reduced formation of DBPs. Nevertheless, for certain DBPs an increased formation has also been found after ozonation. One of the early applications of ozone was its significant potential to mitigate the formation of chlorophenols and bromophenols which are potent taste and odour compounds that can be formed during post-chlorination of phenol-containing waters (Bruchet & Duguet, 2004; Acero *et al*., 2005; Piriou *et al*., 2007). Under typical ozonation conditions, phenol is efficiently destroyed and therefore, halo-phenols cannot be formed any more (Chapter 7). Related to this, ozonation of natural waters generally reduces the formation of trihalomethanes (THMs) and haloacetic acids (HAAs) during post-chlorination (Reckhow *et al*., 1986; Chaiket *et al*., 2002; Chang *et al*., 2002; Gallard & von Gunten, 2002; Chin & Bérubé, 2005; Meunier *et al*., 2006; Hua & Reckhow, 2007; Li *et al*., 2008). HAA formation was found to increase when chlorination was replaced by chloramination (Hua & Reckhow, 2007). The formation of trichloronitromethane (chloropicrin) and other halonitromethanes increased if natural waters were treated with ozone/chlorine compared to chlorine alone (Hoigné & Bader, 1988; Krasner *et al*., 2006). In Br^--containing waters, a shift to bromonitromethanes was observed (Krasner *et al*., 2006; Krasner, 2009).

These studies did not use a biological filtration step between ozonation and post-chlorination/chloramination. It can be expected that some of the halonitromethane-precursors are biodegradable and

that biofiltration would reduce formation of halonitromethanes during post-chlorination/chloramination (Krasner, 2009).

In Br^--containing waters, bromate is the main ozone disinfection by-product of concern (Chapters 11 and 14). However, numerous organic by-products such as bromoform, bromopicrin, (di)bromoacetic acid, dibromoacetonitriles, bromoacetone, cyanogen bromide, bromoketones, bromonitriles, bromoalkanes and bromohydrins can also be formed during ozonation or in combination with chlorine or chloramine (Richardson *et al*., 1999a). In I^--containing waters, ozonation rapidly oxidises I^- to iodate, which hinders the formation of iodo-organic compounds (Chapter 11).

NDMA precursors are generally oxidised during ozonation which leads to a reduction of NDMA formation during post-chloramination (Lee *et al*., 2007b; Krasner, 2009; Shah *et al*., 2012). Ozonation, however, may also enhance NDMA formation, as discussed in Chapters 8 and 11.

3.6 UV ABSORBANCE OF DISSOLVED ORGANIC MATTER

All natural DOMs have in common that they show strong UV absorptions. There is, however, a considerable variation in the specific UV absorbance (SUVA, absorbance at 254 nm per mg DOC) (Huber & Frimmel, 1992) The UV absorption of a typical wastewater is shown in Figure 3.9.

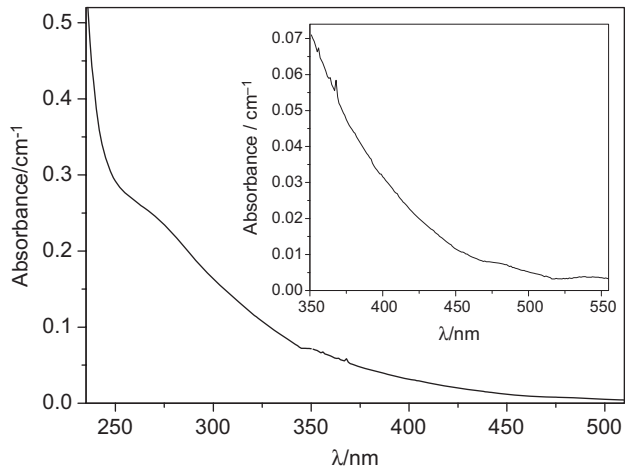

Figure 3.9 UV–Vis spectrum of a typical wastewater (effluent of the municipal WWTP Neuss, Germany). Inset: blow-up of the long-wavelength side. At the short-wavelength side the absorbance rises steeply (not shown). Courtesy T. Nöthe.

The absorption of natural water, drinking water and wastewater DOM is characterised by a continuous increase in absorption on going to shorter wavelength without any noticeable peak. This is most uncommon for any isolated UV-absorbing (e.g. aromatic) compound (Nöthe *et al*., 2009), and it has been convincingly shown that absorptions generally observed with aquatic DOMs must be due to charge transfer transitions of electron-donating (e.g. phenolic or alkoxylated) subunits to electron-accepting (e.g. quinoid) subunits present in close neighbourhood within this polymeric material (Del Vecchio & Blough, 2004). This is schematically shown in Figure 3.10.

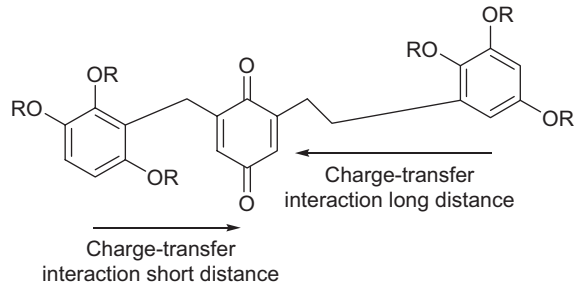

Figure 3.10 Schematic drawing of a quinone (electron acceptor) and alkoxylated benzenes (electron donors) at different distances. Charge transfer interactions between these sites in DOM give rise to electronic transitions (absorptions). The longer the distance the weaker the transition and thus the longer the wavelength of absorption.

The first electronic transition of isolated aromatic compounds that is near 250–260 nm is a forbidden transition with molar absorption coefficients of only a few hundred. Charge transfer transitions such as suggested by the Blough model (Del Vecchio & Blough, 2004) (Figure 3.10) are, however, allowed transitions and are characterised by high absorption coefficients. In a wastewater containing a DOM of 11 mg/L, the absorption at 254 nm was 30 m^{-1} (Schumacher, 2006; Nöthe *et al.*, 2009). Based on the above estimate of the concentration of subunits of this polymeric material, this relates to a molar absorption coefficient of the DOM subunits near 3300 M^{-1} cm^{-1}, which is a much higher value than that of a typical aromatic compound. The featureless absorption, rising from the visible light into the UV region (Figure 3.9) can also be explained on the basis of this model. The absorption maxima of such charge transfer transitions vary with the distance between donor and acceptor (Figure 3.10). Structural conditions as depicted in Figure 3.10 and fluctuations of these distances induced by thermal motions are the reason for this featureless and very broad absorption.

Since the UV-active moieties in DOM (activated aromatic systems) have a certain reactivity with ozone, the UV absorption and SUVA have been used as empirical surrogate parameters to predict the ozone consumption rate in natural waters (Elovitz *et al.*, 2000b). A reasonable correlation between the pseudo-first-order rate constant for ozone decrease and $SUVA_{254}$ with a correlation coefficient $R^2 = 0.79$ was found for nine DOM isolates (Elovitz *et al.*, 2000b). In these correlations, especially Suwannee river humic acid, but also Suwannee river fulvic acid, DOM isolates, often used to simulate drinking water DOM, proved to be outliers with significantly higher ozone reactivity (see Figure 3.2).

The change in the UV absorption of DOM has been used as an empirical parameter for predicting micropollutant removal during ozonation of wastewaters (Nanaboina & Korshin, 2010; Buffle *et al.*, 2006a; Wert *et al.*, 2009b; Bahr *et al.*, 2007), but such changes cannot be used for mechanistic interpretations as attempted by Nanaboina & Korshin (2010).

3.7 RELEVANCE OF OZONE KINETICS FOR THE ELIMINATION OF MICROPOLLUTANTS

For the elimination of micropollutants, competition between DOM of the water matrix and pollutant (P) for ozone has to be taken into account [reactions (21) and (22)].

$$DOM + O_3 \longrightarrow DOM_{ox} \quad (21)$$

$$P + O_3 \longrightarrow P_{ox} \quad (22)$$

The kinetics of the reaction of ozone with DOM thus strongly affects the efficiency of micropollutant transformation by ozone (Katsoyiannis *et al*., 2011). Only those micropollutants that react rapidly stand a chance of being oxidised directly by ozone. Here, we only consider the very first step in the sequence of events that eventually will lead to mineralisation. This is justified, because in most cases, the biological activity of the micropollutant is practically fully suppressed by this very first oxidation step (Chapter 4). For a wastewater (DOC = 10 mg/L, pH 8), one can neglect the slow process for an ozone dose of, for example, 5 mg/L. Based on the example shown in Figure 3.3, the ozone decay can be simulated by breaking up the process into several kinetic phases. A simulation has shown (Nöthe *et al*., 2009) that during the consumption of the first mg ozone per L all micropollutants that have ozone rate constants $>10^5$ $M^{-1}s^{-1}$ are completely (>90%) eliminated, micropollutants that react with 10^4 $M^{-1}s^{-1}$ are eliminated to about 25% remaining, and micropollutants that react an order of magnitude more slowly are practically not affected. This situation is substantially improved by the reaction of the next 4 mg/L ozone. Here, the lower rate constant of ozone consumption by the wastewater matrix and the higher ozone dose cooperate. Complete elimination is now achieved for all micropollutants that react with 3×10^3 $M^{-1}s^{-1}$ and micropollutants that react with 1×10^3 $M^{-1}s^{-1}$ are eliminated to about 50%. For the elimination of less reactive micropollutants, higher ozone doses would be required. For an ozone dose of 10 mg/L (1 gO_3/gDOC), micropollutants that react with 1×10^3 $M^{-1}s^{-1}$ are fully eliminated, and the concentrations of even less reactive ones are noticeably lowered ($k = 300$ $M^{-1}s^{-1}$ to 25%; $k = 100$ $M^{-1}s^{-1}$ to 65% remaining). The elimination of micropollutants with varying second-order rate constants for their reaction with ozone is illustrated in Figure 3.11 as a function of the specific ozone dose.

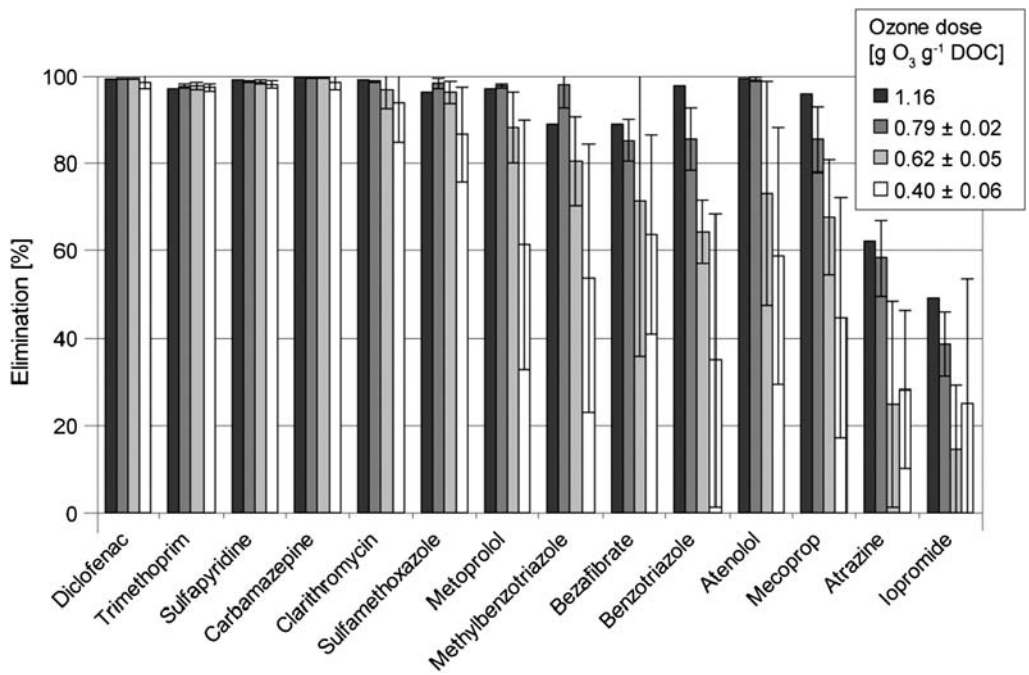

Figure 3.11 Elimination of selected micropollutants during ozonation of secondary effluent of a full-scale ozonation plant for various specific ozone doses (Regensdorf, Switzerland). DOC 5.2 ± 0.6 mg/L, pH 7. Reprinted with permission from Hollender *et al*., 2009. Copyright (2009) American Chemical Society.

Fast reacting compounds from diclofenac to sulfamethoxazole ($k > 10^4$ $M^{-1}s^{-1}$) are fully eliminated at specific ozone doses of 0.4 g ozone per g DOC. For compounds with intermediate ozone reactivity, (metoprolol to atenolol, 2×10^2 $M^{-1}s^{-1} < k < 10^4$ $M^{-1}s^{-1}$) significantly higher specific ozone doses of about 1 g ozone per g DOC are necessary for complete elimination. For compounds with second order rate constants near 100 $M^{-1}s^{-1}$ and below (mecoprop to iopromide), specific ozone doses of 1 $gO_3/gDOC$ lead to eliminations of 50–90%. For these compounds, elimination is dominated by •OH. The dependence of the degree of elimination of micropollutants in a wastewater on the reactivity with ozone and •OH is further illustrated in Figure 3.12 for compounds that cover the full range of ozone and •OH rate constants.

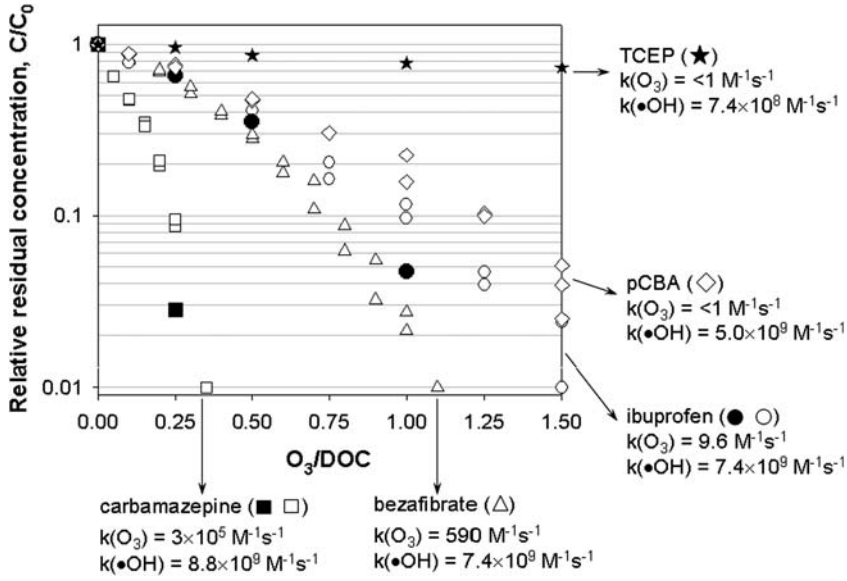

Figure 3.12 Residual concentrations of selected spiked micropollutants at sub to low μg/L ranges after ozonation of Kloten-Opfikon wastewater effluent with variable ozone doses up to ratios of ozone : DOC of 1.5 (g/g). Filled and open symbols represent experiments with low (~1 μg/L) and high dosage (~200 μg/L) of the micropollutants. pCBA: *p*-chlorobenzoic acid, TCEP: Tris-(2-chloroethyl) phosphate. Second order rate constants for the reaction with ozone and •OH are given. According to Lee, Gerrity, Snyder & von Gunten unpublished.

Micropollutants such as the chlorinated trialkylphosphates have considerably lower •OH rate constants than the aromatic x-ray contrast media such as iopromide (Table 3.3). These are hence degraded to an even lesser extent (cf. Figure 3.14).

3.8 HYDROXYL RADICAL YIELD AND •OH-SCAVENGING RATE OF DISSOLVED ORGANIC MATTER

Ozone reacts with a number of organic compounds, notably amines (Chapter 8) and electron-rich aromatic compounds (e.g. phenols and alkoxylated benzenes; Chapter 7) by giving rise to •OH in side reactions, and hence •OH is always formed when drinking water and wastewater are treated with ozone. The •OH yield in wastewater has been determined making use of the tertiary butanol (tBuOH) assay (Chapter 14). In brief,

tBuOH is added in large excess to overrun the •OH scavenging rate of the wastewater (see above), and one of the products of the reaction of •OH with tBuOH, formaldehyde, is determined. Formaldehyde is not formed in the reaction of ozone with wastewater in the absence of tBuOH. As a rule of thumb, the •OH yield is twice the formaldehyde yield (Flyunt *et al.*, 2003a). Using this approach, the data shown in Figure 3.13 were obtained. In the inset of this figure, a competition plot of tBuOH and the water matrix for •OH is shown (for competition kinetics see Chapter 2).

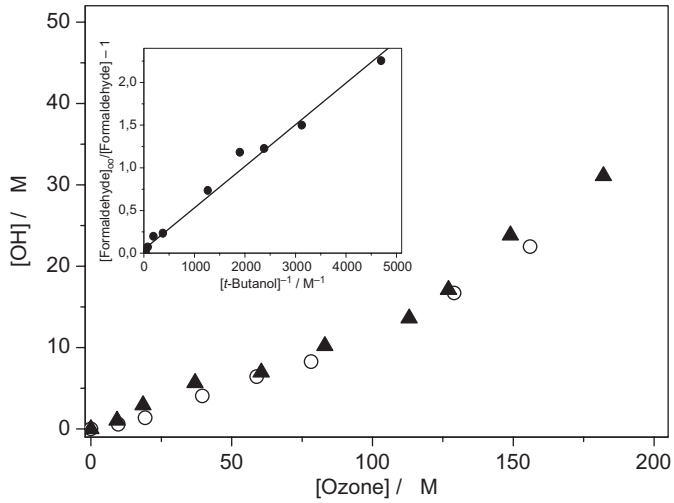

Figure 3.13 The •OH radical yield as a function of the ozone dose in a wastewater (WWTP Bottrop, pH 8, DOC after dilution by ozone-containing water 8.0 mg/L). Inset: Competition of the water matrix and tertiary butanol for •OH radicals formed upon the addition of ozone (112 µM, 5.6 mg/L) to wastewater (WWTP Neuss, pH 8, DOC = 9.05 mg/L, 3.8 mM bicarbonate). Reprinted with permission from Nöthe *et al.*, 2009. Copyright (2009) American Chemical Society.

As seen from Figure 3.13, the •OH yield continues to remain constant or even slightly increases up to an ozone dose of 190 µM. At a DOC of 8 mg/L (67 µM in subunits) the ozone concentration is 2.8 times that of the DOM subunits. Thus, the capacity of the DOM for •OH production does not become exhausted but rather new •OH-generating sites are formed in the reaction of ozone with DOM, as discussed above.

The •OH yield can vary significantly from one water source to another. By increasing the ozone:DOC ratio (g/g) to 2.0 the •OH yield may rise to ~30% (Lee & von Gunten, in preparation). Apparently, there is no general •OH yield, and for each water to be treated with ozone •OH formation has to be assessed.

3.9 ELIMINATION OF OZONE-REFRACTORY MICROPOLLUTANTS BY THE •OH ROUTE

Ozone-refractory micropollutants are eliminated to a certain extent by the •OH route. There is not such a high variation in •OH rate constants [for a compilation see (Buxton *et al.*, 1988)] as for ozone. Yet for ozone-refractory micropollutants that we are concerned with in drinking water and wastewater, a variation of the •OH rate constant by a factor of ten (4.5×10^8 to 7×10^9 $M^{-1}s^{-1}$) is typical (Table 3.3), and this is of relevance for the elimination efficiency and therefore the ozone dose required for achieving a desired elimination.

Table 3.3 Compilation of ozone and •OH rate constants (unit: $M^{-1}s^{-1}$) of selected ozone-refractory micropollutants in drinking water and wastewater at pH 7

Compound	Source/application	*k* (ozone)	*k*(•OH)	Reference
Atrazine	Herbicide	6	3×10^9	Acero *et al.*, 2000
Iopromide	X-ray contrast agent	<0.8	3.3×10^9	Huber *et al.*, 2003
Diazepam	Tranquiliser	0.75	7.2×10^9	Huber *et al.*, 2003
NDMA	Oxidation by-product	5×10^{-2}	4.5×10^8	Lee *et al.*, 2007a
Tris-(2-chloro-isopropyl) phosphate (TCPP)	Flame retardant	$\ll 1$	7×10^8	Pocostales *et al.*, 2010
Tris-(2-chloro-ethyl) phosphate (TCEP)	Flame retardant	$\ll 1$	7.4×10^8	Watts & Linden, 2009
Tri-*n*-butyl phosphate (TnBP)	Plasticiser	$\ll 1$	$\approx 2.8 \times 10^9$	Pocostales *et al.*, 2010

For the elimination of ozone-refractory micropollutants, one may write the competing reactions (23) and (24), where M denotes the water matrix (DOC plus bicarbonate, see above) and P the micropollutant.

$$M + {}^{\bullet}OH \longrightarrow M\text{-ox} \quad (23)$$

$$P + {}^{\bullet}OH \longrightarrow P\text{-ox} \quad (24)$$

The •OH scavenging rate that determines the rate of reaction (24) and •OH yields (in wastewater) has been given above. Based on this, the elimination efficiency of a given ozone-refractory micropollutant can be calculated. This is shown in Figure 3.14 for two organic phosphates.

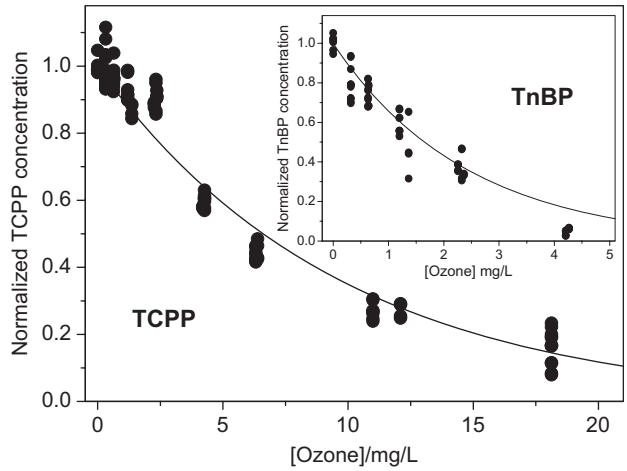

Figure 3.14 Experimental data (symbols) and simulation (solid lines) of the degradation of TCPP and TnBP (inset) in diluted Neuss wastewater (DOC = 5.5 mg/L). Reprinted with permission from Pocostales *et al.*, 2010. Copyright (2010) American Chemical Society.

The $^{\bullet}$OH scavenging rate of a water can be determined by measuring the rate of the apparent rate constant for the decrease of a probe compound [e.g. 4-chlorobenzoic acid (pCBA)] as a function of varying tBuOH concentrations (Katsoyiannis *et al*., 2011). Without knowing the $^{\bullet}$OH scavenging rate of a given water, one can also follow the elimination of an ozone-refractory test compound such as pCBA for which the $^{\bullet}$OH rate constant is known ($k = 5 \times 10^9\ M^{-1}s^{-1}$, Figure 3.12), and with the knowledge of the $^{\bullet}$OH rate constants of other micropollutants, their degradation can be calculated (Acero *et al*., 2000; Acero & von Gunten, 2001; Huber *et al*., 2003; Peter & von Gunten, 2007). The $^{\bullet}$OH rate constants of selected ozone-refractory micropollutants are compiled in Table 3.3.

3.10 OZONE-BASED ADVANCED OXIDATION PROCESSES

There are three ozone-based Advanced Oxidation Processes (AOPs) that lead to the formation of $^{\bullet}$OH, (i) the reaction of ozone with H_2O_2 or, more correctly, with its anion, HO_2^- (peroxone process), (ii) photolysis of ozone with UV light (UV/ozone) and (iii) reaction of ozone with activated carbon (carboxone process). In principle, this can also provide the means for coping with ozone-refractory pollutants, as $^{\bullet}$OH radicals are much more reactive than ozone. To what extent, this expectation can be realised in practice, will be discussed below.

3.10.1 Peroxone process

The best-known of the three ozone-based AOPs is the peroxone process. Details of its chemistry are discussed in Chapter 11. Here, it is recalled that H_2O_2 does not react efficiently with ozone, but that the reaction with HO_2^- is fast, and that the HO_2^- reaction dominates over a wide pH range that extends even into the acid pH region. This pH dependence is given by equation (25).

$$k_{obs} = k(HO_2^- + O_3) \times 10^{(pH - pK_a)} \tag{25}$$

Due to this marked pH dependence and the high pK_a of H_2O_2 [p$K_a(H_2O_2) = 11.8$], this reaction is fast only at high pH. For example at pH 8, k_{obs} is $1.5 \times 10^3\ M^{-1}\ s^{-1}$ and at pH 7 one order of magnitude lower, $k_{obs} = 150\ M^{-1}\ s^{-1}$. This slow reaction has to compete with other ozone decay processes such as the reaction with DOM (for an example see below). Moreover, the $^{\bullet}$OH yield is only half of the value that a simplified stoichiometry (Staehelin & Hoigné, 1982) suggests (von Sonntag, 2008) (for the reason for this, see Chapter 11).

Increasing the rate by increasing the H_2O_2 concentration may under certain conditions not be an advantage as H_2O_2 also acts as an $^{\bullet}$OH scavenger [reaction (26), $k = 2.7 \times 10^7\ M^{-1}\ s^{-1}$ (Buxton *et al*., 1988)].

$$^{\bullet}OH + H_2O_2 \longrightarrow H_2O + HO_2^{\bullet} \tag{26}$$

In a sequence of reactions, $HO_2^{\bullet}$ reacts with ozone [reactions (2)/(3) and (10)/(11)] giving again rise to $^{\bullet}$OH (for details. see Chapter 13). As a result, ozone and H_2O_2 are destroyed without the desired effect of pollutant degradation. Yet compared to other $^{\bullet}$OH reactions, the rate constant of reaction (26) is very low, and this prevents this chain reaction from becoming of importance when the $^{\bullet}$OH scavenging rate of the matrix is high, for example, in surface waters or wastewaters.

For a wastewater, the effect of H_2O_2 on the formation of $^{\bullet}$OH has been simulated on the basis of known rate constants (Figure 3.15).

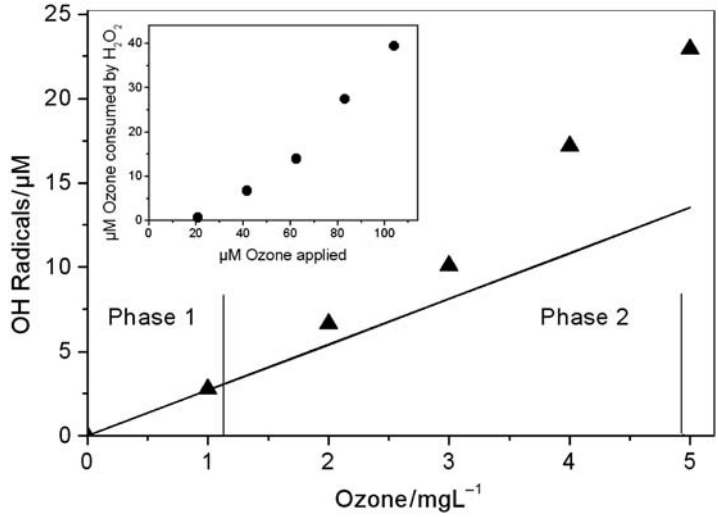

Figure 3.15 Simulation of the •OH yield for a wastewater containing a DOC of 5.5 mgC/L (diluted Neuss wastewater). The solid line is based on 13% •OH yield in the reaction of ozone with the DOC in the absence of H_2O_2 (cf. Figure 3.14). The symbols indicate the total •OH yields formed in the reaction of ozone with the DOC and in the peroxone process (molar ratio ozone/$H_2O_2 = 2.0$). Inset: ozone consumption from the peroxone process as a function of the applied ozone concentration (units: µM, note that 1 mg/L ozone = 21 µM). Lines near 1 and 5 mg/L ozone indicate the ranges of first and second phase in ozone kinetics of this wastewater (cf. Table 3.2). Reprinted with permission from Pocostales *et al*., 2010. Copyright (2010) American Chemical Society.

As •OH formation in the Neuss wastewater is 13% of ozone consumption and in the peroxone process only 50% (see above), the excess gain in •OH formation is only 37% when ozone reacts with H_2O_2 instead of reacting with the wastewater DOM. Because ozone reacts rapidly with the water matrix at the early stage, H_2O_2 can barely compete. Only when the matrix reaction becomes slower and the H_2O_2 concentration higher, is there a surplus of •OH. This surplus of •OH has to be paid for by a considerable depletion of ozone (inset in Figure 3.15) and a shortening of ozone lifetime, with the effect that disinfection and micropollutant destruction by the direct ozone reaction are now much less effective. This mainly affects micropollutants that have a low to medium ozone rate constant. Whether this loss in micropollutant destruction by ozone is offset by an •OH-induced destruction has not yet been tested experimentally.

In water treatment practice, AOPs are often considered as processes with a "magic" touch. In the case of the AOP ozone/H_2O_2, a better elimination of micropollutants is suggested compared to the conventional ozonation process. In Figure 3.16, the ozone stability is shown for a groundwater (DOC 1 mg/L, alkalinity 5.2 mM) and a surface water (DOC 3.2 mg/L, alkalinity 3.8 mM). Ozone stability is affected by the addition of H_2O_2 in both waters even at pH 7 (Figure 3.16).

The effect is more pronounced in the groundwater than in the surface water. The larger effect in the groundwater is due to the lower DOC which results in a higher stability of ozone in the absence of H_2O_2. When H_2O_2 is added, the relative contribution of H_2O_2 to ozone decomposition is very high in the groundwater, whereas in the surface water it is small. The relative residual concentration of pCBA, an ozone-refractory compound, is shown in Figure 3.17 for the same experimental conditions.

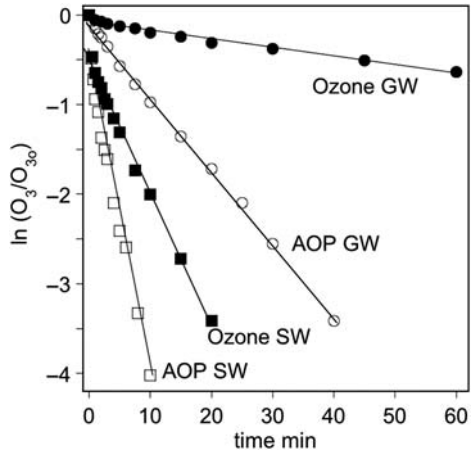

Figure 3.16 Ozonation of a groundwater (GW) (DOC 1 mg/L, alkalinity 5.2 mM) and a surface water (SW) (DOC 3.2 mg/L, alkalinity 3.8 mM). First order kinetic representation of the ozone decrease. Experimental conditions: ozone dose 2.1×10^{-5} M, H_2O_2 dose 1.0×10^{-5} M, pCBA dose 2.5×10^{-7} M, pH 7, 11 °C. Adapted from Acero & von Gunten, 2001. Reprinted by permission *Journal AWWA*. Copyright American Water Works Association.

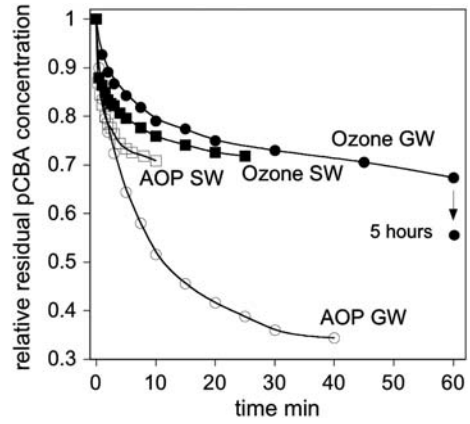

Figure 3.17 Ozonation of a groundwater (GW) (DOC 1 mg/L, alkalinity 5.2 mM) and a surface water (SW) (DOC 3.2 mg/L, alkalinity 3.8 mM). Kinetics of the transformation of pCBA. Experimental conditions: ozone dose 2.1×10^{-5} M, H_2O_2 dose 1.0×10^{-5} M, pCBA dose 2.5×10^{-7} M, pH 7, 11°C. From Acero & von Gunten, 2001, reprinted by permission *Journal AWWA*. Copyright American Water Works Association.

Two features should be highlighted: (i) the kinetics of the transformation of pCBA and (ii) the extent of pCBA transformation. In both waters, the rate of pCBA transformation is higher in the presence of H_2O_2, with a more pronounced effect in the groundwater. For a hypothetical contact time in a reactor of 15 min, the relative transformation in the absence and in the presence of H_2O_2 is 20% and 55%, respectively. This shows

that the addition of H_2O_2 allows a higher degree of transformation for a given hydraulic residence time. The extent of transformation has to be compared for the complete depletion of ozone in the absence and presence of H_2O_2. In the surface water, the overall extent of transformation is fairly similar for both scenarios, whereas in the groundwater, H_2O_2 addition improves the elimination of pCBA from about 40 to 65%. Thus, depending on water quality, a similar or only small increase of the extent of transformation is observed in presence of H_2O_2.

3.10.2 UV photolysis of ozone

In his pioneering work, Taube concluded that only H_2O_2 is formed upon the photolysis of ozone in water (Taube, 1957). This conclusion was based on the apparent 1:1 stoichiometry of ozone consumption and H_2O_2 formation in the presence of acetate as an $^{\bullet}OH$ scavenger. At this time, it was not yet known that in its $^{\bullet}OH$-induced reactions in the presence of O_2, acetate gives rise to relatively large amounts of H_2O_2 (Schuchmann *et al.*, 1985). Later on, when it was realised that $^{\bullet}OH$ radicals are generated in this reaction, the ozone/UV system was widely discussed among potential AOPs (Glaze *et al.*, 1982; Peyton *et al.*, 1982; Peyton & Glaze, 1987, 1988; Takahashi, 1990; Gurol & Vatistas, 1987; Ikemizu *et al.*, 1987; Morooka *et al.*, 1988). The reactions in this rather complex system are now reasonably well understood (Reisz *et al.*, 2003).

Upon photolysis, ozone is decomposed into O_2 and oxygen atoms $O(^1D)$ (excited state) and $O(^3P)$ (ground state) (Wayne, 1987; Schriver-Mazzuoli, 2001; Bauer *et al.*, 2000; Smith *et al.*, 2000; Taniguchi *et al.*, 2000). In the gas phase and below 300 nm, the main processes (quantum yield, $\Phi \approx 0.9$) are reactions (27) and (28), that is, the formation of $O(^1D)$ and singlet oxygen, $O_2(^1\Delta_g)$, as well as oxygen in its ground state, $O_2(^3\Sigma_g{}^-)$. Reactions that yield $O(^3P)$ [reactions (29) and (30)] are of lower importance ($\Phi \approx 0.1$) (Wayne, 1987; Hancock & Tyley, 2001; Wine & Ravishankara, 1982).

$$O_3 + h\nu \longrightarrow O(^1D) + O_2(^1\Delta_g) \quad (27)$$

$$O_3 + h\nu \longrightarrow O(^1D) + O_2(^3\Sigma_g{}^-) \quad (28)$$

$$O_3 + h\nu \longrightarrow O(^3P) + O_2(^1\Delta_g) \quad (29)$$

$$O_3 + h\nu \longrightarrow O(^3P) + O_2(^3\Sigma_g{}^-) \quad (30)$$

The quantum yield of $O(^1D)$ formation falls to a value near 0.1 above a wavelength of about 320 nm but not to zero. This shows that the spin-forbidden formation of $O(^1D)$ and $O_2(^3\Sigma_g{}^-)$ [reaction (28)] is possible (Bauer *et al.*, 2000; Smith *et al.*, 2000; Taniguchi *et al.*, 2000; Jones & Wayne, 1970). $O(^1D)$ is very energetic [heat of formation, 437 kJ mol^{-1} (Taniguchi *et al.*, 1999)] and therefore reacts rapidly even with water [reaction (31), $k = 1.8 \times 10^{10}\ M^{-1}s^{-1}$ (Biedenkapp *et al.*, 1970), by insertion (Taube, 1957)].

$$O(^1D) + H_2O \longrightarrow H_2O_2 \quad (31)$$

In the gas phase, the excess energy of the H_2O_2 molecule so formed results in the fragmentation of the O–O bond [reaction (32); BDE = 210 kJ mol^{-1} (McKay & Wright, 1998)].

$$(H_2O_2)_{hot} \longrightarrow 2\ ^{\bullet}OH \quad (32)$$

In aqueous solution, the rapid thermalisation of the "hot" H_2O_2 [reaction (33)] competes with reaction (32).

$$(H_2O_2)_{hot} \longrightarrow H_2O_2 \tag{33}$$

In addition, the solvent-cage effect inhibits the escape of $^{\bullet}OH$, that is, recombination competes with diffusion into the bulk. Hence, most of the $O(^1D)$ will be converted into H_2O_2.

In contrast, the reaction of $O(^3P)$ with water is endergonic by about 75 kJ mol^{-1} (Amichai & Treinin, 1969) and can be neglected here. Most of the $O(^3P)$ disappears by reacting with ground state oxygen [$O_2(^3\Sigma_g^-)$] regenerating ozone [reaction (34); $k = 4 \times 10^9$ M^{-1} s^{-1} (Kläning *et al.*, 1984)].

$$O(^3P) + O_2(^3\Sigma_g^-) \longrightarrow O_3 \tag{34}$$

Reactions of $O(^3P)$ with organic material are slow in comparison (Bucher & Scaiano, 1994; Herron & Huie, 1969) and may be neglected for typical AOP conditions.

The quantum yield of *direct* ozone photolysis is $\Phi = 0.5$, and, using tBuOH to scavenge $^{\bullet}OH$ radicals, it has been shown that only about 10% of the photolysed ozone furnish $^{\bullet}OH$ ($O_3 + H_2O + h\nu \rightarrow 2\ ^{\bullet}OH$) (Reisz *et al.*, 2003). Thus, the quantum yield of $^{\bullet}OH$ production is relatively low, $\Phi \approx 0.1$, when compared with the photolysis of H_2O_2 [$\Phi(H_2O_2) = 1.0$ (Legrini *et al.*, 1993)].

The UV/ozone process has never gained much practical application in water treatment. In comparison with the UV/H_2O_2 process, it is not capable of minimising the bromate problem. Yet, there are many lab-scale studies. A considerable number of these do not take into account that ozone reacts rapidly with the substrate molecules resulting in an ozone steady-state concentration which is so low that ozone photolysis cannot contribute to product formation. The reported differences in product yields can thus not be related to ozone photolysis but rather to a photolysis of starting material and products.

3.10.3 Reaction of ozone with activated carbon

The reaction of ozone with activated carbon (AC) leads to the formation of $^{\bullet}OH$, and it has been believed that this is a catalytic reaction (Jans & Hoigné, 1998). Yet, a more detailed study has shown that electron-donating residues within AC, notably its nitrogen content, cause this $^{\bullet}OH$ production, and when this source is exhausted, $^{\bullet}OH$ production comes to a halt (Sánchez-Polo *et al.*, 2005). XPS measurements indicated that the pyrrole content of the AC decreases during ozonation. Based on this characterisation and the measurement of $O_2^{\bullet -}$ formation (Sánchez-Polo *et al.*, 2005) by the tetranitromethane method [$O_2^{\bullet -}$ reacts quickly with ozone giving rise to $^{\bullet}OH$ (Chapter 13)], a hypothetical mechanism for the ozone reaction with AC has been formulated [reaction (35)].

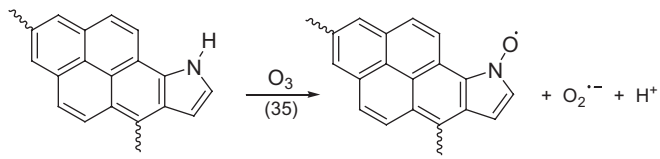

Figure 3.18 shows the kinetics of the transformation of pCBA in the absence and presence of AC. The presence of AC leads to a significant increase of the rate of pCBA transformation (adsorption is much slower and can be excluded). The presence of DOC does not affect the rate of pCBA transformation in the AC experiment.

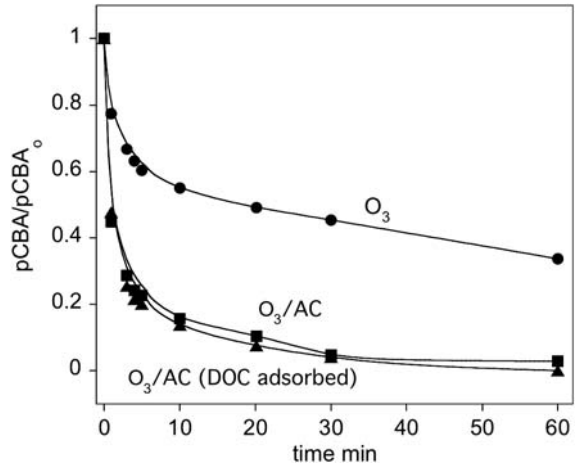

Figure 3.18 Kinetics of the transformation of pCBA during ozonation of Lake Zurich water in absence and presence of activated carbon. All experiments: pH 7, 5 mM phosphate buffer, ozone dose 1 mg/L, activated carbon 0.5 g/L. Circles (O_3), ozone only; squares (O_3/AC), ozone in presence of activated carbon F400; triangles (O_3/AC, DOC adsorbed), ozone in presence of activated carbon F400 pre-equilibrated with DOM. From Sánchez-Polo *et al.*, 2005, with permission.

In this process, AC does not serve as a catalyst. When the pyrrole groups are exhausted upon repeated ozonation, the effectiveness of the AC decreases significantly (Sánchez-Polo *et al.*, 2005). In the case of compounds that adsorb well on AC, adsorption may be the main removal mechanism (Sánchez-Polo *et al.*, 2006). An experiment in the presence of AC and in the absence of ozone shows that the main removal mechanism of atrazine is its adsorption. Therefore, for compounds with high affinity to AC, a combined process has only a limited advantage over AC alone. However, the combination of activated carbon with ozone is an optimal process for removing adsorbable and non-adsorbable ozone-refractory compounds simultaneously in a one treatment step if AC is continuously renewed.

Chapter 4

Inactivation of micro-organisms and toxicological assessment of ozone-induced products of micropollutants

4.1 DISINFECTION KINETICS

The disinfecting power of ozone has already been recognised in the 19th century (Chapter 1). Ozone has been applied for primary disinfection in drinking water treatment since the beginning of the 20th century (Chapter 5). Ozone is the best chemical disinfectant currently applied in drinking water treatment (Katzenelson *et al.*, 1974; Ellis, 1991; von Gunten, 2003b; Dahi, 1976; Hoff & Geldreich, 1981; Trukhacheva *et al.*, 1992; Bünning & Hempel, 1999). It readily copes with viruses (Katzenelson *et al.*, 1979; Kim *et al.*, 1980; Thurston-Enriquez *et al.*, 2005; Katzenelson *et al.*, 1974; Kim *et al.*, 1980; Roy *et al.*, 1980; Nupen *et al.*, 1981; Roy *et al.*, 1981a, b; 1982a, b; Finch & Fairbairn, 1991; Hall & Sobsey, 1993; Botzenhart *et al.*, 1993; Lin & Wu, 2006), with bacteria and their spores (Scott & Lesher, 1963; Broadwater *et al.*, 1973; Katzenelson *et al.*, 1974; Finch *et al.*, 1988; Botzenhart *et al.*, 1993; Finch *et al.*, 1993; Hunt & Marinas, 1997; Driedger *et al.*, 2001; Larson & Marinas, 2003; Facile *et al.*, 2000; Cho *et al.*, 2002; Jung *et al.*, 2008; Komanapalli & Lau, 1996) as well as with protozoa (Wickramanayake *et al.*, 1984a, b; Rennecker *et al.*, 1999).

For bacteria, spores and protozoa, the inactivation kinetics is typically characterised by a shoulder as schematically depicted in Figure 4.1 (right curve). But in many cases, the shoulder is quite small and a fit according to a mono-exponential decay is adequate (Figure 4.1, left curve).

This is analogous to the inactivation of cells by short-wavelength UV-radiation (UVC) and by ionising radiation. In these cases, the target is definitely DNA, whereas with long-wavelength UV-radiation (UVA), a spectral range where DNA absorbs only very little, protein damage, a much less efficient process, is the molecular basis of (solar) disinfection (Bosshard *et al.*, 2010). From UVC and ionising radiation studies, it became apparent that inactivation is not due to a single lesion, but that many DNA lesions are required for preventing reproduction [reproductive cell death, for a study on ozone-induced DNA damage and repair see Hamelin & Chung (1989)]. The shoulder arises from a competition of repairing these lesions with the help of repair enzymes and the attempt to generate a second set of complete double-stranded DNA and for dividing into two daughter cells. Strains that lack such repair enzymes no longer show the shoulder. Moreover, starving the cells ("liquid holding") prevents cells from undergoing rapid reproduction, and repair becomes more efficient. When this competition is not very pronounced, the inactivation curve may show up as a straight line (Figure 4.1, left).

To a certain extent, viruses may also make use of the repair enzymes provided by their host cells.

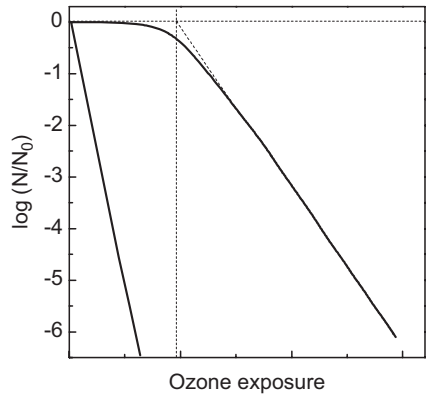

Figure 4.1 Schematic representation of the two types of inactivation curves. Mono-exponential (left), mono-exponential with shoulder (right).

The importance of repair processes may be illustrated by some numbers that are available for the lesions set by ionising radiation. The lesions set by ozone must be different, but some lesions will be similar such as single-base lesions. The more severe lesions such as DNA double-strand breaks and DNA crosslinks are possibly of minor importance in the case of ozone as a damaging agent. With ionising radiation, a dose of 1 Gy induces 0.2–0.8 lethal events in (mammalian) cells and about 1000 DNA single-strand breaks. For the same conditions, many more single-base lesions (for a typical yet not the most abundant damage, 8-oxo-adenine, 700 such lesions were estimated), 40 DNA double-strand breaks and 150 DNA-protein crosslinks occur (von Sonntag, 2006). These extraordinary large numbers show the high efficiency of the cellular repair enzymes, and it is concluded that also in the case of damages set by ozone, the majority can be repaired. It thus does not come as a surprise that some 10^8 ozone molecules are required for the inactivation of a bacterium (Scott & Lesher, 1963; Finch *et al.*, 1988).

Ionising radiation induces chromosome aberration to a similar extent as lethal effects (von Sonntag, 2006), and mutations are also observed with ozone (Rodrigues *et al.*, 1996; Dubeau & Chung, 1982; Dillon *et al.*, 1992).

Starting with Chick and Watson in 1908, there were many attempts to fit experimental data (Zhou & Smith, 1995) and to model inactivation of micro-organisms by disinfectants. A compilation and discussion of current models is given by Gyürék & Finch (1998). All of these models have in common that they neglect repair processes. For the inactivation of micro-organisms showing a shoulder, kinetics can be formulated by an empirical approach (Rennecker *et al.*, 1999; Gujer & von Gunten, 2003) [Equations (1)–(4)].

$$CT_{\text{lag}} = \frac{1}{k}\ln\left(\frac{N_1}{N_0}\right) \tag{1}$$

$$\text{if } CT \leq CT_{\text{lag}} \text{ then } \frac{N}{N_0} = 1 \tag{2}$$

$$\text{else } \frac{N}{N_0} = \frac{N_1}{N_0}\exp\left(-k \times CT\right) \tag{3}$$

$$\text{or } \frac{N}{N_0} = \exp\left(-k \times [CT - CT_{\text{lag}}]\right) \tag{4}$$

N: number of micro-organisms per unit volume; N_0: initial number of micro-organisms; N_1: intercept with ordinate resulting from extrapolating pseudo-first order line; CT: ozone exposure (see below); CT_{lag}: ozone exposure without measureable inactivation of micro-organisms; k: disinfection rate constant.

The surviving fraction (N/N_0) of a given micro-organism population when plotted as $\log(N/N_0)$ vs. the ozone CT or ozone exposure (for definitions see below) shows typically a shouldered curve (right curve in Figure 4.1). There are cases, where the shoulder is so little pronounced that this plot turns into a straight line (left curve in Figure 4.1).

Repair takes place during ozonation and any post-ozonation period including the time required for the assay measuring the surviving fraction. Table 4.1 gives an overview of inactivation parameters for various micro-organisms with ozone.

Table 4.1 Selected kinetic parameters for the inactivation of micro-organisms by ozone at 20−25°C

Micro-organism	k L mg^{-1}min^{-1}	CT_{lag} mg min L^{-1}	Ozone exposure mg min L^{-1} for inactivation of		Reference
			2-log	4-log	
E. coli	7800	*	0.0006	0.0012	Hunt & Marinas, 1997
B. subtilis spores	2.9	2.9 ~3 (varying)	4.5	6.1	Driedger *et al.*, 2001 Larson & Marinas, 2003
Rotavirus[a]	76	*	0.06	0.12	Langlais *et al.*, 1991
G. lamblia cysts	29	*	0.16	0.32	Wickramanayake *et al.*, 1984b
C. parvum oocysts	0.84	0.83	6.3	11.8	Rennecker *et al.*, 1999

[a]5°C; *very small, not detectable by applied methods

The rate of inactivation of micro-organisms by ozone depends on the type of organism and varies over about four orders of magnitude (Table 4.1). Although, compared to the reactivity of organic compounds, this is a narrower distribution, it is very important for the design of disinfection systems. Disinfection parameters (k, CT_{lag}) depend strongly on temperature (data in Table 4.1 are given for 20−25°C only), with a higher disinfection efficiency at higher temperature (Gallard *et al.*, 2003; Rakness *et al.*, 2005). Reactor hydraulics are critical for disinfection because inactivation of micro-organisms over several orders of magnitude is required (Gujer & von Gunten, 2003; Do-Quang *et al.*, 2000). This is only possible if disinfection systems approach plug-flow behaviour (Roustan *et al.*, 1992). In practice, this can be achieved by a series of completely stirred tank reactors (CSTRs), for example by dividing a reactor into chambers with baffles (Roustan *et al.*, 1991). It is the most ozone-resistant target micro-organism that determines the required ozone exposure. Lag phases are most important for the required ozone exposure as may be seen from columns 4 and 5 in Figure 4.1. Stochastic modelling indicates that the largest uncertainty in predicting inactivation of *C. parvum* oocysts lies more in the experimental determination of the lag-phase than in the inactivation rate constant (Neumann *et al.*, 2007).

There is only scarce information in the literature concerning the inactivation mechanisms of micro-organisms by ozone. During chlorination, the inactivation of *E. coli* proceeds in the following order of viability indicators: (i) loss of culturability, (ii) loss of substrate responsiveness, (iii) loss of membrane

potential, (iv) loss of respiratory activity, and finally (v) loss of membrane integrity (Lisle *et al.,* 1999). Today, culturability is the main parameter for the assessment of disinfection. With a better understanding of other endpoints, (ii)–(v), and the development of new analytical tools [e.g. flow cytometry (Hammes *et al.*, 2011)], other parameters might gain in importance for the assessment of disinfection efficiency in practice.

In waters containing significant concentrations of bromide, the required ozone exposures for a certain degree of inactivation may lead to high bromate concentrations (Driedger *et al.*, 2001; Kim *et al.*, 2004, 2007a; Buffle *et al.*, 2004). Thus bromate formation may be a limiting factor, and measures have to be taken to comply with the drinking water standard (cf. Chapters 11, 14).

4.2 INACTIVATION MECHANISMS: ROLE OF MEMBRANES AND DNA

The relatively narrow distribution of inactivation rate constants for various micro-organisms may be caused by the similar types of constituents that are attacked during inactivation of all micro-organisms. Main targets for ozone may be the nucleic acids; to what extent membrane damage contributes is as yet not known.

The kinetic parameters for the inactivation of viruses are given for rotavirus in Table 4.1. In viruses, the genetic information, represented by the nucleic acids DNA or RNA, is only protected against ozone attack by a thin protein coat. Generally, only a few protein constituents react with ozone with high rate constants. The aliphatic amino acids and also phenylalanine (note that benzene reacts at $2\ M^{-1}\ s^{-1}$) are barely reactive. The basic amino acids, incorporated in the protein, will only show ozone reactivity to the extent present as free bases. Intrinsically high reactivity can only be expected from histidine (Chapter 8) and the sulfur-containing amino acids methionine, cysteine and cystine (Chapter 9). It is thus conceivable that the viral coat is not an efficient barrier for ozone diffusing to the nucleic acids. Therefore, the high rate constant (Table 4.1) is probably due to the attack of ozone on DNA/RNA.

With bacteria, the situation is more complex. Here, DNA is attached to the bacterial membrane. Some 10^8 ozone molecules are required for the inactivation of a bacterium (Scott & Lesher, 1963; Finch *et al.*, 1988). Based on this assumption for a lake water with a total cell count of 10^9 cells/L (Hammes *et al.*, 2008), 10^{17} ozone molecules/L will be required for their inactivation. This corresponds roughly to 0.2 μM (0.01 mg/L) ozone which is far below typically applied ozone doses ($>10\ \mu M = 0.5$ mg/L). Therefore, disinfection processes do not contribute significantly to the ozone consumption under typical treatment conditions. It has been suggested that inactivation of planktonic bacterial cells is due to a destruction of the bacterial cell wall and subsequent leakage of cellular contents (Scott & Lesher, 1963). Even though there is membrane damage in the early stage of ozonation, cell viability of *E. coli* is only affected by the oxidation of DNA (Komanapalli & Lau, 1996). This is supported by the fact that the inactivation rate constant for *E. coli* (Table 4.1) is only a factor of two different from that of rotavirus, suggesting that DNA might still be the main target for ozone. Upon ozonation of a natural consortium of bacteria, membrane damage occurs simultaneously to the loss of cell numbers. For other disinfectants such as chlorine dioxide, chlorine and monochloramine, membrane integrity decreases before cell numbers are reduced (Ramseier *et al.*, 2011a). The kinetics of membrane damage of natural bacteria is slower than the kinetics of inactivation of pure cultures as determined by cultivation methods. Even though this points towards DNA damage, the two experimental systems cannot be compared directly (Ramseier *et al.*, 2011a). Therefore, further studies are needed to fully elucidate the importance of membrane damage in disinfection processes.

In addition to inactivation, ozone also causes mutations (Rodrigues *et al.*, 1996; Dubeau & Chung, 1982; Dillon *et al.*, 1992). This may be taken as evidence for DNA damage (with the cell remaining adequately

intact), but the possibility that ozone by-products (e.g. formed in the reaction with the cell wall) have caused the mutagenic effect cannot be excluded. For example, hydroperoxides and H_2O_2 are typical ozonation by-products, and the latter is known to be weakly mutagenic (Thacker, 1975; Thacker & Parker, 1976). With this in mind, ozone by-products derived from membrane damage may also contribute to cell mortality.

4.3 REACTIONS WITH NUCLEIC ACID COMPONENTS

The ozone-reactive components of the nucleic acids are the nucleobases: thymine, cytosine, adenine and guanine in DNA. Some viruses contain RNA instead of DNA, and here thymine is replaced by uracil.

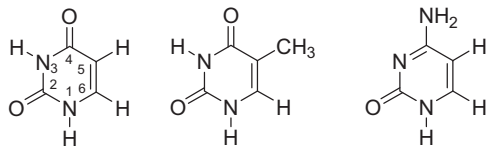

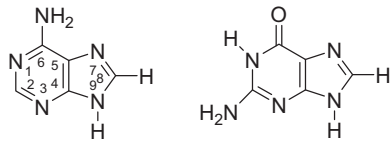

There is a remarkable spread of ozone rate constants among the nucleic acid constituents (Chapter 6, Table 6.1). Notably, the rate constants of the Ade nucleosides, adenosine (Ado) and deoxyadenosine (dAdo), are very low. This is in great contrast to $^{\bullet}OH$ reactions that are close to diffusion-controlled for all nucleobases (von Sonntag, 2006).

The ozone chemistry of thymine and thymidine has been elucidated in quite some detail (Flyunt *et al.*, 2002) (Chapter 6). The reactive site is the quasi-olefinic C(5)–C(6) double bond. This may also hold for uracil and cytosine. The substantial increase in the rate of reaction of the pyrimidines with ozone upon deprotonation may be largely due to an increase in the electron density in the reacting double bond. With Cyt and cytidine (Cyd)/deoxycytidine (dCyd), protonation at the exocyclic nitrogen acts in the opposite direction, that is, it lowers the rate of reaction.

With the pyrimidine free bases, the formation of some singlet oxygen, notably at high pH is observed, but not with the corresponding nucleosides (Table 6.7) (Muñoz *et al.*, 2001). Mechanistic aspects are also discussed in Chapter 6.

The rate of reaction of Ado and dAdo are very low, and this may be due to the fact that the aromatic ring contains two nitrogens. Nitrogen-containing heteroaromatics react only very slowly with ozone (Chapter 8). The electron density at the exocyclic amino group must be also low, but the formation of singlet oxygen (20%, Table 6.7) and of $^{\bullet}OH$ radicals [43% (Flyunt *et al.*, 2003a)] point to this nitrogen as the preferred site of attack. The *N*-oxide at N1 is formed upon the reaction of H_2O_2 with dAdo (Mouret *et al.*, 1990). This *N*-oxide is not formed in the reaction of ozone with dAdo (Muñoz *et al.*, 2001). A more detailed product study is still missing, but reactions (5)–(8) may be tentatively suggested to account for the formation of $^1O_2$ and of $^{\bullet}OH$. Potential precursors of $^{\bullet}OH$ are $O_3^{\bullet-}$ [reaction (7)] or $O_2^{\bullet-}$ [reaction (8); for the ensuing chemistries see Chapter 8].

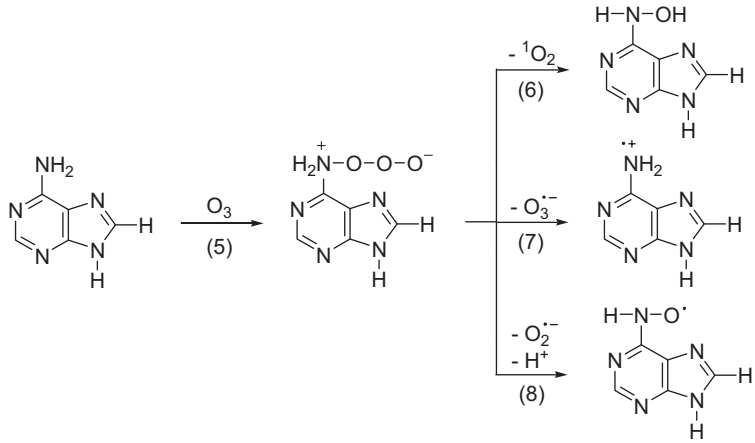

Singlet oxygen (40%, Table 6.7) but no $^{\bullet}$OH (Flyunt *et al.*, 2003) are formed with Gua derivatives. The latter is surprising as the reduction potential of the guanine riboside Guo is lower ($E_7 = 1.29$ V) than that of adenine riboside Ado ($E_7 = 1.56$ V) (von Sonntag, 2006). This may exclude reaction (7) and favour reaction (8) as the precursor of $^{\bullet}$OH.

4.4 REACTION WITH DNA

In the reaction of ozone with DNA, $^{\bullet}$OH plays an important role (Van der Zee *et al.*, 1987; Theruvathu *et al.*, 2001). This $^{\bullet}$OH formation must be due to the reaction of ozone with the adenine moiety (Ishizaki *et al.*, 1984; Theruvathu *et al.*, 2001). For the determination of the intrinsic ozone rate constant with DNA, tertiary butanol has to be added. Under such conditions, the rate of reaction of DNA is only 410 $M^{-1}s^{-1}$ (in the absence of tertiary butanol $k_{obs} = 1.1 \times 10^3$ $M^{-1}s^{-1}$), i.e. much lower than that of the weighted average of the nucleobases. In the case of $^{\bullet}$OH, which reacts with the nucleobases and their derivatives at close to diffusion-controlled rates [$k \approx 3 \times 10^9$ $M^{-1}s^{-1}$ (Buxton *et al.*, 1988)], the rate constant of $^{\bullet}$OH with DNA is considerably lower [$k = 2.5 \times 10^8$ $M^{-1}s^{-1}$ (Udovicic *et al.*, 1994)], since in this non-homogeneous reaction with the macromolecule DNA two terms, a diffusion term (k_{diff}) and a reaction term (k) have to be considered (Udovicic *et al.*, 1991). The observed overall rate constant (k_{obs}) is the harmonic mean of these two rate constants [cf. Equation (9)].

$$\frac{1}{k_{\text{obs}}} = \frac{1}{k} + \frac{1}{k_{\text{diff}}} \tag{9}$$

In contrast to $^{\bullet}$OH, ozone reacts with the nucleobases at rates much below the diffusion-controlled limit, and the second term must fall away. Hence, the rate of reaction of ozone with the nucleic acids is only given by the first term, that is, it should be close to that of the weighted average of the concentrations of the various nucleobases in the nucleic acid times their rate constants with ozone. This is not observed. The reason for this is as yet not understood. As on this basis, the dAdo moiety can barely contribute (cf. the low rate constant given in Table 6.1) and the explanation that $^{\bullet}$OH production must be due to an ozone reaction with this moiety must fall away. It is tentatively suggested that in double-stranded DNA, hydrogen bonding between the nucleobases and base stacking may be the reason for these unexpected effects.

Corresponding experiments with RNA are as yet not available. From the rate constants given in Table 6.1, one would assume that in RNA the guanine moiety is the most likely one to become degraded upon ozone treatment. This has indeed been observed (Shinriki *et al.*, 1981). In DNA, the situation might be somewhat different. Besides guanine, thymine may be the other preferred target.

4.5 APPLICATION OF OZONE FOR DISINFECTION IN DRINKING WATER AND WASTEWATER

To assess the disinfection efficiency in water treatment, the CT-concept is applied. C stands for the concentration of disinfectant (ozone) and T for the contact time; CT is the product of the aqueous disinfectant concentration and contact time. In laboratory systems where ozone can be directly measured, the CT can be expressed as ozone exposure. This corresponds to the integral under the ozone decay curve of an ozone vs. time plot (von Gunten & Hoigné, 1994). In real reactor systems, the CT value is not easily accessible. Often, time-resolved ozone concentration profiles and contact times are not readily available. To overcome this problem, several concepts have been developed (Rakness, 2005; Rakness *et al.*, 2005). A conservative approach is the calculation of CT_{10}, where C is the reactor effluent concentration (or concentration at last sampling point) and T_{10} is the travel time of the first 10% of the water going through the reactor. T_{10} is typically much shorter than the hydraulic retention time τ; the T_{10}/τ ratio is often around 0.5 (Roustan *et al.*, 1993). This approach does not take into consideration that the ozone concentration is significantly higher near the influent of the reactor, and ozone exposure is underestimated. Especially for ozone-resistant micro-organisms such as *C. parvum* oocysts (Table 4.1), this approach may lead to higher required ozone doses and hence to an increased formation of disinfection by-products such as bromate (Chapters 11 and 14). To make a better approximation of the real ozone concentration in the reactor, calculating the geometric mean of the ozone concentrations at the inlet and outlet $[C = (C_{in} \times C_{out})^{0.5}]$ has been suggested (Rakness *et al.*, 2005). This method is an improvement compared to the standard CT_{10} approach. Yet, it is still far from the real ozone exposure. To further improve the prediction of disinfection efficiency, combined models including reactor hydraulics (determined by tracer experiments), ozone decay kinetics and disinfection kinetics have to be used (Roustan *et al.*, 1993; von Gunten *et al.*, 1999; Do-Quang *et al.*, 2000; Gallard *et al.*, 2003; Kim *et al.*, 2004; Smeets *et al.*, 2006). To include the variability of parameters such as inactivation rate constant, CT_{lag}, ozone decay rate, temperature, changes in water quality and hydraulics, "uncertainty modelling" is a powerful tool for assessing the variability in the disinfection efficiency (Neumann *et al.*, 2007). With increasing computing power, methods based on computational fluid dynamics can make even more accurate predictions and are a valuable tool in reactor design (Wols *et al.*, 2010).

In wastewater, ozone decay is typically too fast for using measured ozone concentrations to calculate CT values (Chapter 5). Parameters for process design in wastewater disinfection by ozone have been discussed (Xu *et al.*, 2002).

4.6 TOXICOLOGICAL ASSESSMENT OF OZONE INDUCED TRANSFORMATION PRODUCTS

The abatement of organic micropollutants during ozonation does typically not lead to their mineralisation but to the formation of transformation products (Huber *et al.*, 2004; McDowell *et al.*, 2005; Radjenovic *et al.*, 2009; Benner & Ternes, 2009a, b; Dodd *et al.*, 2010; Lange *et al.*, 2006; Schumacher *et al.*, 2004a). Thus, ozonation products may contain more or fewer structural similarities to the original

compounds, and the question arises, whether the original biological effects (e.g. antimicrobial activity, oestrogenicity, herbicidal properties, etc.) are lost even when the molecules are only slightly modified. There is also some concern about new biological effects resulting from the transformation of micropollutants. Since these questions can rarely be answered by elucidating the structures of the transformation products only, ozonated solutions of a biologically active compound may have to be tested for remaining or new biological activity (Mestankova *et al.*, 2011; Escher & Fenner, 2011). In the following, some of the most important classes of biologically active compounds and the change in biological activity upon ozonation will be discussed.

4.7 ENDOCRINE DISRUPTING COMPOUNDS

Compounds behaving like hormones and disturbing the hormonal status of an organism are called endocrine disrupting compounds (EDCs). Among many other bioactive compounds, they are considered the most important class in terms of adverse effects to aquatic life (Runnalls *et al.*, 2010). The general implication for the water industry of the presence of EDCs and other micropollutants and their removal has been addressed (Snyder *et al.*, 2003, 2006; Broséus *et al.*, 2009). The simplest way to disturb the hormonal system of an organism is to interact with a receptor in a way similar to the hormone itself. The receptor of the female hormone oestrone is a typical example and is called an oestrogen receptor, because it also binds other oestrogenic compounds such as the natural hormone oestradiol and the synthetic hormone 17α-ethinyloestradiol. These oestrogenic compounds are phenols, and the phenolic group is essential for binding to the oestrogen receptor (Lee *et al.*, 2008). They are found in WWTP effluents in concentrations of up to several ng/L (Andersen *et al.*, 2003; Ning *et al.*, 2007a). One of the main concerns of the release of oestrogenic compounds is the feminisation of male fish (Sumpter & Johnson, 2008). In an experimental lake in north-western Ontario, Canada, the fish population was almost extinct after a seven-year exposure to 5−6 ng/L 17α-ethinyloestradiol (Kidd *et al.*, 2007).

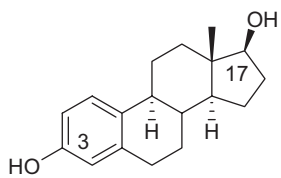

Oestradiol (E2)

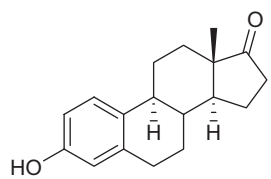

Oestron (E1)

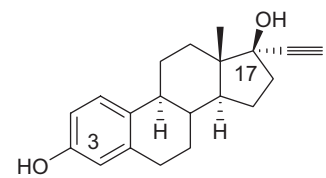

17α-Ethinyloestradiol (EE2)

Besides the phenol function, there are hydrophobic binding sites that influence the equilibrium constant of equilibrium (10).

$$\text{EDC} + \text{oestrogen receptor} \rightleftarrows \text{bound EDC} \tag{10}$$

Because of structural similarities to oestrogenic compounds, many industrial and natural compounds can also bind to oestrogen receptors with different equilibrium constants of equilibrium (10) and hence exert different endocrine disrupting potentials (Bonefeld-Jörgensen *et al.*, 2007). A critical review on *in vitro* and *in vivo* effects of synthetic organic chemicals including phenol-containing compounds is available (Tyler *et al.*, 1998). Some examples of such compounds will be discussed in the following.

Bisphenol A, *t*-butylphenol, octylphenol and nonylphenol are technical products and abundant in wastewaters and surface waters (Ahel *et al.*, 1994; Voutsa *et al.*, 2006; Ning *et al.*, 2007a).

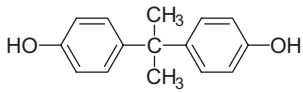

Bisphenol A

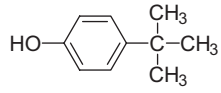

***t*-Butylphenol**

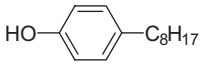

Octylphenol

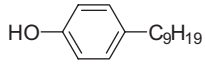

Nonylphenol

The isoflavone family (formononetine, daidzein, equol, biochanin, genistein) is typically found in surface waters (Hoerger *et al.*, 2009).

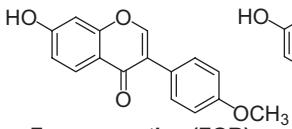

Formononetine (FOR)

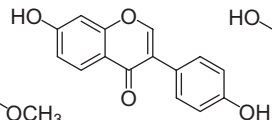

Daidzein (DAI)

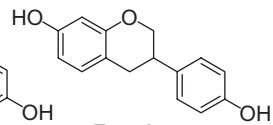

Equol

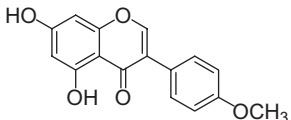

Biochanin (BIO)

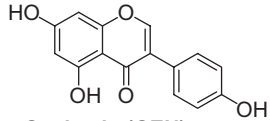

Genistein (GEN)

Parabenes, esters of the *p*-hydroxybenzoic acid, also belong to the group of EDCs. They seem to be mainly taken up by cosmetics (Darbre & Harvey, 2008).

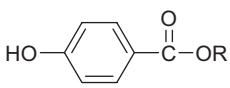

Parabene

A typical example of an endocrine disruptor is nonylphenol. There are more than 500 isomers, including stereoisomers, conceivable (Günther, 2002). To visualise this, four of them are shown below.

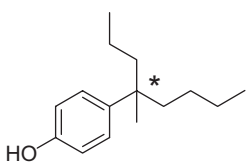

4-[1-Methyl-1-propyl-pentyl]-phenol

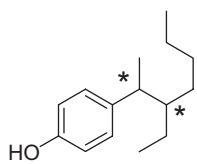

4-[2-Ethyl-1-methyl-phexyl]-phenol

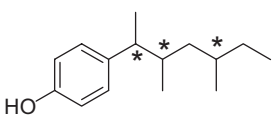

4-[1,2,4-Trimethyl-hexyl]-phenol

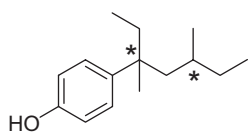

4-[1-Ethyl-1,3-dimethyl-pentyl]-phenol

They differ by orders of magnitude in their binding constants and hence in their endocrine disrupting potential. The daily intake of nonylphenols by food has been estimated at 7.5 µg for an adult in Germany (Günther, 2002). This high value indicates that drinking water may not be the major source of EDCs to man, but the main concern of these EDCs is related to their adverse effects on aquatic life (Oehlmann *et al.*, 2000, 2006; Kidd *et al.*, 2007; Sumpter & Johnson, 2008). Nonylphenols lead to feminisation of aquatic organisms and a decrease in male fertility and the survival of juveniles at concentrations below 10 µg/L (Soares *et al.*, 2008). Prosobranch snails have been suggested as test organisms (Duft *et al.*, 2007; Oehlmann *et al.*, 2007). For a comparison of prosobranch snails and fish see Jobling *et al.* (2004). Similar concerns are related to bisphenol A. Its mode of action and potential human health effects have been reviewed (Vandenberg *et al.*, 2009).

Tin compounds show a strong endocrine disrupting activity for aquatic life (Duft *et al.*, 2003a; Duft *et al.*, 2003b; Wirzinger *et al.*, 2007). Tributyl- and triphenyl tin have a very different mode of action as xeno-androgens (Schulte-Oehlmann *et al.*, 2000).

Even drugs such as carbamazepine (Oetken *et al.*, 2005) or the herbicide atrazine (Hayes *et al.*, 2002) seem to have endocrine disrupting properties.

As there are so many different compounds that give rise to endocrine disrupting activity, *in vivo* and *in vitro* test systems have been developed to assess water samples experimentally. Two test systems that are widely used for *in vivo* and *in vitro* oestrogenicity assessment are based on *in vivo* measurement of the blood plasma vitellogenin (VTG) concentrations in male rainbow trout (*Oncorhynchus mykiss*) and *in vitro* measurement of the oestrogen binding to a human oestrogen receptor (yeast oestrogen screen, YES) [for a review see (Sumpter & Johnson, 2008), for some recent developments requiring shorter reaction times (LYES) see (Schultis & Metzger, 2004)]. For the YES assay, two plasmids have been introduced into a yeast cell. The first plasmid generates the human α-oestrogen receptor. Upon addition of the EDC to be tested, it binds to the receptor according to equilibrium (10) and changes its structure. This receptor complex now binds to the second plasmid and triggers the formation of a marker enzyme. The resulting enzyme activity is measured. In these assays, bisphenol A and the mixture of technical nonylphenols are about four orders of magnitude less potent than oestradiol.

The effect of ozonation on the oestrogenic activity of natural and synthetic EDCs has been investigated in laboratory and full-scale studies.

4.7.1 Laboratory studies

Ozonation of nonylphenols leads to an intermediate increase in the oestrogenicity (Sun *et al.*, 2008). Hydroxylation is a major process in the ozone chemistry of phenols (Chapter 7), and 4-nonylcatechol has a higher oestrogenic activity than 4-nonylphenol itself. When all phenolic compounds are degraded, oestrogenic activity disappears. In contrast to this study, it has been reported that there is still some residual oestrogenicity (E-screen assay with MCF-7 cells) even after full transformation of bisphenol A, E1 and EE2 (Alum *et al.*, 2004). This is in contrast to studies that have shown a stoichiometric loss of the oestrogenicity with the transformation of EE2 by ozone and $^{\bullet}OH$ radicals (Huber *et al.*, 2004; Lee *et al.*, 2008). Figure 4.2 shows the decrease of the relative EE2 concentration (open circles) as a function of the ozone dose (in presence of tBuOH as a scavenger for $^{\bullet}OH$ radicals) and as a function of the fluence in the UV/H_2O_2 process (oxidation by $^{\bullet}OH$ radicals; direct photolysis can be neglected) (Lee *et al.*, 2008).

Figure 4.2 also shows the oestrogenic activity expressed as EEEQ (17α-ethinyloestradiol equivalents, open circles). In the insets, the relative EEEQ is plotted vs. the relative EE2 concentrations. The good correlation between the two parameters with a slope of unity indicates that both oxidants lead to a loss of oestrogenicity by the first attack on the EE2 molecule. Loss of oestrogenicity upon $^{\bullet}OH$ attack was also

confirmed for E2 and EE2 (Linden *et al.*, 2007). Other oxidants such as chlorine, bromine, chlorine dioxide and ferrate (VI) also efficiently destroy the oestrogenicity of EE2 (Lee *et al.*, 2008).

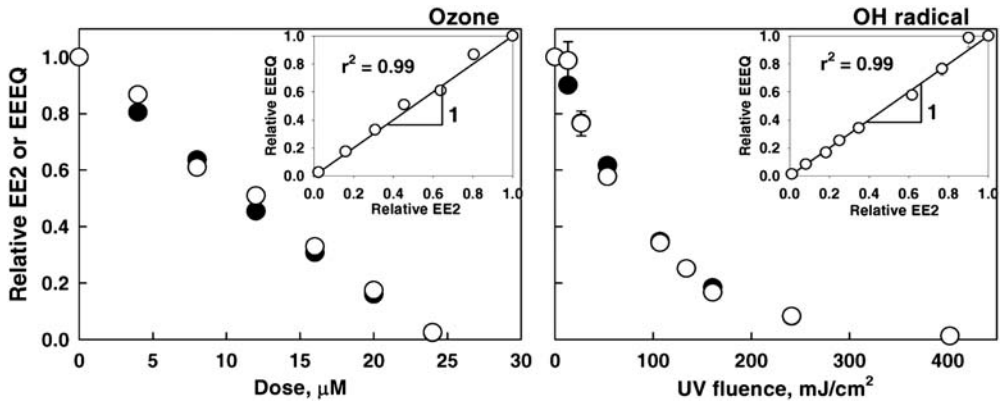

Figure 4.2 Decrease of the relative EE2 concentration (filled circles) and oestrogenic activity (open circles) EEEQ, 17α-ethinyloestradiol equivalents due to the oxidation by ozone and •OH radicals. Insets show plots of the relative EEEQ versus the relative EE2 concentration. Experimental conditions: $[EE2]_0 = 10$ μM, pH = 8, $T = 23$°C, ozonation in presence of tBuOH (5 mM). When filled circles are invisible, data overlap with open circles. Reprinted with permission from (Lee *et al.*, 2008). Copyright (2008) American Chemical Society.

4.7.2 Full-scale studies

A considerable number of EDCs have been detected in WWTPs (Spengler *et al.*, 2001). In many WWTPs, oestrogenicity is controlled by oestrogenic compounds (E1, E2 and EE2) with concentrations in the ng/L range rather than industrial compounds such as alkylphenols, alkylphenolmonoethoxylates and alkylphenoldiethoxylates, even though present in μg/L levels (Aerni *et al.*, 2004). However, this might be different in WWTPs with a high contribution of industrial wastewater. Oestrogenicity in wastewater is eliminated well by activated sludge processes (> 90% removal) (Escher *et al.*, 2009). Since many EDCs are phenols, they are readily eliminated by an ozonation step and lose their hormonal activity upon attack by chemical oxidants (see above). This was demonstrated in a full-scale WWTP in Switzerland where a > 95% elimination of oestrogenicity (YES assay) was found upon ozonation (Escher *et al.*, 2009). In another study, the oestrogenicity was reduced by 90% for an ozone dose of about 0.4 mgO_3/mg DOC (Stalter *et al.*, 2011). The effective removal of oestrogenic activity by ozonation has been confirmed by an additional test with yolk-sac larvae (Stalter *et al.*, 2010b). A significant reduction of vitellogenin levels was observed in fish exposed to ozonated wastewater compared to fish reared in conventionally treated wastewater.

In other WWTPs, oestrogenicity (YES assay) decreases in parallel to the degradation of bisphenol A by ozone (Figure 4.3).

The same effect is also apparent in the effluent of two other WWTPs where bisphenol A and EEQ were 10% (Köln-Stammheim) and 1% (Bottrop) of the given example. In these wastewaters, there is a very close correlation between the presence of the technical product bisphenol A and oestrogenicity. This points to the predominance of industrial sources (contraceptives were below detection) for the observed oestrogenicity in these wastewaters. However, bisphenol A and alkylphenols (data not shown) can only account for about 10% of the observed oestrogenicity. Therefore, there must be other, as yet unknown, oestrogenic

micropollutants that give rise to the YES assay response. They may belong to the phenol family, as bisphenol A and YES assay show the same ozone response (Figure 4.3). Such a discrepancy between YES assay and detected micropollutants with ED activity is not uncommon. Also in estuarine sediments the oestrogenic activity is not adequately reflected ($<1\%$) by the concentrations of known oestrogens (Thomas *et al.*, 2004). Nevertheless, in other municipal wastewaters with less industrial influence the oestrogenicity could be reasonably well predicted by summing up the effects of individually measured compounds such as E1, E2 and EE2 (Aerni *et al.*, 2004).

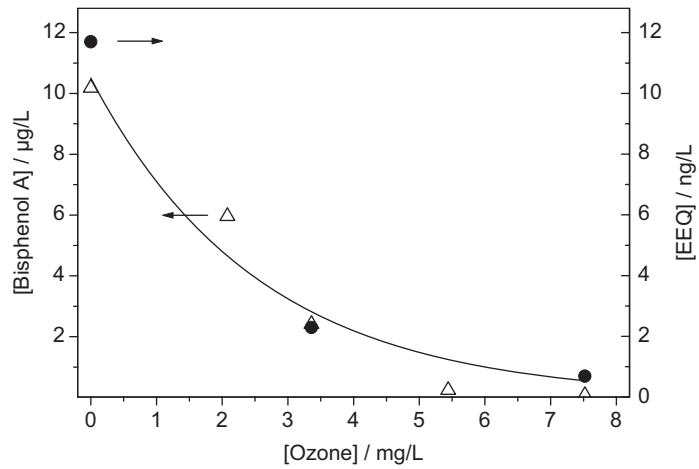

Figure 4.3 Decrease of the bisphenol A concentration (triangles, left axis) and of the oestrogenicity (YES assay, E2 equivalent (EEQ), circles, right axis in the effluents of the WWTPs of Düsseldorf-Süd (DOC = 16 mg/L). Adapted from (Nöthe, 2009), with permission.

4.8 ANTIMICROBIAL COMPOUNDS

A quasi-definition of a micropollutant is that the compound in question must show some biological activity. Two commonly asked questions are whether ozonation decreases or increases the biological activity, and when it decreases the biological activity, how many moles of ozone are required for reducing the biological activity to an insignificant level. A group of compounds that lose their biological activity are the phenolic EDCs discussed above. The fact that after ozonation $\leq 3\%$ of the starting material is slowly regenerated after ozonation (Chapter 7) is considered insignificant in the present context. Clinically important antibiotics are found in individual concentrations from 0.5 to 3 µg/L in raw and primary wastewaters, and a reduction of 60−90% of their concentration typically occurs during activated sludge treatment [(Dodd *et al.*, 2006a) and references therein]. In general, resulting effluent concentrations are below levels affecting bacteria and aquatic life, but there might still be effects of certain antibiotics on aquatic organisms and on bacteria in the activated sludge process (Dodd *et al.*, 2006a). The main concern related to antibiotics is the development of antibiotic resistance in microbial consortia (Kümmerer, 2009a, b). To date it is, however, not yet clear, whether this can happen in activated sludge processes or in the aquatic environment (Kümmerer, 2009b). Antibiotics comprise many classes of compounds containing ozone-reactive moieties: macrolides (tertiary amines, Chapter 8), sulfonamides (anilines, Chapter 8), fluoroquinolones (piperazines, Chapter 8), lincosamide (thioether, Chapter 9), β-lactams (olefins, Chapter 6; thioethers, Chapter 9), tetracycline (olefins, Chapter 6;

phenols, Chapter 7), glycopeptides (phenols, methoxytoluene, Chapter 7), aminoglycosides (primary amines, Chapter 8) (Dodd *et al.*, 2006a). With the exception of β-lactams, all investigated antibiotics (9 classes, 14 compounds) lost their antimicrobial activity during ozonation in parallel to the loss of the parent compound (Dodd *et al.*, 2009; Lange *et al.*, 2006). This means that the primary attack of ozone (exclusion of $^{\bullet}OH$ reactions) on the parent compound efficiently removes its antimicrobial activity. This is shown in Figure 4.4 for macrolides and Figure 4.5 for fluoroquinolones.

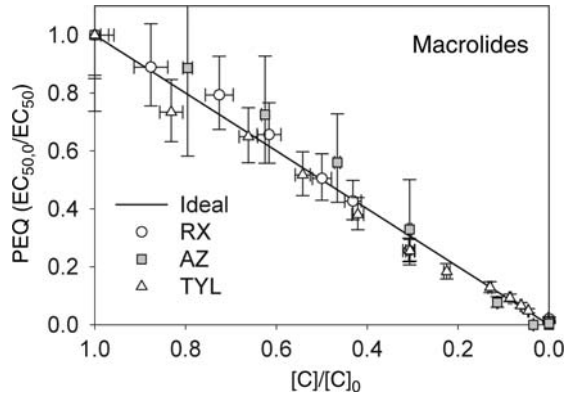

Figure 4.4 Deactivation stoichiometries of macrolides by ozone at pH 7 (tBuOH = 5 mM). PEQ: Potency equivalent derived from growth inhibition tests; RX: roxithromycin; AZ: azithromycin; TYL: tylosin. Reprinted with permission from (Dodd *et al.*, 2009). Copyright (2009) American Chemical Society.

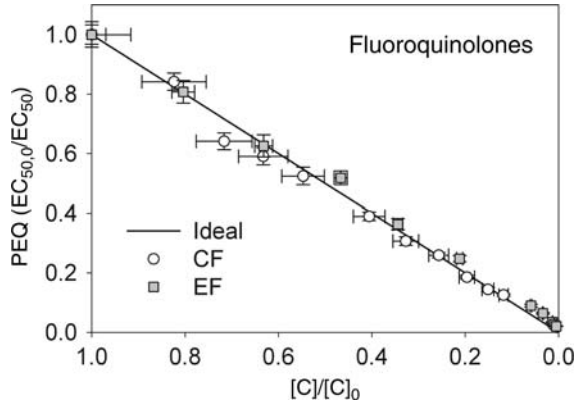

Figure 4.5 Deactivation stoichiometries of fluoroquinolones by ozone at pH 7 (tBuOH = 5 mM). PEQ: potency equivalent derived from growth inhibition tests; CF: ciprofloxacin; EF: enrofloxacin. Reprinted with permission from (Dodd *et al.*, 2009). Copyright (2009) American Chemical Society.

Similar data as shown in Figure 4.4 have been reported for the macrolide antibiotic clarithromycin (Lange *et al.*, 2006). For the attack of $^{\bullet}OH$ on antibiotics, a slight deviation of the ideal loss of antibacterial activity was observed for β-lactams (Dodd *et al.*, 2009). This was attributed to the formation of hydroxylated analogues of the parent compounds which are known to exert an antibacterial activity similar to or

higher than the parent compounds themselves (Kavanagh, 1947). For higher degrees of transformation, however, the residual antibacterial activity was destroyed.

A discussion of ozone-reactivity of the two β-lactams penicillin G and cephalexin and the products formed upon ozone attack (Dodd *et al.*, 2010) is given in Chapter 9. The (*R*)-sulfoxides have some residual antimicrobial activity. With cephalexin, this is of no importance, because an attack of ozone on the remaining olefinic function leads to an efficient loss of the antibacterial activity. In the case of penicillin G, however, the (*R*)-sulfoxide is ozone-resistant and retains about 15% of the antibacterial activity of penicillin G. Yet during wastewater ozonation, penicillin-G-(*R*)-sulfoxide is efficiently oxidised by $^{\bullet}$OH, and the antibacterial activity is removed at typical ozone doses (Dodd *et al.*, 2010).

The antiviral drug oseltamivir acid (active metabolite of Tamiflu®, see Chapter 6) may be applied in high quantities during pandemic influenza outbreaks and significant concentrations can be expected in wastewaters, even more so because this compound is not efficiently removed in biological wastewater treatment (Prasse *et al.*, 2010). The loss of antiviral activity due to treatment with ozone and $^{\bullet}$OH was investigated by measuring neuraminidase inhibition of two viral strains (Mestankova *et al.*, 2012). For both oxidants and low doses, an increased activity was produced that disappeared at high degrees of transformation of the parent and also when solutions were analysed after 24h. Primary unstable products exerting a higher antiviral activity than the parent compound must thus be formed (Mestankova *et al.*, 2012).

Biocides are also ubiquitous compounds found in wastewater effluents. Triclosan, a common additive to soaps and personal care products reacts quickly with ozone (Chapter 7). Its antibacterial properties are lost upon the first attack of ozone (Suarez *et al.*, 2007) while some dioxin-like activity is formed (Mestankova *et al*., in preparation.). The dioxin that is formed in the photolysis of triclosan has been characterised as 2,8-dichlorodibenzo-*p*-dioxin (Latch *et al.*, 2005).

4.9 TOXICITY

Tests on biological activity can reveal valuable information as to the feasibility of ozone application in micropollutant abatement (Gerrity & Snyder, 2011). Additional tests in real water systems might be necessary for ascertaining further endpoints and the role of mixtures of micropollutants and of the water matrix (e.g. DOM). Table 4.2 summarises effect-oriented studies on ozone-treated secondary wastewater effluents.

Table 4.2 Biological test results from *in vivo* and *in vitro* tests on secondary effluents treated with ozone

Treatment system	Test systems	Results	References
Full-scale ozonation wastewater	Pre-concentration of samples –Bioluminescence inhibition –Oestrogenicity –Arylhydrocarbon receptor response –Genotoxicity –Neurotoxicity –Phytotoxicity	Significant decrease of all effects upon ozonation step	Macova *et al.*, 2010; Reungoat *et al.*, 2010

(*Continued*)

Table 4.2 Biological test results from *in vivo* and *in vitro* tests on secondary effluents treated with ozone (*Continued*)

Treatment system	Test systems	Results	References
Full-scale ozonation of secondary effluent	Pre-concentration of samples –Bioluminescence inhibition –Growth inhibition –Inhibition of photosynthesis –Oestrogenicity –Inhibition of acetylcholinesterase –Genotoxicity	Significant removal of all effects during ozonation –No genotoxicity formation during ozonation	Escher *et al.*, 2009
Ozonation of secondary effluent	*In vitro* tests after pre-concentration –*In vivo* tests with whole effluent –Genotoxicity –Retionic acid receptor (RAR) agonist activity –Acute ecotoxicity (*Daphnia magna*) –Japanese medaka embryo exposure tests	Significant removal of genotoxicity, RAR agonist activity and acute ecotoxicity – Higher ozone doses lead to a reduction in hatching success rate of Japanese medaka embryos	Cao *et al.*, 2009
Tertiary treated sewage effluent (ozonation)	*In vivo* tests with juvenile rainbow trout *O. mykiss* in liver and kidney tissues –Glutathione *S*-transferase (GST) –Total glutathione (GSH) –Glutathione peroxidase (GPX) –Lipid peroxidase (LPO) –Haem peroxidase	Liver: Increased haem peroxidase, LPO and GST –Total GSH depleted –Kidney: Increased LPO, GPX observation shows oxidative stress of organism –Coagulation after ozonation reduces these effects	Petala *et al.*, 2009
Ozonation of secondary effluent	*In vivo* tests –*Lemna minor* growth inhibition –Chironomid toxicity test with the non-biting midge *Chironomus riparius* –*Lumbriculus variegatus* toxicity –Genotoxicity –Oestrogenicity	Growth inhibition –Removal of oestrogenicity –Increased genotoxictiy –Enhanced toxicity for *Lumbriculus variegates* –Effects disappear after rapid sand filtration after ozonation	Stalter *et al.*, 2010a

(*Continued*)

Table 4.2 Biological test results from *in vivo* and *in vitro* tests on secondary effluents treated with ozone (*Continued*)

Treatment system	Test systems	Results	References
Ozonation of secondary effluent	Fish early life stage toxicity test (rainbow trout, *O. mykiss)*	Development retardation –Effect disappears after post-sand filtration –Removal of oestrogenicity	Stalter *et al.*, 2010b

Toxicity is not as well-defined as, for example, endocrine disruption. Endocrine disruption can be well-described by a relatively simple assay, for example, the YES assay that provides a reasonable answer. Other tests may be used for confirmation, but are not strictly required. In contrast for describing toxicity, many different test systems may have to be utilised depending on the relevant endpoints for ecosystems (Stalter *et al.*, 2010a). Different toxicity tests have been carried out with ozonated wastewater (Table 4.2). For example, the *Lumbriculus variegatus* test, based on the development of this worm within 28 days, revealed a significantly enhanced toxicity after ozonation compared to conventional treatment (Stalter *et al.*, 2010a). Moreover, a significantly increased genotoxicity was observed, detected with the comet assay using haemolymph of the zebra mussel (Stalter *et al.*, 2010a). The comet assay, originally developed for radiation-induced DNA strand breakage caused by ionising radiation in cells (Ostling & Johanson, 1984), has been later applied to the assessment of DNA-reactive agents (Collins *et al.*, 1997). Also the fish early life stage toxicity test (FELST) using rainbow trout (*Oncorhynchus mykiss*) revealed a considerable developmental retardation of test organisms exposed to ozonated wastewater (Stalter *et al.*, 2010b). All these effects were removed by subsequent sand filtration to the level of conventional treatment. Activated carbon treatment even resulted in a significant reduction of genotoxicity. The build-up of toxicity upon ozonation and its subsequent removal during post-sand filtration points to the formation of biodegradable organic compounds such as aldehydes and ketones from the reaction of ozone with DOM (Chapter 3). Apparently, these compounds show toxicity in certain test systems but not in others. It is very unlikely that the increased toxicity is caused by transformation products from micropollutants.

The above statement, that toxicity is not a simple parameter, is illustrated by the fact that other parameters that can measure toxicity such as the *Lemna minor* growth inhibition test and the *Chironomid* toxicity test did not give a response on ozonated wastewater (Stalter *et al.*, 2010a).

It seems fair to conclude that ozone-induced toxicity is mostly transient and can be eliminated by biological sand filtration or biological activated carbon filtration. Hence, toxicity may not be a major obstacle for introducing ozonation as a polishing step in wastewater treatment.

Chapter 5

Integration of ozonation in drinking water and wastewater process trains

5.1 HISTORICAL ASPECTS

5.1.1 Drinking water

In France, the earliest test with ozonation for disinfection dates back to 1886. In 1906, ozonation for full-scale drinking water disinfection, after slow sand filtration, was installed in Nice (France) (Le Palouë & Langlais, 1999). In the early applications of ozone in water treatment, ozonation was basically a replacement for chlorine disinfection. Especially in water supplies treating groundwater, there was a substantial carryover of ozone into reservoirs and the distribution systems, because in these waters ozone is quite stable due to the low DOC concentration and the high carbonate alkalinity (Chapter 3). In Germany, ozonation of groundwaters and surface waters also started around 1900. Several plants (Wiesbaden, Paderborn, Hermannstadt) were closed down, however, after only a few years of operation, mainly due to the lower costs of chlorination (Böhme, 1999). In the USA, the first ozone installations for taste and odour or colour removal were established in the early 1900s. Significant capacity was only installed in the mid-1980s (Rice, 1999). In other countries such as Japan, Canada, UK, The Netherlands, Belgium and Switzerland, ozone application for drinking water treatment started between the 1940s and the 1960s (Matsumoto & Watanabe, 1999; Lowndes, 1999; Kruithof & Masschelein, 1999; Geering, 1999; Larocque, 1999). A compilation of the estimated number of drinking water treatment plants in Europe and North America is shown in Table 5.1. From this comparison, it is evident that the number of ozonation plants per capita is very high in France and Switzerland, whereas it is rather low in the USA and Japan. This reflects the high affinity of many water suppliers to chlorine and related products, despite the many disadvantages of these oxidants compared to ozone (Sedlak & von Gunten, 2011).

5.1.2 Municipal wastewater

So far, there is only a limited number of wastewater treatment plants that use ozonation. Most of these plants are located in Canada, Germany, Japan, South Korea and the USA (Paraskeva & Graham, 2002) with the main objective of disinfection. Disinfection of wastewater effluent is mandatory in some states in the USA. In Europe, it is only applied occasionally for achieving bathing water quality goals. Disinfection of wastewaters is typically also applied for irrigation or other reuse purposes. Disinfection of wastewaters, however, is often achieved with chlorine or UV rather than ozone. Nevertheless, the growing importance of water reuse and the discussion on enhanced treatment of wastewaters for micropollutant removal may

render ozone more attractive because of its dual role as disinfectant and as oxidant (Ternes *et al*., 2003; Reungoat *et al*., 2010; Hollender *et al*., 2009; Oneby *et al*., 2010; Zimmermann *et al*., 2011).

Table 5.1 Estimated number of drinking water plants using ozone in Europe, North America and Japan (numbers from period 1997–2011)

Country	Number of plants	Number of plants per million capita	References
Switzerland	108	13.8	von Gunten & Salhi, 2003
France	700	10.6	Langlais *et al*., 1991
Canada	68	2	Larocque, 1999
Germany	>100	1.2	Böhme, 1999; Loeb *et al*., 2011
United Kingdom	50	0.8	Lowndes, 1999
BENELUX	ca. 20	0.72	Kruithof & Masschelein, 1999
USA	200	0.64	Rice, 1999
Japan	>50	>0.39	Loeb *et al*., 2011

5.2 DRINKING WATER TREATMENT SCHEMES INCLUDING OZONATION

Even though ozone was originally used in one- or two-step processes, today it is widely accepted that ozone should at least be combined with a biological treatment step for removal of AOC/BDOC (Chapter 3). Nowadays, ozonation is mostly used for treatment of surface waters and is integrated into multi-barrier treatment systems (Kruithof & Masschelein, 1999). The development of the integration of ozonation into water treatment trains is shown schematically in Figure 5.1(a) for the evolution of lake water treatment in Switzerland from the 1950s to 2005.

This is representative for the development of treatment trains in other industrialised countries as well. Figure 5.1(b) shows the evolution of the phosphate concentration in Lake Zurich which is an indicator of the degree of eutrophication with a peak in the early 1970s. Drinking water treatment had to follow this development (additional treatment steps) to cope with the various problems related to eutrophication (turbidity, high DOC concentrations, taste and odour issues, etc.). The phosphate concentration in Swiss lakes was reduced by rigorous measures in water pollution control (phosphate elimination in wastewater treatment plants, phosphate ban from textile washing detergents). In the 1950s, lake water treatment started with conventional treatment (sand filtration followed by chlorination) which was supplemented with a pre-chlorination followed by a flocculation process. The introduction of activated carbon was a consequence of increasing taste and odour problems but in other contexts also a barrier against micropollutants which started to emerge in the 1970s. In the mid-1970s, the discovery of trihalomethanes and the formation of chloro- and bromophenols [potent taste and odour compounds (Acero *et al*., 2005)] which are formed during chlorination was a motivation for moving away from chlorination to ozonation. First, an intermediate ozonation was introduced followed by biological activated carbon filtration (see also Chapter 3). Then, pre-chlorination was replaced by pre-ozonation. The combination of ozone with biological activated carbon filtration is also known as the Mülheim process which was developed in 1974 (Sontheimer *et al*., 1978; Heilker, 1979). Mülheim is one of the cities in the most densely populated industrial area in Germany, the Ruhr area (ca. 4 million people), and draws its water from the river Ruhr. A rigorous and efficient treatment scheme was necessary to provide high-quality drinking water to the population (Figure 5.2 and discussion below).

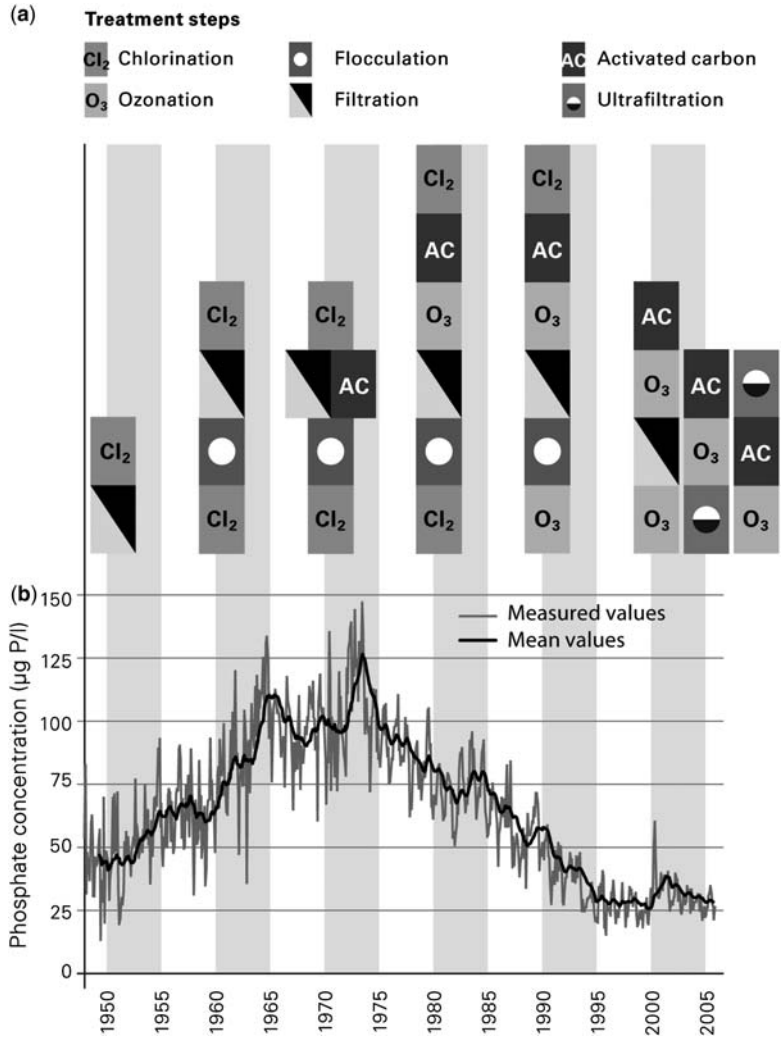

Figure 5.1 (a) Evolution of lake water treatment for Lake Zurich water from 1950 to 2005. (b) Evolution of the phosphate concentration as an indicator for the trophic state of the lake. According to von Gunten, 2008, with permission.

When lake water quality in Switzerland improved in the 2000s and membranes became affordable for drinking water treatment, treatment trains were simplified including a membrane filtration step (ultrafiltration, UF). Hence, treatment schemes could be reduced to three steps, always including the combination of ozone with biological activated carbon filtration and membranes. This combination guarantees a high drinking water quality with respect to hygiene, aesthetic properties and chemical contaminants and allows a distribution of drinking water without residual disinfectants such as chlorine, chloramine and chlorine dioxide. This has the advantage that no disinfection by-products are formed in the distribution system (Sedlak & von Gunten, 2011).

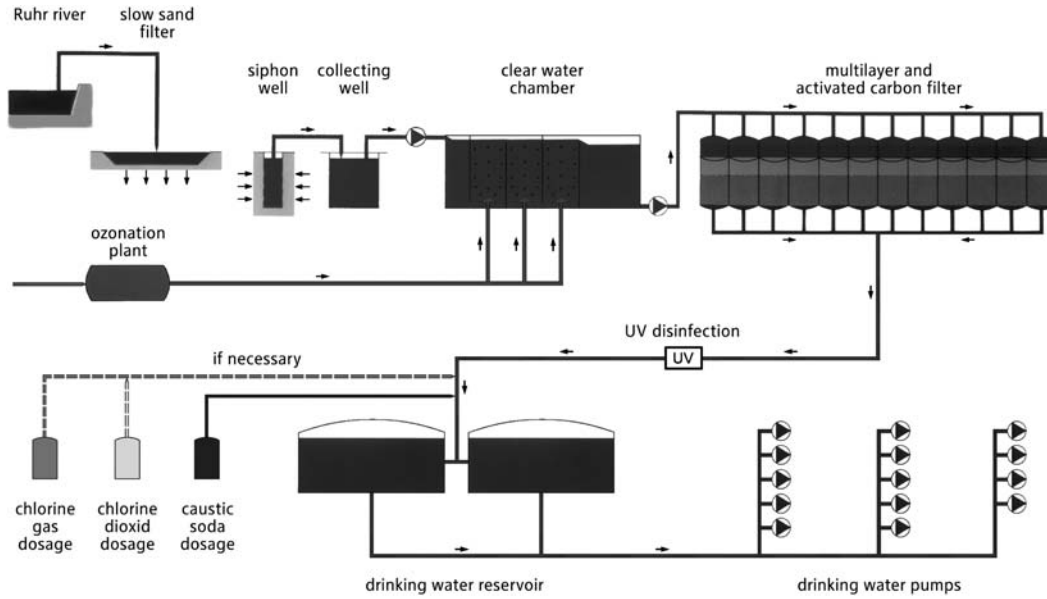

Figure 5.2 The Mülheim process with the characteristic combination of ozonation and biological filtration. With permission of RWW Rheinisch-Westfälische Wasserwerksgesellschaft mbH.

As mentioned above, the implementation of the Mülheim process in 1974 was a considerable break-through in chlorine-free drinking water treatment. In a first step, the water passes through a slow sand filter. Thereby, suspended particles are retained and part of the organic matter is consumed by microbial processes. Subsequent ozonation oxidises micropollutants and transforms part of the remaining DOM to AOC/BDOC (Chapter 3), which leads to a further reduction of DOC in the following biofiltration step with multi-layer filters containing activated carbon (AC). The water is then UV-disinfected prior to distribution. In case of emergency, chlorine or chlorine dioxide dosing is possible.

Since the 1990s, membrane filtration, in particular UF, has become an interesting alternative to deep bed sand filtration processes. UF is an efficient barrier against micro-organisms (viruses, bacteria and protozoa) but does not retain organic micropollutants (Jacangelo *et al*., 1997). Therefore, a combination of UF with ozone oxidation and adsorption processes leads to a drinking water with good hygienic and chemical qualities.

Figure 5.3 shows a conventional process combination including ozonation and deep bed filtration processes and two possible process combinations including UF, ozonation and AC filtration (Pronk & Kaiser, 2008).

All three process combinations are currently used for the treatment of Lake Zurich water in Switzerland. Combination C may require a final disinfection with UV, because AC filters lose significant numbers of micro-organisms. In a pilot study with combination B, the total cell count determined by flow cytometry was $\approx 10^3$ cells/mL after ozonation and $>10^5$ cells/mL after AC filtration (cf. Figure 5.4) (Hammes *et al*., 2008).

In the AC filter, bacteria can grow on AOC/BDOC, which leads to a significant increase in the total cell count (Figure 5.4). In combination B which is reflected in Figure 5.4, bacteria are removed by UF to below detection limit of flow cytometry, whereas in combination C, where AC filtration is the last treatment step, they would be released into the distribution system if not properly disinfected.

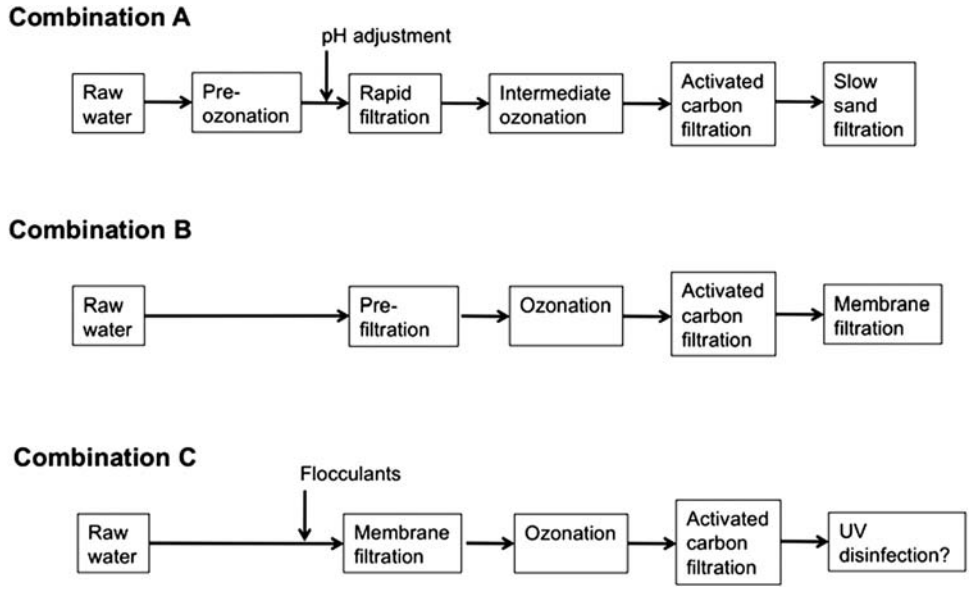

Figure 5.3 Conventional multi-barrier treatment with ozonation (Combination A) and two possible alternative process combinations (B and C) including ozonation and ultrafiltration. Adapted from Pronk & Kaiser, 2008, with permission.

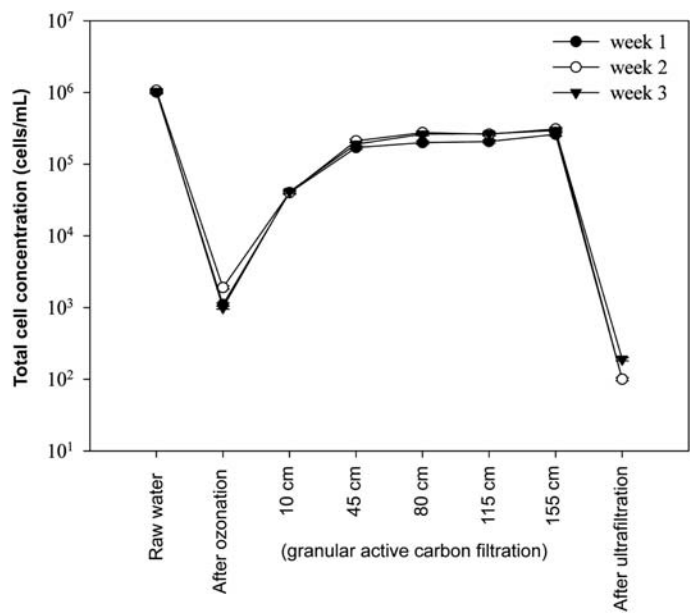

Figure 5.4 Total cell concentration determined with flow cytometry as a function of the treatment step for process combination B in Figure 5.3. According to Hammes *et al.*, 2008, with permission.

5.3 MICROPOLLUTANTS IN WATER RESOURCES, DRINKING WATER AND WASTEWATER

A large body of compounds found in waters and wastewater are considered as micropollutants (Fahlenkamp *et al*., 2004). There is vast literature on the occurrence of micropollutants in water resources such as ground-water and surface waters and in urban water management systems. They have also been monitored in wastewater before and after biological treatment. These studies are too numerous to be dealt with in this book and the reader is referred to some review articles and books on this topic (Ternes, 1998; Kolpin *et al*., 2002; Snyder *et al*., 2003; Vanderford *et al*., 2003; Schwarzenbach *et al*., 2006, 2010; Kümmerer, 2010; Ternes & Joss, 2006; Benotti *et al*., 2009; Kim *et al*., 2007b; Richardson & Ternes, 2011).

Micropollutant abatement is one of the objectives of ozone in water treatment (Gerrity & Snyder, 2011). Mechanistic studies on the degradation of micropollutants by ozone are found in Chapters 6–13. Ozone rate constants of micropollutants as much as they are known thus far are also given in these chapters. Some micropollutants react too slowly with ozone to be eliminated by ozone under such conditions. They are typically called ozone-refractory, although this is not fully correct. Their reaction is just too slow to be of relevance. They may be eliminated by the much more reactive $^{\bullet}$OH radicals. For the formation of $^{\bullet}$OH in the reactions of ozone with the organic part of the water matrix (DOM) and the contribution of $^{\bullet}$OH to micropollutant abatement see Chapter 3. The chemistries of $^{\bullet}$OH and the ensuing peroxyl radicals are discussed in Chapter 14.

Combination B in Figure 5.3 was tested with regard to the potential for micropollutant removal from Lake Zurich water in pilot-scale ($\approx$10 m^3/h). Three compounds with different physical chemical properties (rate constants for reactions with ozone and $^{\bullet}$OH, adsorption behaviour on AC, see legend of Table 5.3) were investigated, the fuel additive methyl-*t*-tbutylether (MTBE) and the taste and odour compounds 2-isopropyl-3-methoxypyrazine (IPMP) and β-ionone [for a compilation of typical taste and odour compounds see Table 5.2, for their occurrence in Swiss lakes see Peter *et al*. (2009)].

Table 5.2 Some abundant taste and odour compounds according to Peter & von Gunten (2007)

Compound	Odour	Odour threshold/ng L^{-1}	Source	Formula in Chapter
β-Cyclocitral	Fruity	19000	Cyanobacteria	6
Geosmin	Earthy	4	Cyanobacteria, Actinomycetes	14
cis-3-Hexen-1-ol	Grassy	70000	Algae	6
β-Ionone	Violets	7	Cyanobacteria, algae	6
2-Isopropyl-3-methoxypyrazine (IPMP)	Decaying vegetation	0.2	Actinomycetes	8
2-Methylisoborneol (MIB)	Musty	15	Cyanobacteria, Actinomycetes	14
trans,*cis*-2,6-Nonadienal	Cucumber	20	Algae	6
1-Penten-3-one	Fishy-rancid	1250	Cyanobacteria, algae	6

(*Continued*)

Table 5.2 Some abundant taste and odour compounds according to Peter & von Gunten (2007) (*Continued*)

Compound	Odour	Odour threshold/ng L^{-1}	Source	Formula in Chapter
2,6-Di-*t*-butyl-4-methylphenol	Plastic	Not available	Leaching from polyethylene pipes	7
2,4,6-Tribromoanisole (TBA)	Earthy–musty	0.03	Methylation of bromophenol by micro-organisms	7
2,4,6-Trichloroanisole (TCA)	Musty	0.03	Methylation of chlorophenol by micro-organisms	7

After ozonation, the relative residual concentrations of MTBE, IPMP and β-ionone are 80%, 50% and <5%, respectively (Table 5.3).

Table 5.3 Elimination of selected micropollutants in a multi-barrier system including ozonation, activated-carbon filtration and ultrafiltration (combination B in Figure 5.3). Relative residual concentrations are given in %. For MTBE and IPMP data are given for various activated-carbon running times (10, 150 and 200 days) MTBE: $k(O_3) = 0.15\ M^{-1}\ s^{-1}$, $k(^{\bullet}OH) = 1.9 \times 10^9\ M^{-1}\ s^{-1}$, $\log K_{ow} = 0.94$; IPMP: $k(O_3) = 50\ M^{-1}\ s^{-1}$, $k(^{\bullet}OH) = 5 \times 10^9\ M^{-1}\ s^{-1}$, $\log K_{ow} = 2.41$; β-ionone: $k(O_3) = 1.6 \times 10^5\ M^{-1}\ s^{-1}$, $k(^{\bullet}OH) = 7.8 \times 10^9\ M^{-1}\ s^{-1}$, $\log K_{ow} = 3.84$. According to von Gunten, unpublished

Micropollutant	After ozonation	After activated-carbon filtration	After ultrafiltration
	Relative residual concentrations in %		
MTBE (10 days)	80	<d.l.	<d.l.
MTBE (150 days)	75	78	77
IPMP (10/200 days)	50	<d.l.	<d.l.
β-Ionone	1	<d.l.	<d.l.

MTBE methyl-*t*-butylether; IPMP 2-Isopropyl-3-methoxypyrazine; d.l. detection limit.

This can be explained on the basis of the rate constants for the reaction of these compounds with ozone and $^{\bullet}OH$. MTBE has the lowest reactivity towards ozone and $^{\bullet}OH$; IPMP is in an intermediate range, whereas β-ionone reacts rapidly with ozone and $^{\bullet}OH$ (Table 5.3). For short running times, AC removes MTBE well, but at longer operation times (150 days) MTBE breaks through. IPMP is fully retained even after 200 days of operation of the granular activated carbon (GAC) filter. This behaviour of the two compounds can be explained by their octanol–water partitioning coefficients (K_{ow}) taken as a measure for the affinity to GAC. Based on the K_{ow} value, β-ionone would be even better adsorbed. But this has no consequences, since β-ionone is already fully removed by ozonation. For improving MTBE removal, the AOP ozone/H_2O_2 (Chapter 3 for details) was tested by injecting H_2O_2 in the third chamber of the four-chamber ozone reactor. An increase in the ozone dose in combination with H_2O_2 addition allowed a full elimination of MTBE (for the reaction of $^{\bullet}OH$ with MTBE see Chapter 14).

5.4 ENHANCED WASTEWATER TREATMENT WITH OZONE

As discussed above, wastewater treatment with ozone has mainly been installed for disinfection purposes. In Europe and some other countries, the need for enhanced wastewater treatment for micropollutant removal to protect aquatic ecosystems is now considered (Ternes *et al*., 2003; Joss *et al*., 2008; Ort *et al*., 2009). Currently, there are two options for enhanced treatment of secondary wastewater effluent, namely the addition of a powdered AC (Nowotny *et al*., 2007) or ozonation (Joss *et al*., 2008). For investigating ozonation of wastewater systems, a considerable number of pilot- and full-scale tests have been performed over recent years (Ternes *et al*., 2003; Huber *et al*., 2005; Wert *et al*., 2009a; Hollender *et al*., 2009; Reungoat *et al*., 2010; Zimmermann *et al*., 2011; Stalter *et al*., 2010a, 2011; Macova *et al*., 2010).

A typical treatment train for enhanced wastewater treatment with an ozonation step is shown in Figure 5.5. For minimising ozone consumption, ozone is placed after the activated sludge treatment, where DOC concentration is lowest.

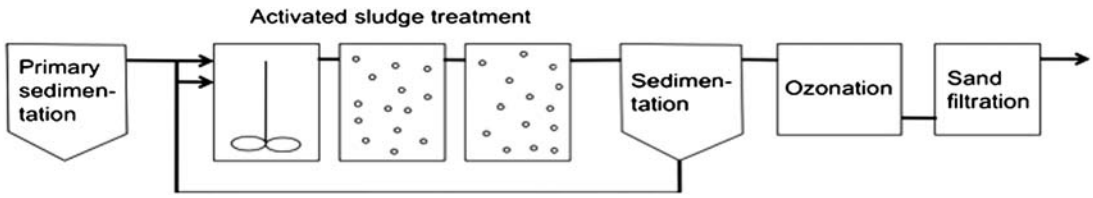

Figure 5.5 Treatment train for enhanced wastewater treatment with ozone.

Ozonation should be followed by biological sand filtration for degrading AOC/BDOC formed during ozonation (Zimmermann *et al*., 2011) (Chapter 3). Ozonated wastewater leads to a developmental retardation of rainbow trout, but this effect disappears after sand filtration (Stalter *et al*., 2010b). This might be an indication that easily biodegradable compounds such as aldehydes are responsible for these adverse health effects on fish (cf. Chapter 4). Aldehyde formation during ozonation of wastewater is quite significant (Wert *et al*., 2007).

Formation and the degradation of AOC during ozonation and post-sand filtration is shown in Figure 5.6 for a full-scale wastewater treatment plant for a specific ozone dose of 1.24 g O_3/g DOC (Zimmermann *et al*., 2011). The main increase in AOC is observed at the first sampling point in the ozone reactor (P1), where most of the ozone is consumed. Thereafter, AOC remains almost constant, mainly due to the small residual ozone concentration. After sand filtration, AOC is considerably reduced, indicating that a significant portion of low-molecular-weight compounds that are potentially toxic to fish can be removed by this process.

Figure 5.6 also shows the evolution of total cell counts (TCC) during ozonation and post-sand filtration. Depending on the ozone dose, TCC decreases by 2−4 orders of magnitude (Zimmermann *et al*., 2011) reflecting the efficiency of ozone as a disinfectant. After sand filtration, total cell count increases again leading to an overall efficiency of the process of 1–2 logs reduction of TCC. This is in line with the observation of cell growth in activated carbon filters in drinking water treatment (Hammes *et al*., 2008). A 0.5–3 log inactivation of *E. coli* was observed during ozonation of the same wastewater. In this case, however, sand filtration did not lead to an increase of bacterial counts for *E. coli* (Zimmermann *et al*., 2011) suggesting that there is also no re-growth of pathogenic bacteria in the sand-filtered water after ozonation.

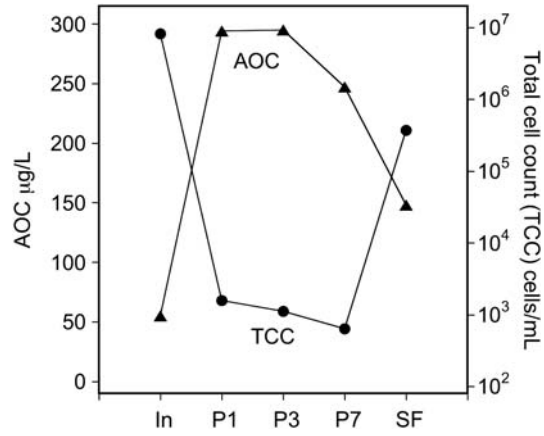

Figure 5.6 Assimilable organic carbon (AOC) formation and total cell counts (TCC, determined by flow cytometry) for ozonation followed by biological sand filtration for a full-scale wastewater treatment plant, Regensdorf, Switzerland (25000 population equivalent). Ozone dose 1.24 g O_3/g DOC. In: Secondary effluent, inlet to ozone reactor; P1, P3, P7 sampling points within the reactor; SF sand filtration. Adapted from Zimmermann *et al.*, 2011, with permission.

5.5 ENERGY REQUIREMENTS FOR MICROPOLLUTANT TRANSFORMATION IN DRINKING WATER AND WASTEWATER

Energy requirements for micropollutant transformations during ozonation and advanced oxidation processes (AOPs) depend on the matrix of the water that consumes oxidants (Chapter 3, mainly type and concentration of DOM) and the rate constant for the reaction of a target compound with ozone and $^{\bullet}OH$ radicals. Table 5.4 shows a comparison of the energy requirements for a 90% transformation of selected compounds during ozonation and the AOP UV/H_2O_2 for laboratory experiments. In general, an increase in energy of about 25% for O_3/H_2O_2 relative to the conventional ozonation is estimated based on production energy of 15 kWh/kg and 10 kWh/kg for ozone and H_2O_2, respectively (Katsoyiannis *et al.*, 2011). For ozonation, Table 5.4 shows that for a given water quality, the required energy increases in the order SMX < pCBA < ATR < NDMA. This can be explained by a decrease in the second order rate constants for the reaction of these compounds with ozone and $^{\bullet}OH$ from SMX to NDMA. Energy requirements also increase significantly from Lake Zurich water to Dübendorf wastewater, due to the higher concentrations of DOM (consumption of ozone and $^{\bullet}OH$, Chapter 3) and carbonate (consumption of $^{\bullet}OH$, Chapter 3). For a given water, energy requirements for UV/H_2O_2 are typically significantly higher and depend on the penetration depth of UV radiation. Only for NDMA, with low reactivity towards ozone and $^{\bullet}OH$ (Lee *et al.*, 2007b), does the energy requirement for UV/H_2O_2 become comparable to ozonation. This is due to the fact that NDMA undergoes mainly direct photolysis (Sharpless & Linden, 2003).

For a particular full-scale study (Hollender *et al.*, 2009), the energy consumption for ozonation of secondary effluent, including all contributions (production of liquid oxygen, its transport, generation of ozone) was calculated. The energy requirement at the plant remained constant for process gas in the range of 100–170 g O_3 m^{-3} at 12 kWh/kg O_3. This translates into an energy requirement of 0.035 kWh m^{-3} for a specific ozone dose of 0.6 g O_3/g DOC, which corresponds to about 12% of the total energy consumption of a nutrient (C, N, P) removal plant (0.3 kWh m^{-3}). In addition,

production of pure oxygen requires 0.01–0.015 kWh m^{-3}. Therefore, the overall energy requirement at this ozone dose (removal of SMX) is quite similar to that shown in Table 5.4 for laboratory systems. For a large range of wastewaters (10,000 to 500,000 person equivalents) and DOC contents (6 to 20 g DOC m^{-3}), total costs of ozonation (investment and operation including post-filtration step) were estimated to range between 0.05 and 0.15 € m^{-3}, depending on plant size and secondary effluent quality (Joss *et al.*, 2008).

Table 5.4 Energy requirements in kWh m^{-3} for 90% transformation of selected micropollutants by conventional ozonation in Lake Zurich water and Dübendorf wastewater and by using UV(254 nm)/H_2O_2 (0.2 mM) for varying optical path lengths (cm) in Lake Zurich water. Experimental conditions: target compound concentration = 0.5 μM, pH 8, $T = 20$ °C. According to Katsoyiannis *et al.*, (2011), with permission

	Lake Zurich Water	Dübendorf wastewater	Lake Zurich Water		
Target compound	**Ozonation**	**Ozonation**	**UV/H_2O_2 1 cm**	**UV/H_2O_2 5 cm**	**UV/H_2O_2 10 cm**
SMX	0.0015	0.045	0.39	0.15	0.11
pCBA	0.035	0.2	0.75	0.23	0.17
ATR	0.05	0.3	0.98	0.28	0.2
NDMA	0.5	0.9	1.62	0.44	0.3

SMX sulfamethoxazole; pCBA *p*-chlorobenzoic acid; ATR atrazine; NDMA *N*-nitrosodimethylamine; Lake Zurich water, DOC 1.3 mgC/L, carbonate alkalinity 2.6 mM; Dübendorf wastewater, DOC 3.9 mg C/L, carbonate alkalinity 6.5 mM.

5.6 SOURCE CONTROL

The removal of micropollutants from the wastewater stream by enhanced treatment of secondary wastewater effluent is an end-of-pipe solution. Other options include treatment of source-separated urine (Larsen & Gujer, 1996) or treatment of other point sources such as hospital wastewater. Urine separation and treatment with ozone has been demonstrated to be a feasible process for micropollutant removal. Even though it only accounts for about 1% of the wastewater stream, it requires more energy to remove micropollutants by ozonation than in wastewater (Dodd *et al.*, 2008). When the treatment of source-separated urine is combined with nutrient recovery (N, P), the overall energy requirement becomes even favourable for urine treatment compared to wastewater treatment (Dodd *et al.*, 2008). Nevertheless it has to be considered that some chemicals, among them high risk chemicals such as the antiarrhythmic compound amiodarone (cf. Chapter 8), are excreted via faeces (Escher *et al.*, 2011). Therefore, the full spectrum of compounds will not be removed by this approach. The contribution of hospital wastewater to the overall load of pharmaceuticals in municipal wastewater is typically quite low in the order of $<15\%$ (Ort *et al.*, 2010). Nevertheless, source control in hospitals has quite high acceptance among stakeholders, especially if the contribution of hospitals to the overall load is high (Lienert *et al.*, 2011). In this context it is noted that municipal wastewater receives an integrated load of chemicals used in households, which also include biocides, pesticides, personal care products, etc., which will also be removed by an ozone treatment of secondary effluents (Hollender *et al.*, 2009).

5.7 RECLAMATION OF WASTEWATER

Reclamation of wastewater as a resource for drinking water and for irrigation purposes (agriculture, golf courses, etc.) has become an important issue in arid and semi-arid areas due to population growth and climate change. Today, wastewater reuse is heavily based on membrane processes. Secondary effluent is typically treated by a combination of microfiltration/ultrafiltration with reverse osmosis (RO) (Figure 5.7) (Asano *et al.*, 2007). Even in coastal areas this approach (<1 kWh/m^3) is more energy efficient than seawater desalination [3.5–4.5 kWh/m^3, (Sommariva, 2010)]. Water desalination has become increasingly important worldwide with large-scale plants (30,000–320,000 m^3/d) in Kuwait, Singapore, USA, Australia and China (Hemmi *et al.*, 2010). The RO process is frequently followed by UV disinfection, and the water is then mostly used for replenishment of natural water bodies such as groundwaters or surface waters. In the treatment scheme outlined in Figure 5.7, ozonation is not applied. In principal, ozonation could be used to treat secondary wastewater effluent for removing NDMA precursors (Lee *et al.*, 2007a). Such (unknown) precursors may lead to NDMA during chloramination which is routinely applied to hinder biofilm growth on the RO membrane. Typically, the rejection of micropollutants by RO is $>90\%$ (Busetti *et al.*, 2009). Advanced oxidation of the RO permeate (UV/H_2O_2, UV/ozone or ozone/H_2O_2 is an option for an additional barrier for removing micropollutants such as NDMA, which are not fully retained by RO. AOPs in post-RO water are expected to be very efficient, because its $^{\bullet}OH$ scavenging rate is very low due to its low DOC of <0.1 mg/L.

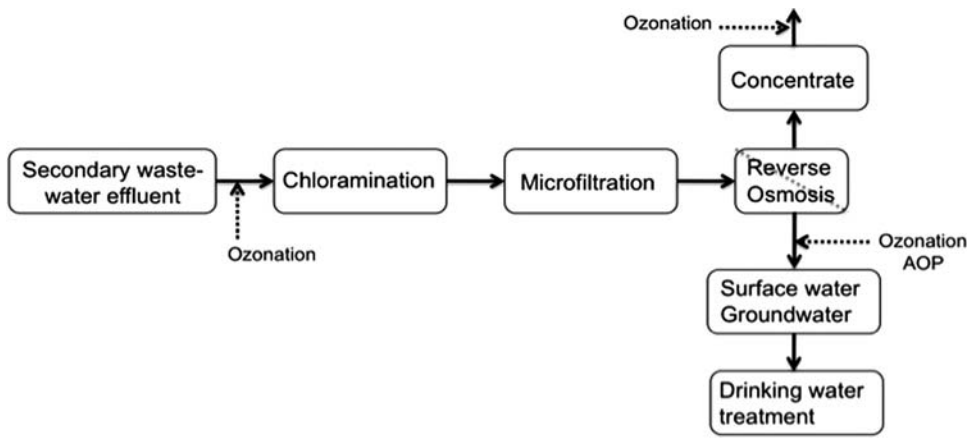

Figure 5.7 Water reuse scheme based on ultrafiltration/reverse osmosis. Points for potential ozonation steps are also indicated.

One of the problems in the RO-based water reuse scheme is the discharge of the RO concentrate. The concentration factor for micropollutants during RO treatment of wastewater is of the order of four. In a recent study, ozonation was investigated for the elimination of beta blockers from an RO concentrate with a DOC of 46 mg/L (Benner *et al.*, 2008). For metoprolol (cf. Chapter 8) [$k(O_3) = 2 \times 10^3$ M^{-1} s^{-1} (pH 7), $k(^{\bullet}OH) = 7.3 \times 10^9$ M^{-1} s^{-1}] an ozone dose of >10 mg/L (≈ 0.25g O_3/g DOC) was required for a removal of $>90\%$. The bromate concentration for these conditions was of the order of <40 µg/L, which is relatively low considering the high Br^- levels (1200 µg/L) in the RO concentrate. The ozonated water can then be released to the environment with less toxicological concern.

An alternative strategy for wastewater reuse consists of a combination of conventional processes such as ozonation, dissolved air flotation and active carbon filtration. Figure 5.8 shows a schematic representation of such a potential treatment train (Reungoat *et al*., 2010). Overall, this multi-barrier treatment removed, very efficiently, micropollutants and DOC. Fifty of fifty-four compounds detected in the secondary effluent were eliminated to below detection limits. The DOC concentration was reduced by 55–60%. Furthermore, toxicity determined by various biological endpoints (e.g. oestrogenicity, neurotoxicity, phytotoxicity), was significantly lower than in the influent, often very similar to the blank (Reungoat *et al*., 2010).

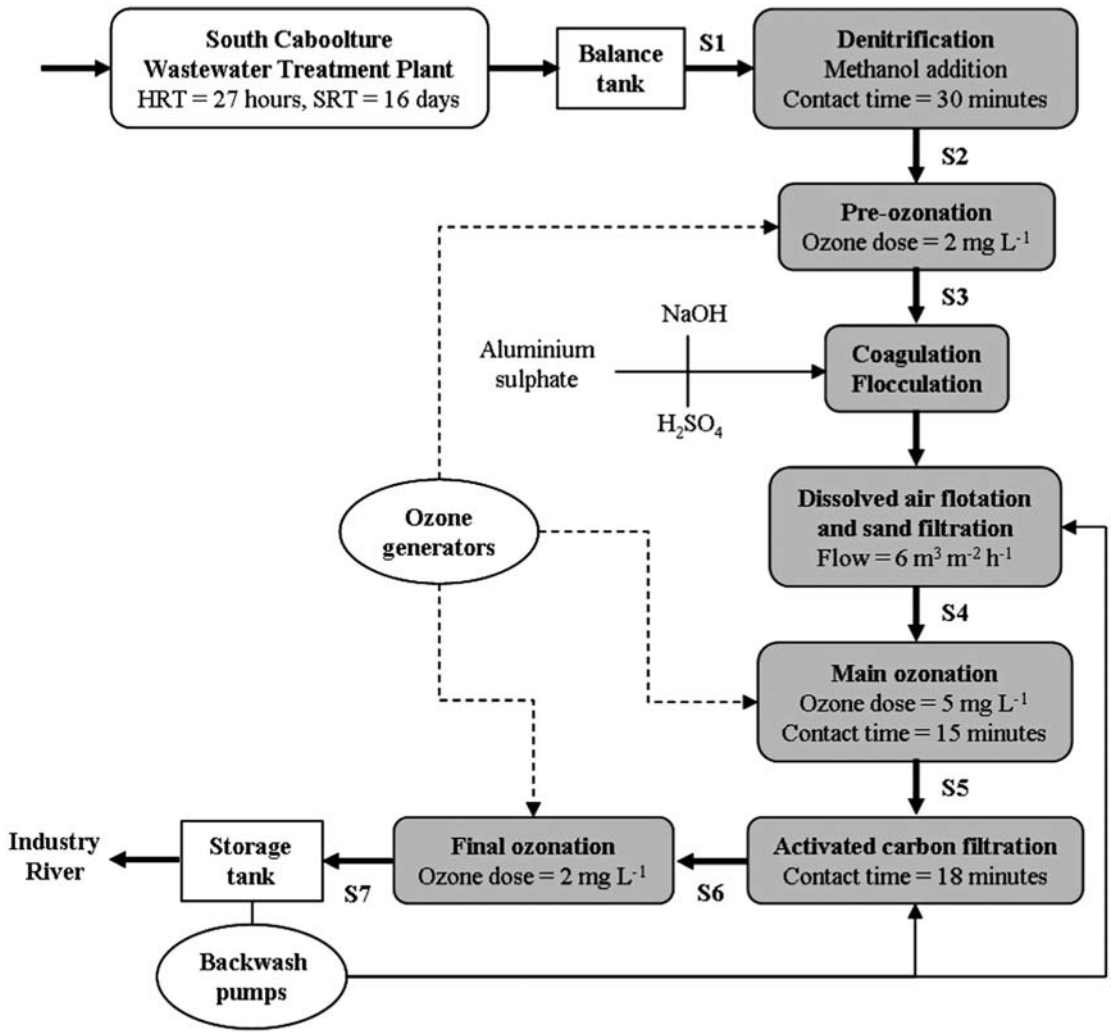

Figure 5.8 Water reuse scheme based on conventional processes such as ozonation, dissolved air flotation and activated carbon filtration. SRT: sludge retention time. According to Reungoat *et al*. (2010), with permission.

5.8 COMPARISON OF THE APPLICATION OF OZONE IN THE URBAN WATER CYCLE

Based on the discussion above, potential points of application of ozonation processes for micropollutant abatement in the urban water cycle are shown in Figure 5.9.

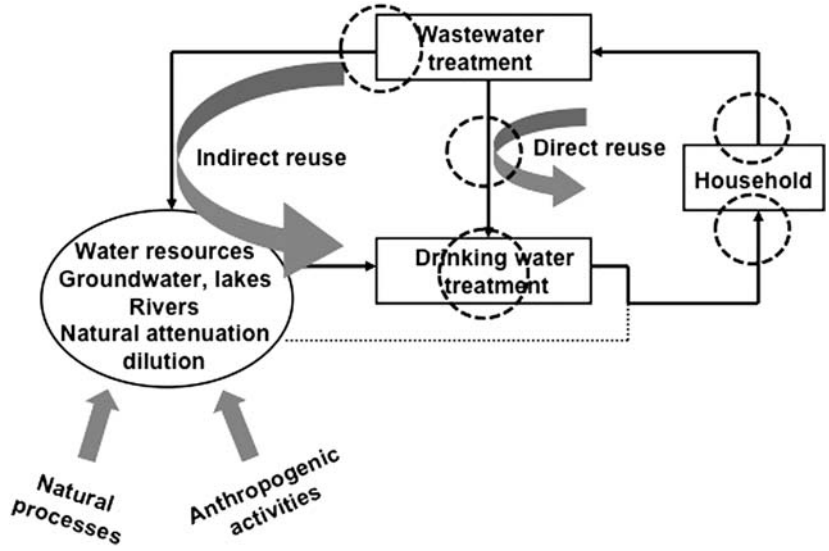

Figure 5.9 The urban water cycle with potential points of ozonation (marked with circles).

In principle, ozonation can be applied in households as point-of-entry or point-of-use treatment and to the wastewater, e.g. source separated urine (Dodd *et al*., 2008). Once the wastewater is collected, oxidative treatment may be carried out as post-treatment of secondary wastewater effluent (see above). Compared to treatment of source-separated urine, this also allows oxidative transformation of micropollutants which are derived from sources other than households. Both the treatment at the household level and the treatment in centralised wastewater treatment plants lead to a reduction of the micropollutant discharge to the receiving water bodies. As a consequence, ecosystems and water resources are protected from adverse impacts. When the urban water system is mainly driven by human toxicology, oxidative treatment (mainly ozonation or AOPs) may be placed within the drinking water treatment scheme (Westerhoff *et al*., 2005; Broséus *et al*., 2009; Vieno *et al*., 2007; Kruithof *et al*., 2007; Ternes *et al*., 2002).

This scenario has the advantage that micropollutants from diffuse sources such as agriculture, traffic and natural sources (e.g. cyanotoxins and taste and odour compounds) will also be removed (Acero *et al*., 2000, 2001; Benitez *et al*., 2007; Rodriguez *et al*., 2007; Peter & von Gunten, 2007; Onstad *et al*., 2007). For direct or indirect potable water reuse, an oxidation can be applied after a reverse osmosis treatment (Asano *et al*., 2007). The water quality for each treatment scenario is decisive for the efficiency of an ozonation process. The main parameter is the content of the dissolved organic matter, typically expressed as DOC concentration (Chapter 3). In addition, pH, alkalinity and ammonia also play an important role (Chapter 3). Table 5.5 summarises water qualities of hydrolysed and electrodialysed urine, municipal wastewater and water resources used for drinking water production.

Table 5.5 Water quality parameters relevant for oxidation processes, from Dodd *et al*. (2008); Pronk *et al*. (2006); Udert *et al*. (2003)

Water type	pH	DOC mg/L	Alkalinity mM	NH_3/NH_4^+ mg/L
Hydrolysed urine	9	≈2000	≈300	≈4000
Electrodialysed urine diluate*	8	≈400*	≈30	≈400
Wastewater effluent	7–8	≈5−20	2–4	≈20
Water resources for drinking water production				
Surface water	7–8	1–20	1–2	< 0.005 to >1
Groundwater	7–8	<1 to 20	1–5	< 0.005 to >1

*contained some methanol from dosing of micropollutants

A dramatic decrease of DOC is observed from hydrolysed urine to wastewater effluent. This is partially caused by dilution and partially by the DOC removal during activated sludge treatment. The DOC concentration in surface and groundwaters is typically much smaller and dominated by natural processes (soil weathering, algal growth, etc.). Because ozone demand is closely related to the DOM concentration, it is evident that ozone consumption gets smaller further away from the household source. However, it has to be taken into account, that human urine represents <1% of the total flow of municipal wastewater. Therefore, it might still be a feasible option for micropollutant elimination.

The water quality data (Table 5.5) have consequences for the efficiency of micropollutant elimination. A comparison of the required ozone doses for 90% micropollutant elimination is shown in Table 5.6 for hydrolysed urine, electrodialysed urine diluate, wastewater effluent and two surface waters for 17α-ethinyloestradiol (EE2) a synthetic steroid oestrogen and ibuprofen (IP) an antiphlogistic.

Table 5.6 Required ozone doses (mg/L) and corresponding O_3/DOC ratios (w/w) for a 90% elimination of 17α-ethinyloestradiol (EE2) and ibuprofen (IP) in various water sources (Lee & von Gunten, 2010; Dodd *et al*., 2008; Huber *et al*., 2003, 2005)

Water type	EE2		IP	
	O_3 dose mg/L	O_3/DOC w/w	O_3 dose mg/L	O_3/DOC w/w
Hydrolysed urine	≈500	0.25	≈1000	0.5
Electrodialysed urine diluate*	≈150	0.375	≈600	1.5
Wastewater 1 (7.7 mg/L DOC)	>1	>0.13	n.d.	n.d.
Wastewater 2 (5 mg/L DOC)	0.5	0.1	≈4	0.8
Lake water (3.7 mg/L DOC)	0.1	0.03	n.d.	n.d.
River water (1.3 mg/L DOC)	<0.1	<0.08	>2	>2

n.d.: not determined;
*contained some methanol from dosing of micropollutants

While EE2 reacts quickly with ozone and $^{\bullet}OH$ (pH 7: $k(O_3) \approx 3 \times 10^6\ M^{-1}\ s^{-1}$, $k(^{\bullet}OH) = 9.8 \times 10^9\ M^{-1}\ s^{-1}$), IP reacts mostly with $^{\bullet}OH$ (pH 7: $k(O_3) = 9.6\ M^{-1}\ s^{-1}$, $k(^{\bullet}OH) = 7.4 \times 10^9\ M^{-1}\ s^{-1}$) (Huber *et al.*, 2003).

The efficiency of ozonation increases with decreasing DOC concentrations. For a 90% elimination of EE2, the ozone dose varies over more than three orders of magnitude, reflecting the difference in the DOC concentration between hydrolysed urine and the pre-treated river water. While this difference seems quite large, it has to be considered, that the volume of urine that needs to be treated is about two orders of magnitude smaller than that of wastewater. Furthermore, the ozone dose normalised to the DOC concentration for 90% abatement of the selected ozone-reactive and ozone-resistant compounds is similar for hydrolysed urine and wastewater. Therefore, urine treatment at the household level seems to be feasible, however as mentioned above, only part of the micropollutant load in the wastewater will be treated at this level. In addition, small-scale ozonation systems would have to be implemented at the household level which would require the appropriate maintenance. Table 5.6 also shows that the ozone doses and O_3/DOC ratios for drinking water sources are significantly smaller for compounds reacting rapidly with ozone and in a similar range as urine and wastewater for ozone-resistant compounds.